ZIAD A. ELSAHN

SMOOTH UPGRADE OF EXISTING FTTH ACCESS NETWORKS : SAC-OCDMA AND DENSE SS-WDM SOLUTIONS

Thèse présentée
à la Faculté des études supérieures de l'Université Laval
dans le cadre du programme de doctorat en génie électrique
pour l'obtention du grade de Philosophiæ Doctor (Ph. D.)

DÉPARTEMENT DE GÉNIE ÉLECTRIQUE ET DE GÉNIE INFORMATIQUE
FACULTÉ DES SCIENCES ET DE GÉNIE
UNIVERSITÉ LAVAL
QUÉBEC

2010

Such is the Bounty of Allah, which He bestows on whom He will: and Allah is the Lord of the highest bounty [Quran: 62-4]

To whom I love and respect

Résumé

Pour satisfaire les futures besoins de bande passante, les réseaux d'accès existants de fibre-au-domicile (FTTH) doivent être améliorés pour garantir au moins une connexion dédiée de 100 Mb/s par abonné. Étant donné que la durée de vie de l'infrastructure d'un réseau optique passif (PON) doit dépasser 25 ans, le remplacement des infrastructures existantes n'est pas désiré lors de l'amélioration du 'throughput' du réseau. Dans cette thèse, nous proposons des solutions peu coûteuses pour la prochaine génération des PONs utilisant l'infrastructure existante basée sur les coupleurs passifs. Les mises à jour nécessaires sont effectuées à base d'abonné permettant un déploiement progressif des clients à haut débit, sans affecter les anciens usagers. Dans notre étude, nous considérons deux types de solutions utilisant des sources de lumière incohérente.

La première approche que nous proposons est d'utiliser le codage spectral d'amplitude à accès multiple par répartition de codes (SAC-OCDMA) pour la prochaine génération des PONs. La performance des architectures basées sur des sources de lumière locales ou des sources centralisées sont examinées en fonction du taux d'erreur binaire (BER), du budget de puissance, et des exigences d'amplification. Nous avons, avec succès, démontré la liaison montante d'un 7×622 Mb/s SAC-OCDMA PON au-dessus d'un lien de 20 km, avec l'opération en mode rafale (burst-mode). Malgré les pertes supplémentaires dans les architectures avec des sources centralisées, nous avons atteint une transmission sans erreurs pour un système chargé, en utilisant un code correcteur d'erreurs (FEC) Reed-Solomon RS(255,239). En utilisant le récepteur 'burst-mode', nous avons atteint un rapport de perte de paquets (PLR) nul, pour un maximum de quatre usagers simultanés et plus de deux ordres de grandeur d'amélioration du PLR pour un PON chargé.

La deuxième approche que nous proposons est un chemin de migration du multiplexage par répartition temporel (TDM) vers le multiplexage dense de tranches de spectres (SS) par répartition en longueur d'onde (WDM). Nous utilisons un nouvel amplificateur optique réfléchissant à semi-conducteur (RSOA) auto-injecté, comme un transmetteur, et

un récepteur balancé récemment proposé pour atténuer le bruit d'intensité. Nous utilisons un réseau de Bragg (FBG) ayant une réflectivité de *p*% pour l'auto-injection, et nous optimisons sa réflectivité pour un compromis entre la puissance de sortie et l'effet de nettoyage du bruit. Nous avons découvert qu'en utilisant le FBG optimal ($p = 18 \pm 2\%$), on peut transmettre jusqu'à 4.5 dBm de puissance dans un canal de 25 GHz. Nous avons démontré expérimentalement une transmission SS-WDM dense à 1.25 Gb/s, et traité la possibilité d'avoir une unité de réseau optique (ONU) incolore en plaçant le FBG au nœud de distribution (RN). Une transmission sans erreurs a été réalisée sur un lien de 20 km pour l'auto-injection locale, alors qu'un plancher de BER autour de 10^{-9} a été atteint pour l'auto-injection à distance. Pour un lien de 10 km, une transmission sans erreurs a été atteinte pour les deux cas. Le budget de puissance a permis jusqu'à 32 usagers d'être supportés au-dessus de l'infrastructure existante de PON sans amplification au terminal de ligne optique (OLT). A l'aide des simulations, nous avons estimé que la capacité peut être augmentée à 128 usagers lorsqu'un FEC est utilisé. Nous avons montré que, malgré les pertes élevées au RN, notre solution permet une plus grande efficacité spectrale que celle des SS-WDM PON traditionnels basés sur des rangées de réseaux à guide d'ondes (AWG).

Abstract

To satisfy future bandwidth demands, existing fiber-to-the-home (FTTH) access networks must be upgraded to guarantee at least a 100 Mb/s dedicated connection per subscriber. Since the lifetime of the outside plant of a passive optical network (PON) is expected to be greater than 25 years, replacing the existing PON infrastructure is not desirable when upgrading the network throughput. In this thesis, we propose inexpensive solutions for next generation PONs using the existing passive splitter-based infrastructure. The necessary upgrades are made on a per subscriber basis allowing a gradual rollout of high bit rate clients without affecting the legacy PON users. In our study, we consider two different solutions using incoherent light sources.

The first approach we propose is to use spectral amplitude coded (SAC) optical code-division multiple-access (OCDMA) for next generation PONs. Both local sources and centralized light sources architectures are examined in terms of the bit error rate (BER) performance, the power budget, and the amplification requirements. We successfully demonstrated the uplink of a 7×622 Mb/s SAC-OCDMA PON over a 20 km link, with burst-mode operation. Despite the extra losses in centralized light sources architectures, we achieved error free transmission for a fully loaded system using a Reed-Solomon RS(255,239) forward-error correcting (FEC) code. Using the burst-mode receiver, we reported zero packet loss ratio (PLR) for up to four simultaneous users, and more than two orders of magnitude improvement in the PLR for a fully loaded PON.

The second approach we propose is a migration path from time-division multiplexing (TDM) to dense spectrum-sliced (SS) wavelength-division multiplexing (WDM). We use a novel self-seeded reflective semiconductor optical amplifier (RSOA) as a transmitter, and a recently proposed balanced receiver to mitigate the intensity noise. We use a p% reflective fiber Bragg grating (FBG) for self-seeding, and we optimize its reflectivity to tradeoff the output power versus the noise cleaning effect. We found out that using the optimum FBG ($p = 18 \pm 2\%$), we can transmit up to 4.5 dBm of power within a 25 GHz

channel. We experimentally demonstrated a 1.25 Gb/s dense SS-WDM transmission, and addressed the possibility of colorless optical network unit (ONU) operation by placing the FBG at the remote node (RN). Error free transmission was achieved over a 20 km feeder for local self-seeding, whereas a BER floor around 10^{-9} was reported for the remote self-seeding. For a 10 km feeder, error free transmission was achieved for both cases. The power budget allowed up to 32 users to be supported over the existing PON infrastructure without optical line terminal (OLT) amplification. Through simulations we estimated that the capacity can be increased to 128 users when a FEC is used. We showed that despite the high splitting losses at the RN, our solution achieves a higher spectral efficiency than that of traditional arrayed waveguide grating (AWG)-based SS-WDM PONs.

Preface

Two chapters of this thesis consist of *IEEE* journal papers, which are fully presented. My contributions in these papers are detailed here.

Paper 1

Z. A. El-Sahn, B. J. Shastri, M. Zeng, N. Kheder, D. V. Plant, and L. A. Rusch, "Experimental demonstration of a SAC-OCDMA PON with burst-mode reception: local versus centralized sources," *IEEE J. Lightwave Technology*, vol. 26, no. 10, pp. 1192-1203, June 2008, [16].

This paper was accepted and published in 2008. It is presented in Chapter 4 as a solution for next generation PONs. This paper is a result of a collaborative work between Laval University and McGill University. The design of the burst-mode receiver was carried by Bhavin J. Shastri, Ming Zeng, and Noha Kheder from McGill University, under the supervision of Prof. David V. Plant. I proposed the SAC-OCDMA PON physical architectures and built the experimental setup. I performed the BER measurements with a global clock, and did the required characterizations. All other experiments reported in this article were also carried in our labs at Laval University using the setup I prepared. I participated actively in all the BER and PLR measurements, including those with the burst-mode receiver. I analyzed the results, performed the FEC simulations to fit the measurements, and analyzed the power budget for the proposed architectures. Finally, I wrote the paper, it was then revised by Bhavin J. Shastri, Prof. David V. Plant, and my supervisor, Prof. Leslie A. Rusch. This collaboration was very fruitful; it resulted in four different publications: two journal papers and two conference papers.

Paper 2

Z. A. El-Sahn, W. Mathlouthi, H. Fathallah, S. LaRochelle, and L. A. Rusch, "Dense SS-WDM over legacy PONs: Smooth upgrade of existing FTTH networks," accepted in *IEEE J. Lightwave Technology*, February 2010, [18].

This paper was submitted to the *IEEE Journal of Lightwave Technology* in June 2008 and was accepted in February 2010. It is presented in Chapter 6, as another alternative for future PONs. Serge Doucet (acknowledged in the paper) fabricated the FBGs we used; he is a research assistant in the research group of Prof. Sophie LaRochelle. I completed the experimental work presented in this paper. The balanced receiver used in this experiment was recently proposed by Walid Mathlouthi, whereas the idea of concentrating the power of a broadband source into a specific band was suggested by Dr. Habib Fathallah. I proposed accomplishing the self-seeding with a *p*% reflective FBG while directly modulating the RSOA. Optimizing the reflectivity of the FBG to balance the output power versus the noise cleaning effect was also my contribution. Further, I analyzed the results, performed the FEC simulations, and analyzed the power budget for both local and remote self-seeding. Finally, I wrote the paper, which was in turn revised by Prof. Leslie A. Rusch. The discussions with Walid Mathlouthi and Dr. Habib Fathallah contributed to the success of this work.

Acknowledgement

First, I would like to express my special thanks to my supervisor, Prof. Leslie A. Rusch, for her academic advice, constant encouragement, guidance, and support during my graduate study at Laval University. I am really grateful to her for contributing many suggestions and improvements. I feel honored to have been given the opportunity to contribute to research under her supervision. Also, I would like to express my gratitude to Prof. Hossam M. H. Shalaby and Prof. El-Sayed A. El-Badawy for their support during my M.Sc. degree at Alexandria University, and for encouraging me to continue my research here at the *Centre d'Optique Photonique et Laser* (COPL).

My appreciation also goes to my colleagues in our lab, and more specifically in our research group, for the friendly academic atmosphere, the useful discussions and their encouragement. I am not going to mention names not to forget anyone, but let me thank especially my co-authors: Prof. David Plant from McGill University and his research group, Walid Mathlouthi, Dr. Habib Fathallah, and Prof. Sophie LaRochelle. I really feel so proud working hand in hand with them throughout my Ph.D.

I would also like to thank my friends in Québec, mostly Robert Raad, Wissem Mbarek, Adel Ziadi and the others, for their sense of humor. Besides, my friends in Egypt are always in memory; I thank them all for the nice time we spent together on Skype, for their loyal listening ears and their kind words that kept me motivated. In addition, I cannot forget Dr. Mohamed Khelifi and his family for their warm welcome, for offering me a family-like environment, and for being so generous and kind to me.

Finally, I would like to pay my humble respects to my parents. I am extremely grateful to them to have sacrificed themselves to give me the finest education and the best in everything. From my early childhood, they raised me to love learning, and supported me to develop my interest in science and engineering. I would also like to thank them for their continuous support, for their patience, encouragement and extra care. The deepest thanks from my heart go to my precious wife who really changed my life to the best in

everything, and even changed my research from *SAC-OCDMA* to *Dense SS-WDM*. I would like to express my gratitude and appreciation to her for her kind support, for her tremendous care, for being my source of inspiration, and even more… To my parents, my wife and to all my family: Words do not exist to describe your importance in my life.

Ziad A. Elsahn

February 2010

Table of Contents

List of Figures

List of Tables

Acronyms

APD	Avalanche Photodiode
APON	ATM PON
ASE	Amplified Spontaneous Emission
ASK	Amplitude Shift Keying
ATM	Asynchronous Transfer Mode
AWG	Arrayed Waveguide Grating
BBS	Broadband Source
BEDFA	Bidirectional EDFA
BER	Bit Error Rate
BERT	BER Tester
BIBD	Balanced Incomplete Block Design
BiDi	Bidirectional
BPF	Band Pass Filter
BPON	Broadband PON
BR	Balanced Receiver
CAPEX	Capital Expenses
CATV	Cable Television
CDMA	Code-Division Multiple-Access
CDR	Clock-and-Data Recovery
CID	Consecutive Identical Digits
CIP	Center for Integrated Photonics
CLK	Clock
CLS	Centralized Light Sources
CO	Central Office
CPA	Clock-and-Phase Alignment

CR	Conventional Receiver
CSF	Channel Select Filter
CW	Continuous Wave
CWDM	Coarse WDM
DBA	Dynamic Bandwidth Allocation
DC	Direct Current
DCF	Dispersion Compensation Fiber
DDF	Distribution Drop Fiber
DEC	Decoder
DES	Deserializer
DFB	Distributed Feed-Back
DOCSIS	Data-over-Cable Service Interface Specifications
DR	Degenerate Receiver
DSL	Digital Subscriber Line
EAM	Electro-Absorption Modulator
EDF	Erbium-Doped Fiber
EDFA	Erbium-Doped Fiber Amplifier
EFMA	Ethernet in the First Mile Alliance
ENC	Encoder
EPON	Ethernet PON
ER	Extinction Ratio
ESA	Electrical Spectrum Analyzer
FBG	Fiber Bragg Grating
FEC	Forward-Error Correction
FFH	Fast-Frequency Hop
FP	Fabry-Perot
FPGA	Field Programmable Gate Array

FSAN	Full Service Access Network
FSK	Frequency Shift Keying
FTTH	Fiber-to-the-Home
FTTP	Fiber-to-the-Premise
FTTx	Fiber-to-the-x
GFP	Generic Framing Procedure
GPON	Gigabit PON
HD	High Definition
HDTV	HD Television
HFC	Hybrid Fiber-Coaxial
HPF	High Pass Filter
IC	Integrated Circuit
IEEE	Institute of Electrical and Electronic Engineering
IP	Internet Protocol
ITU	International Telecommunication Union
LD	Laser Diode
LED	Light Emitting Diode
LPF	Low-Pass Filter
LS	Local Sources
MAC	Media Access Control
MAI	Multiple-Access Interference
MQC	Modified Quadratic Congruence
N/A	Not Applicable
NF	Noise Figure
NRZ	Non-Return-to-Zero

NTT	Nippon Telegraph and Telephone
OCDM	Optical Code-Division Multiplexing
OCDMA	Optical CDMA
ODL	Optical Delay Line
ODN	Optical Distribution Network
OLT	Optical Line Terminal
ONU	Optical Network Unit
OSNR	Optical SNR
P2MP	Point-to-Multipoint
P2P	Point-to-Point
PD	Photodiode
PLL	Phase Locked Loop
PLM	Power Leveling Mechanism
PLR	Packet Loss Ratio
PMD	Physical Medium-Dependent
PON	Passive Optical Network
PRBS	Pseudo-Random Binary Sequence
PSD	Power Spectral Density
QoS	Quality of Service
R^3T	Round Robin Receiver/Transmitter
RF	Radio Frequency
RIN	Relative Intensity Noise
RN	Remote Node
RS	Reed-Solomon
RSOA	Reflective SOA
Rx	Receiver
RZ	Return-to-Zero

SAC	Spectral Amplitude Coding
SCM	Sub-Carrier Multiplexing
SMF	Single Mode Fiber
SNR	Signal-to-Noise Ratio
SOA	Semiconductor Optical Amplifier
SONET	Synchronous Optical Network
SS-WDM	Spectrum Sliced WDM
TDM	Time-Division Multiplexing
TDMA	Time-Division Multiple-Access
TV	Television
Tx	Transmitter
UI	Unit Interval
US	United States
USA	United States of America
VOA	Variable Optical Attenuator
WDM	Wavelength-Division Multiplexing
WDMA	Wavelength-Division Multiple-Access

Chapter 1

Introduction

1.1. Motivation

Fiber-to-the-home (FTTH) is the end game for many service providers [1]-[5]. As more and more IP services are transported over broadband access networks, it is important to identify the technologies and architectures that will enable cost-effective transport of this traffic all the way to the home via an access network. As compared to other broadband access technologies such as digital subscriber line (DSL), and cable/modem, passive optical network (PON) technology seems to be the best solution to alleviate the bandwidth bottleneck in the access network [1], [6]-[8]. From a historical perspective, the

first bandwidth breakthrough in the access network was the arrival of DSL and cable based solutions (Figure 1.1). They provided nearly a 1000-fold increase in data rates over traditional 'dial-up' modems. With the arrival of FTTH access solutions, another 1000-fold increase in data rates over DSL was achieved.

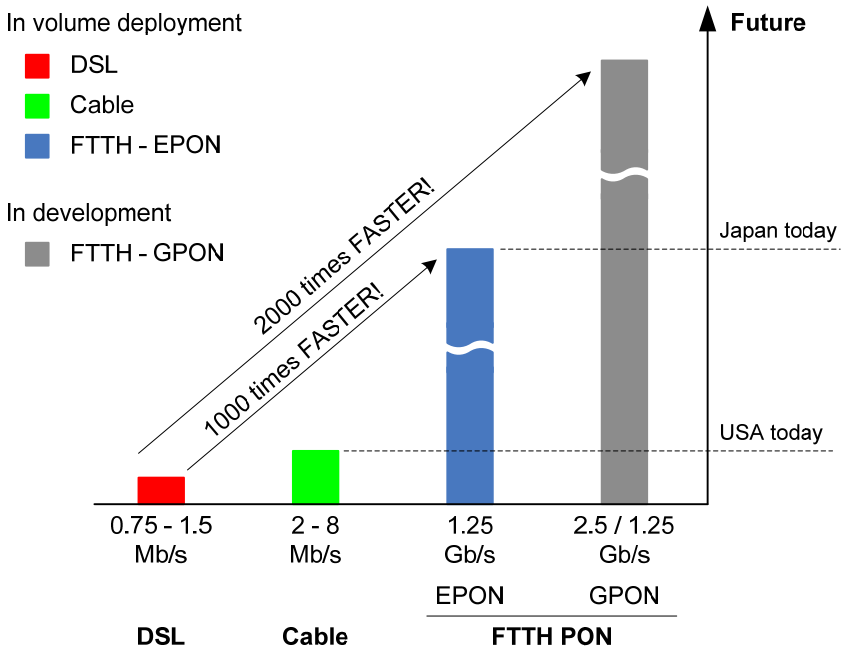

Figure 1.1. Access network technologies: Market and technology overview [7], (EPON: Ethernet PON, GPON: gigabit PON).

Although several PON standards already exist with gigabit capabilities, the actual user bit rate is less than 100 Mb/s as users share the entire bandwidth using time-division multiple-access (TDMA). A typical gigabit symmetric PON for example, provides only 40 Mb/s for 32 customers and up to 80 Mb/s for 16 users.

From the other side, advances in cable networks allow similar bit rates to be supported [9]. Using higher order modulation formats and forward error correcting (FEC) codes, the existing DOCSIS[1] 2.0 standard provides 40 Mb/s for downstream and 30 Mb/s for upstream. The new specifications, referred as DOCSIS 3.0, describe data rates of 160 Mb/s and 120 Mb/s for the downstream and upstream, respectively [10]. However,

[1] Data-over-Cable Service Interface Specifications, http://www.cablemodem.com

the high attenuation in coaxial cables, compared to optical fibers, has limited their maximum reach to only a few kilometers. In practical systems, an optical fiber runs from the central office to the distribution node, and then the signals are dropped to the users through coaxial cables. Such systems are known as hybrid fiber-coaxial (HFC) networks [11].

It is clear that because of the limited bandwidth of a coaxial cable, the complexity of the cable systems is expected to be higher than that of PONs. However, when exploiting an existing cable-based infrastructure, the cost is not significantly high. On the other hand for green field deployment (*i.e.*, new housing developments) of access networks, operators are encouraged to invest on a PON infrastructure.

Incorporating wavelength-division multiplexing (WDM) offers a good solution to increase the capacity of standard PONs, by assigning different wavelengths to different users [12]-[14]. Although WDM technology is mature for backbone networks, its price is still considered high for access networks. Therefore, there is still a need to find low cost solutions for WDM in FTTH access networks.

An alternative to WDM is the use of optical code-division multiple-access (OCDMA) to upgrade existing PONs. OCDMA is receiving considerable attention because it combines the large bandwidth of the fiber medium with the flexibility of the code-division multiple-access (CDMA) technique to achieve high-speed connectivity [15]. As there are no standards or commercial systems for OCDMA networks, the question of the best implementation, and indeed the suitability of OCDMA for PONs remains open.

1.2. Objectives and Major Contributions

While applications drive the development for faster and more efficient network technology, network technology also opens up the opportunity for the development of new applications. Applications that were not feasible or even imaginable a few years ago are now widely used. This increasing demand makes imperative the use of some new

technology that is not only capable of meeting today's demands, but is also flexible to accommodate tomorrow's growth.

In this thesis we focus on simple and inexpensive solutions for upgrading existing PONs without changing the outside plant and without altering the legacy PON users. The passive splitter-based PON infrastructure is still exploited, and the upgrades are made on a per subscriber basis allowing a gradual rollout of high bit rate clients. The contributions of this work are mainly proposing two new solutions for upgrading existing PONs using OCDMA and WDM, based on low cost incoherent sources.

Our first approach is to use spectral amplitude coded (SAC)-OCDMA for next generation PONs [16], [17]. We examine the relative merits (cost and performance) of both local sources and centralized light sources architectures. We experimentally demonstrate the uplink of a 7×622 Mb/s SAC-OCDMA PON with burst-mode operation. We analyze the power budget and study the amplification requirements for both architectures. The selection of appropriate light sources plays an important role in the power budget, and can help increase the link margin. Despite the extra splitting and propagation losses in centralized light sources architectures, we report error free transmission (over a 20 km link) for a fully loaded system when using FEC codes.

The other alternative we propose, is to use dense spectrum-sliced (SS)-WDM to upgrade existing PONs [18]. A reflective semiconductor optical amplifier (RSOA) is used as a transmitter. The RSOA is directly modulated and is self-seeded using a reflective fiber Bragg grating (FBG). The reflectivity is optimized to maximize the output power and for optimal noise cleaning. At the receiver side, a recently proposed balanced receiver is used to preserve the noise cleaning effect [19]. We experimentally demonstrate a 1.25 Gb/s transmission, where error free transmission is achieved over a 20 km feeder. We further investigate the possibility of colorless optical network unit (ONU) operation by placing the FBG at the remote node. The power budget and the spectral efficiency issues are also addressed, up to 32 SS-WDM users can be easily supported over the existing PON infrastructure. Through simulations we show that the capacity can be increased to 128 users when a Reed-Solomon RS(255,239) FEC is used.

1.3. Thesis Organization

Chapter 1 summarizes the motivation, the objectives and the main contributions of this research. Chapter 2 then presents an overview of PON standards, focusing on the physical layer gigabit capable PONs. Various PON standards are outlined and a technical comparison between Ethernet PON (EPON) and Gigabit PON (GPON) is presented. Further, the requirements and needs for future PONs are outlined.

In Chapter 3 we focus on next generation gigabit PONs. We report recently proposed OCDMA and WDM solutions to increase the per user capacity of existing PONs. We discuss their architectural considerations as well as the migration path towards future FTTH access networks. The basics of semiconductor optical amplifiers (SOAs), their noise cleaning capability and their benefits as key enablers in PONs, are also addressed. This chapter lays the groundwork for our contributions presented in the following chapters.

Our proposed physical architectures for the next generation SAC-OCDMA PONs are described in Chapter 4. Both local sources and centralized light source approaches are considered over single-feeder and two-feeder topologies. The operation and the functionalities of a burst-mode receiver (developed at McGill University) at the central office are also verified in our OCDMA system setup. The experimental results and the impact of the PON size on local sources versus centralized light sources PON architectures are presented as well.

Our examination of the performance of a self-seeded RSOA transmitter for SS-WDM PONs is reported in Chapter 5. The transmitter architecture and the bit error rate (BER) performance for different network configurations are presented. The wavelength coverage of the transmitter over the entire C-band is studied. We discuss the noise cleaning effect, the post-filtering effect, and we explain the wavelength dependence of the performance. We benefit from our results in this chapter, to propose (in the following chapter) a novel self-seeded RSOA transmitter that provides simultaneously noise cleaning and high output power.

In Chapter 6 we present our innovative method to upgrade existing PONs using dense SS-WDM over the legacy infrastructure. We outline our FBG-based self-seeded RSOA transmitter, as well as the challenges in combining noise cleaning to self-seeding. We further discuss the architectural aspects and the migration path from time-division multiplexing (TDM) to dense SS-WDM. We present experimental results of transmitter optimization and BER measurements. We further study the possibility of colorless ONU operation through remote self-seeding. The power budget and the spectral efficiency issues are also addressed. Moreover, we run FEC simulations (based on our measurements without FEC) to estimate the coding gain as well as the maximum network capacity that can be achieved.

Finally, the thesis is concluded in Chapter 7, where we also give the direction for future work and other research opportunities.

Chapter 2

Passive Optical Networks for FTTH Access Networks

2.1. Introduction

The increasing need for advanced telecommunication services presents an excellent opportunity for service providers. A single operator offering basic voice, data, and video services at a reasonable price is very likely to have a high penetration rate. Delivering advanced services in addition to the traditional ones attracts subscribers even more. Additionally, if the bandwidth capacity of the network is scalable, then the operator will be able to maintain those customers and grow revenue in the future, as new bandwidth-hungry applications are developed.

Fiber-to-the-Home (FTTH) has long been recognized as a technology that provides future proof bandwidth [1]-[8], but has generally been too expensive to implement on a wide scale. However, reductions in the cost of electro-optic components and improvements in the handling of fiber optics now make FTTH a cost effective solution in many situations. The transition to FTTH in the access network is also a benefit for both consumers and service providers because it opens up the near limitless capacity of the core long-haul network to the local user.

Passive optical networks (PONs) are identified as an economic and future safe solution to alleviate the bandwidth bottleneck in the access network [1], [2]. As the name implies, passive optical networks are typically passive, in the sense that they do not have active components for data transport.

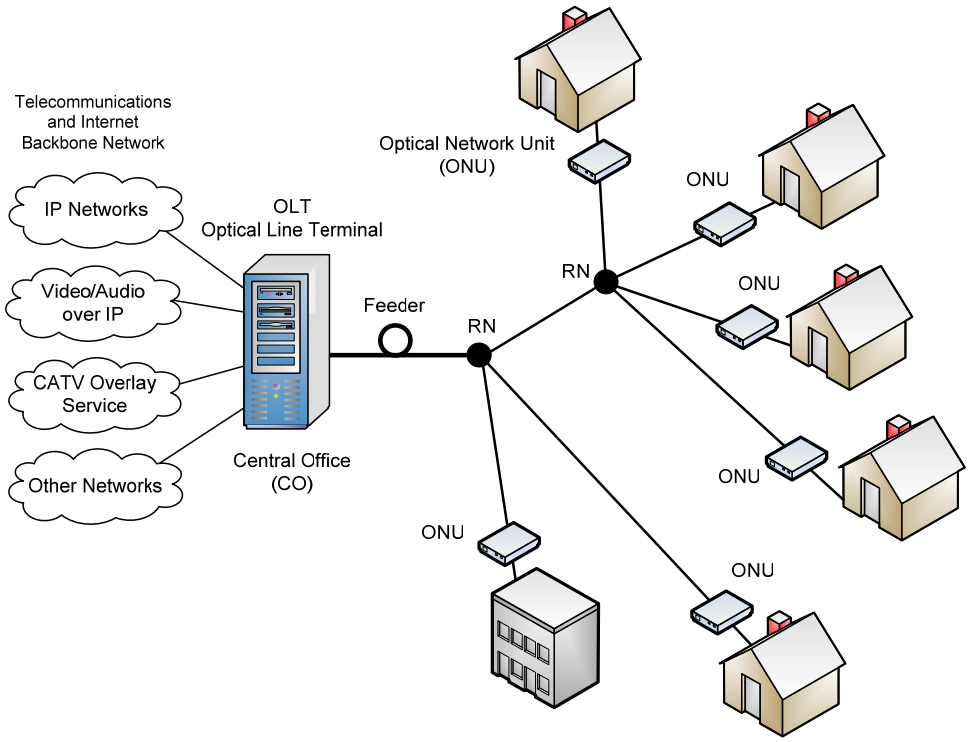

Figure 2.1. Basic architecture of FTTH access network (CATV: cable television, RN: remote node).

Typically, a PON has a physical tree topology with the central office (CO) located at the root and the subscribers connected to the leaf nodes of the tree, as shown in Figure 2.1. At the root of the tree is an optical line terminal (OLT), which is the service provider

equipment. Multiple optical network units (ONUs) are connected to the OLT through a passive optical coupler, and may be at different distances.

Each ONU can serve a single or multiple subscribers. The ONU buffers data received from its attached subscriber(s) and may use priority queues, for different traffic classes. Due to the directional properties of the optical splitter/combiner, the OLT is able to broadcast data to all ONUs in the downstream direction. In the upstream direction, however, ONUs cannot communicate directly with one another. Instead, each ONU is able to send data only to the OLT. Thus, in the downstream direction the PON may be considered as a point-to-multipoint (P2MP) network, whereas for the upstream direction it may be viewed as a point-to-point (P2P) network.

While this thesis is concerned with next generation PONs, in this chapter we review the standards environment for today's first generation PONs. Understanding the current state of PON deployment will provide the context for development of the next generation requirements and constraints.

2.2. Existing PON Standards

The existing PON standards are the results of two different groups of network providers and equipment vendors; namely, the Full Service Access Network (FSAN)[1] and the Ethernet in the First Mile Alliance (EFMA)[2]. The standards represent the different views and attitudes of these groups towards the problem and the possible future of the telecommunication market.

Although, in this thesis focus is oriented towards gigabit access networks, we will rapidly highlight the other flavors of PONs in this section [20], [21]. Selected characteristics of the different PON standards are summarized in Table 2.1. Asynchronous Transfer Mode (ATM) PON (APON) was initiated in 1995 by the FSAN group and standardized as ITU-T G.983. APON was the first PON based technology developed for FTTH

[1] http://www.fsanweb.org
[2] http://www.efmaalliance.org

Table 2.1. Selected characteristics of different versions of PONs.

	APON/BPON	**EPON**	**GPON**
Standard	ITU-T G.983	IEEE 802.3ah	ITU-T G.984
Data Packet Cell Size	53 bytes (48 payload and 5 overhead)	1518 bytes	Variable size from 53 bytes up to 1518
Data Rates	1.25 Gb/s downstream 622 Mb/s upstream	Up to 1.25 Gb/s	Downstream configurable from 1.25 Gb/s to 2.5 Gb/s Upstream configurable in 155 Mb/s, 622 Mb/s, 1.25 Gb/s, or 2.5 Gb/s
Downstream Wavelength	1480 nm – 1500 nm	1500 nm	1480 nm – 1500 nm
Upstream Wavelength	1260 nm – 1360 nm	1310 nm	1260 nm – 1360 nm
Traffic Modes	ATM	Ethernet	ATM, Ethernet, TDM
Maximum PON Splits	32	16	64 or even 128
Bit Error Rate (BER)	-	10^{-12}	10^{-10}
Efficiency	72%	49%	94%

deployment as most of the legacy network infrastructure was ATM based. Since the services offered by this architecture include video distribution, leased line services, and Ethernet access, and to express the broadband capability of PON systems, APON was renamed as broadband PON (BPON). It was standardized by ITU-T recommendations G.983.1, G.983.2, G.983.3.

The progress in the technology, the need for larger bandwidths and the complexity of ATM forced the FSAN group to look for better technology. Gigabit PON (GPON) standardization work was initiated by FSAN in the year 2001 for designing networks over 1 Gb/s and up to 2.5 Gb/s. GPON enables transport of multiple services in their native format, specifically TDM and data. In order to enable easy transition from BPON to GPON, many functions of BPON are reused for GPON. In January 2003, the GPON standards were ratified by ITU-T and are known as ITU-T recommendations G.984.1, G.984.2 and G.984.3. The GPONs use the Generic Framing Procedure (GFP) protocol to provide support for both voice and data oriented services.

Noticing that the majority of traffic in the network is data oriented and that efficient mechanisms enabling support for real time services were in place, the EFMA decided that the sophisticated functionality of the APON/BPON and GPON protocols was no longer needed. Instead, as the Ethernet protocol had became widespread and had a dominant role in the data oriented local and metropolitan networks, the EFMA decided to promote its functionality in PONs. The final version of the new protocol was accepted and released as IEEE 802.3ah in September 2004. The main goal was to achieve a full compatibility with other Ethernet based networks. Hence, the functionality of Ethernet's Media Access Control (MAC) layer is maintained and extensions are provided to encompass the features of PONs. The solution is simple and straightforward, and allows legacy equipment and technologies to be reused. EPON is largely a vendor-driven standard and it is fundamentally similar to APON, but transports Ethernet frames/packets instead of ATM cells.

2.2.1. Physical Medium Dependent (PMD) Layer

The PMD layer characteristics for GPON and EPON are quite similar [20]-[25]. We will state here the major differences other than the ones listed in Table 2.1:

- GPON specifies a lower dynamic range for the OLT receiver, compared to EPON. This is due to the inclusion of a power leveling mechanism (PLM) in the GPON standard, through which the OLT can request ONUs, for whom the received power exceeds specific thresholds, to decrease the transmitter power.
- EPONs can support up to 20 km of logical reach. GPONs can support up to 60 km, with 20 km maximum differential logical reach between the farthest and the nearest subscribers.
- EPON uses 8B/10B encoding and the large burst overhead results in less complex OLT receiver.

GPONs can be classified into three different classes, namely, Class A, B, and C depending on the attenuation losses through the optical distribution network (ODN). An attenuation range of 5-20 dB, 10-25 dB, and 15-35 dB, for Class A, Class B, and Class C,

respectively is tolerated [21]. In this section we quickly review the main parameters of the PMD layer of a class B GPON (symmetrical link at 1.25 Gb/s), showing the major challenges in the design of upstream burst mode receivers at the OLT side.

2.2.1.1. Downstream and Upstream Traffic

In a symmetrical GPON a continuous downlink in the wavelength band of 1480-1500 nm carries 1.25 Gb/s time-division-multiplexed (TDM) data from the OLT towards multiple ONUs [2]. A burst-mode link in the 1310 nm window collects all ONUs upstream traffic toward the OLT as variable-length packets at the same rate, in a time-division multiple-access (TDMA) scheme. This can be viewed in Figure 2.2. While waiting for its opportunity, an ONU buffers all incoming data. The contents of the queues are transmitted in a single burst using the whole available bandwidth of the channel upon the start of an allocated transmission window.

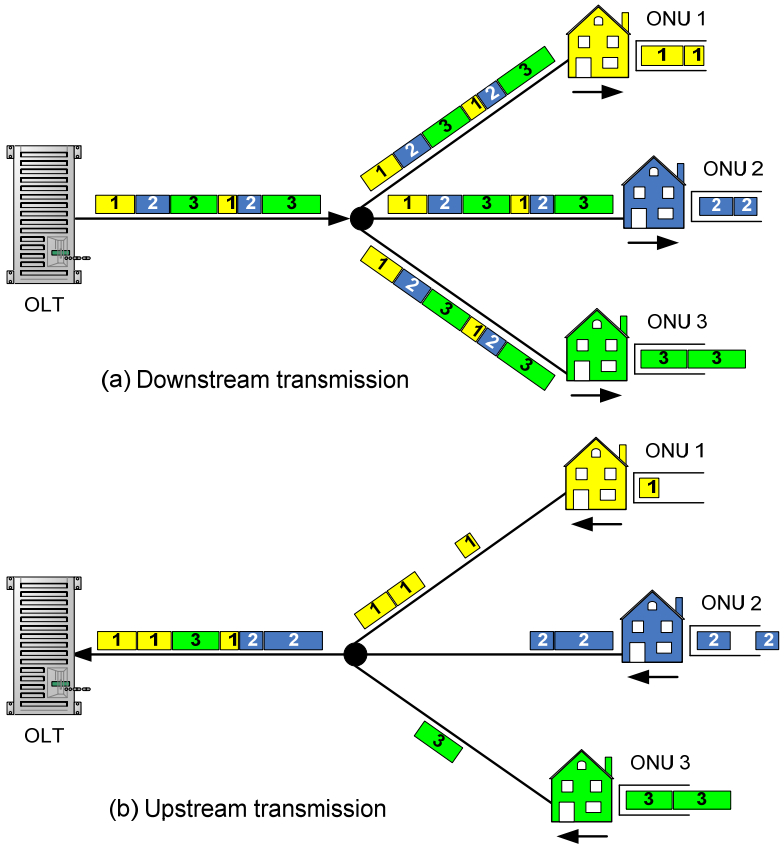

Figure 2.2. Traffic flow in PONs: (a) downstream, (b) upstream.

Table 2.2. Key PMD parameters of a 1.25 Gb/s uplink of a class B GPON.

Item	Value
Extinction Ratio	> 10 dB
Minimum Sensitivity	-28 dBm at BER = 10^{-10}
Receiver Dynamic Range	21 dB
Receiver Dynamic Range with PLM	15 dB
Consecutive Identical Digits	72 bits (57.6 ns)
Overhead length	4 Bytes

Normally, the uplink is more difficult to design due to its bursty nature. The OLT receives packets from all active subscribers, with varying signal level and phase from packet to packet. The average signal level may vary 21 dB in the worst case from packet to packet (Class B). These packets are of variable length and are interleaved with a guard time of 4 B at 1.25 Gb/s (or 25.6 ns) as specified in G.984.2. Other important PMD specifications of such networks are listed in Table 2.2.

2.2.1.2. Burst-Mode Receivers

In [21], X. Qiu *et al.* developed a new upstream GPON OLT burst-mode receiver. Performance measurements on the new burst-mode upstream PMD modules complied with GPON uplink simulations. A receiver sensitivity of -32.8 dBm at a bit error rate (BER) of 10^{-10} was measured, combined with a dynamic range of 23 dB at a fixed avalanche photodiode (APD) gain of 6. Full compliance was achieved with the recently approved ITU-T Recommendation G.984.2 supporting an innovative overall PLM.

The main challenges in the design of this receiver can be summarized in these points:

- Optimizing the APD factor for achieving both high sensitivity and wide dynamic range is not straightforward. The fast succession of upstream bursts do not allow for a change of the APD gain between bursts.

- The receiver must provide fast but accurate threshold settings on individual incoming packets to perform dynamic level detection and amplitude recovery.
- The receiver must quickly extract the decision threshold within a preamble length of a few bytes at the beginning of each packet.
- Due to the short guard time, the burst-mode receiver needs an active reset to erase the threshold of a preceding packet, [26].
- As small amounts of optical power may be present during the guard time, it is difficult to distinguish between transmitted 0's and the dark level during the guard time. Therefore, the receiver cannot know precisely when a packet ends and an external reset signal is necessary to signal the end of a packet.
- A power level measurement circuit must be integrated, which allows the OLT to tell a specific ONU to either increase or decrease its launched power.

Figure 2.3 shows a typical burst-mode signal, which consists of a quick succession of packets [26].

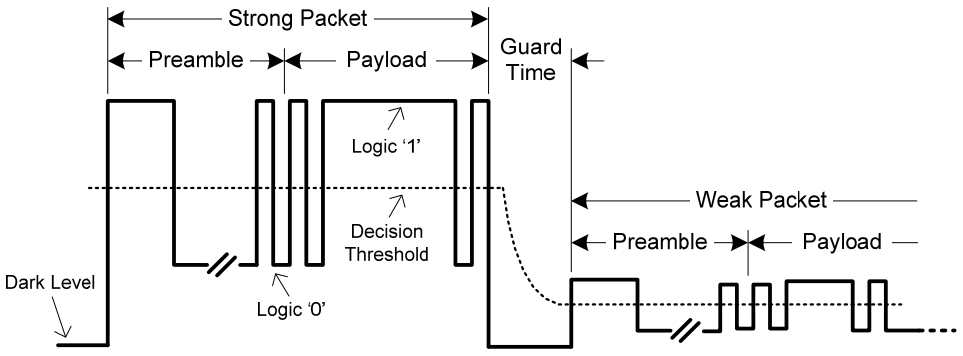

Figure 2.3. Example of burst-mode receiver input signal [26].

2.2.1.3. Operating Parameters Used to Examine Next Generation PONs

The main factors influencing the performance of PONs are the devices and materials used to build the network. The transmitter power and receiver sensitivity are two parameters that define the possible reach of the access network. In Table 2.3 typical parameters of commercially available burst-mode transceivers that support up to 1.25 Gb/s are shown.

Table 2.3. Burst-mode transceiver comparison for 1.25 Gb/s.

Manufacturer/Model	Transmitter Power min	Transmitter Power max	Receiver Sensitivity
Infineon Technologies AG[1] V23870-G5131-x610	-1 dBm	4 dBm	-24 dBm
LuminentOIC[2] SFFB-34-1250-BP-SCA-T	-2 dBm	3 dBm	-24 dBm
Fiberxon[3] FTM-9712P-F20	2 dBm	7 dBm	-30 dBm

In our proposals for next generation FTTH networks, we will try to respect GPON standards power budgets. In our experiments, we will always exploit the existing PON infrastructure, assuming a typical 20 km feeder and passive splitters at the remote node (RN). Via the available power budget, we will be able to calculate the maximum PON reach and/or the PON capacity.

We will concentrate on the design of the more challenging uplink, and the ONU transmitter. We will consider a user bit rate of 622 Mb/s and 1.25 Gb/s for our proposed SAC-OCDMA and dense SS-WDM solutions, respectively. These bit rates comply with the GPON uplink line rates. In Chapter 4, we will examine the performance of our proposed SAC-OCDMA PON in burst-mode operation. In Chapter 6 we will study the performance of our proposed dense SS-WDM PON in continuous mode, but over the existing PON infrastructure.

2.2.2. Gigabit PON Market Overview

With the market for high-speed broadband access continuing to accelerate, the future for gigabit PON is bright [1], [7], [8], [27], and [28]. According to the FTTH council, the number of the worldwide FTTH subscribers reached more than 28 million by the end of June 2008. This represents more than 23% increase in less than six months. The Asian market accounted for 80% of the total FTTx subscribers, with Japan still leading the way.

[1] http://www.infineon.com
[2] http://www.luminentoic.com
[3] http://www.fiberxon.com

However, FTTH customer growth rates in Europe (32% growth) and in the United States (38%) were higher than that in Asia[1]. As a result, the market for PON hardware is forecast to grow sharply. Worldwide OLT and ONU PON equipment revenue reached more than $2.2 billion in 2008. PON manufacturer revenue is forecast to grow at a rapid compound annual growth rate of 23% between 2008 and 2013, as the shift from copper to fiber based broadband access drives growth in this market around the world[2].

In Japan the transition from DSL to FTTH has begun very early. NTT the major carrier in Japan began deploying EPON based FTTH in 2003. For the first time, in the first quarter of 2005, the number of new FTTH subscribers was greater than that of new DSL subscribers according to the Japanese Ministry of Internal Affairs and Communications. With 13.1 and 6 million subscribers, respectively, Japan and South Korea were home to the largest number of ultra-high-speed Internet users in the world in 2008. There was a sharp rise in FTTx subscribers in South Korea (800,000 new customers) and in Japan (close to 1.8 million) in the first half of 2008. Despite high growth rates and other impressive figures, Asia is slowly losing ground to Europe and North America. On the operator front, NTT still had the largest subscriber base worldwide, with more than 9.5 million FTTx customers.

In North America there were about 150,000 Fiber-to-the-Premise (FTTP) subscribers and a million homes passed by late 2004. These are mostly deployments by the small operators. However, carriers such as Verizon, SBC and others, are looking to GPON to advance their FTTH rollout efforts. It is expected that nearly 78 million US consumers will have broadband access by 2010.

In Europe there is a considerable early FTTP deployment (about 400,000 FTTP subscribers in 2003). In 2004 Sweden had the highest FTTx penetration worldwide. Growth had also been particularly substantial in Belgium, Switzerland, and Germany. In 2008 six countries accounted for 83% of the total number of subscribers in Europe: Sweden, Italy, Norway, France, Denmark, and the Netherlands.

---

[1] R. Montagne, “The global FTTH/B panorama shifts,” February 2009 (http://lw.pennnet.com)

[2] Infonetics, “GPON market share race heats up, Motorola challenging Alcatel-Lucent,” March 2009 (http://lw.pennnet.com)

2.3. Requirements and Needs for Future PONs

We are entering a new high-definition-(HD)-video-centric world that will enable new applications and services including HDTV, video on demand, video conferencing, high-quality interactive video gaming, and others [29]-[31]. Video-centric services demand not only a high speed connection but also a high quality of service (QoS). In addition, there has been a trend in traffic patterns to shift from being bursty and highly asymmetric to becoming steadier and more symmetric. This is being driven by the increase in peer-to-peer applications and the constant streaming data rates required for video signals. To satisfy these future demands, it is expected that dedicated and symmetric data rates of 100 Mb/s and greater per subscriber will be required [5]. This places challenges on the development of future access networks since any long-term infrastructure should be capable of supporting large symmetric data rates with high QoS.

When building a PON infrastructure, analysis by Corning has shown that the installation for the outside plant costs about 60% with the remaining 40% required for the service equipment [5]. Therefore the lifetime of the outside passive plant should be greater than 25 years to justify the installation costs and maximize savings in operational expenses. The costs and disruptions associated with installing additional fiber plant should be kept to a minimum. Keeping these constraints in mind, we can estimate possible evolution paths for existing and future PONs. Later in this thesis we present two newly proposed future-proof solutions to smoothly upgrade the existing TDM PONs using the legacy PON infrastructure.

Lowering the per-subscriber cost of FTTH systems is another key issue that should be considered for next generation PONs [8]. It has a dollar-for-dollar impact on the cost of the overall system and helps the technology penetrating more into the market. This is driven by the technological advances in chip integration solutions, and by volume manufacturing [32], [33]. Not only advances in optical transceivers are needed, but also advances in cable management technology, outside plant cabinet technology and fiber performance technology are required [2].

2.3.1. Long Reach PONs

In practice most commercial GPON systems conform to the class B+ specification that allows a maximum optical loss budget of 28 dB; this is often used to deploy a split size of 32 and reach of up to 20 km. Recently, research has focused on extending the reach of GPON via mid-span optical amplifiers or transponders [34]. This concept has recently been standardized in ITU-T Recommendation G.984.6.

Operators value greatly the passive nature of the access network enabled by the PON architecture, and it is not the intention of PON reach extension to move away from this. Nevertheless, having the option of an active mid-span reach extender can provide several benefits mainly reducing the number of central offices [35]. Clearly, there are significant capital and operational costs associated with building a central office. Moreover, deploying a full OLT in a street cabinet is not recommended. An attractive alternative could therefore be a simple mid-span PON extender box deployed in a street cabinet (or underground footway box). To offer benefits over the street-based OLT approach, the PON extender should be compact, low-power, and cost-effective and require minimal configuration and management.

Semiconductor optical amplifiers (SOAs) are attractive candidates for GPON reach extension because of their high gain, low noise figure (NF), low polarization dependent loss, and fast gain dynamics allowing them to operate in burst-mode for the upstream. Moreover, they can be designed to provide gain in the wavelength bands used by GPON. Other attractive advantages of SOAs for this application include their small size, high reliability and low power consumption. Recently, an all-optical GPON reach extender prototype has been developed by a team at Motorola [34]. The prototype was tested in the field and is now ready for commercialization and deployment extending the physical reach of existing GPONs to 60 km and supporting 128 split. Research efforts are trying to push these numbers to 100 km and 512 split for 10 Gb/s next generation PONs. We will not be examining range extension, but we will examine the fundamental power budgets in our systems to determine either their maximum reach or capacity.

2.3.2. Green PONs

Currently, energy consumption is becoming an environmental and therefore social and political issue. In particular, for network operators it is also of an economical concern, since the energy consumption contributes to operational expenditures. The access network part is a major energy consumer in communication networks, since it usually contains a huge number of distributed active network elements. Unlike DSL, cable networks and other access technologies, FTTH based PONs are able to deliver high access bit rates in a more energy efficient way due to their passive nature. However, the need for higher bit rates for next generation PONs will linearly increase the energy and power consumption [36]. Therefore the need for new low power consumption, high speed equipment is necessary. The energy consumption of FTTH access networks has been studied extensively in [37], [38]. Guidelines for choosing the suitable FTTH strategy concerning energy and power consumption issues prior to the network planning and actual deployment are presented. Although we will not be studying the power and energy consumption of our proposed PONs, it is good to mention that PONs are energy efficient and preserve the green nature of the environment compared to other access technologies.

2.3.3. Architectural Considerations for our Proposed Future PONs

Concerning our proposed solutions for next generation PONs, we consider exploiting the existing outside plant for gradual upgrades from TDM to SAC-OCDMA or to dense SS-WDM as will be discussed in Chapter 4 and Chapter 6, respectively. We target low cost solutions by using incoherent light sources instead of laser sources. In order to support future bandwidth-hungry applications, we demonstrate user bit rates of 622 Mb/s and 1.25 Gb/s for our OCDMA and SS-WDM PONs, respectively. Furthermore, our solutions exploit the 1550 nm band (reserved for video distribution) and therefore can co-exist with the legacy PON users, creating a smooth migration path from TDM to future PONs without altering the existing systems. Moreover, we consider our next generation FTTH networks to be attractive as they provide pay-as-you-grow updates.

The architectural aspects of our proposed PONs, the power budget analysis, the spectral efficiency and the bandwidth usage issues, as well as the maximum PON reach/capacity will be examined later through Chapter 4 and Chapter 6.

2.4. Summary and Conclusion

Having briefly discussed the standards for existing FTTH access networks, we have been motivated by the urgent need for upgrading the legacy PONs to meet for future needs and bandwidth demands. In this chapter, we have also outlined the basic needs and general requirements for future PONs, showing the needs for our proposed PONs. We next review in Chapter 3 recent research in next generation PONs, focusing on OCDMA and WDM solutions. In the following chapters we present our contributions for gradually upgrading legacy PONs to SAC-OCDMA or to dense SS-WDM PONs.

Chapter 3

Next Generation Passive Optical Networks

3.1. Introduction

Bandwidth demand is expected to grow rapidly as high-quality multimedia applications begin to be used in daily life. A typical service configuration for the home includes several high-quality video streams for broadcast and video on demand sessions, a number of multimedia communication sessions, high-bandwidth peer-to-peer sessions, online gaming, and web surfing. The bandwidth required for this service set can range from tens of megabits per second to 100 Mb/s and beyond depending on the quality requirements for multimedia streams. To provide users with a multimedia experience comparable or

superior to the current TV experience, it is envisioned that Internet-based multimedia streaming service will support HDTV quality for media broadcasting, and standard TV quality for multimedia communication sessions. Considering that the typical HD media stream requires up to 20 Mb/s, access network bandwidths of 50-100 Mb/s are considered minimal to accommodate future broadband Internet traffic [1].

To provide the required bandwidth as a universal service, service providers need to upgrade their access network. In other words, they need to migrate from TDM to other multiplexing techniques such as wavelength-division multiplexing (WDM), sub-carrier multiplexing (SCM) and optical code-division multiplexing (OCDM). Sharing the PON architecture using wavelength-division multiple-access (WDMA) is a highly efficient method [12]-[14]. In this scheme, each subscriber is virtually point-to-point connected through a dedicated wavelength to the OLT. While several schemes of WDM PONs have been proposed, the cost of the system has been of main concern. Further, the wavelength management of the ONU transmitters is a significant burden for network operators. Wavelength-independent ONU transmitters are required if WDM is to be used in the access network [39].

Another alternative for upgrading existing PONs is to use SCM by assigning a different radio frequency (RF) channel for each subscriber [5]. The TDM PON infrastructure and the passive splitters already installed at the RN would not need to be upgraded. In contrast, deploying WDM requires that these couplers be replaced by arrayed waveguide gratings (AWGs). Another possibility for future PONs is to use OCDMA to increase the capacity of the existing PONs, which would not require a RN upgrade. In such systems, users simultaneously share the same bandwidth using orthogonal codes. Although this solution is still under research and in its infancy compared to WDM, it offers several advantages and can be interesting for future PONs, in the long term. Hybrid solutions combining different multiple-access techniques have also been proposed for PONs. For example using TDM over WDM allows several users to share the same wavelength on a TDMA basis [14], [40]-[42]. Combining SCM with WDM is another option for future PONs [43], [44]. Using OCDMA over WDM for gigabit symmetric PONs was also proposed for next generation PONs [45].

In this chapter we present some of the recent research and the state of the art for future PONs. We focus on both OCDMA and WDM solutions for gigabit capable PONs. In the case of WDM, we are particularly interested in spectrum-sliced WDM (SS-WDM) systems as a low cost solution for PON upgrade.

We start by introducing semiconductor optical amplifiers as key enablers for next generation FTTH access networks. Focus is oriented towards the physical layer; however, we highlight the important aspects of the MAC layer and discuss the possible upgrades to be considered for next generation PONs. We next review various proposals for OCDM, WDM and SS-WDM, often exploiting SOAs. Finally, we end the chapter with a summary and conclusion to anticipate what we propose in the following chapters and to justify our choice of the different technologies for OCDMA and WDM.

3.2. Semiconductor Optical Amplifier as a Key Component

Due to advances in optical semiconductor fabrication techniques, device design and packaging technologies, the semiconductor optical amplifier (SOA) and the reflective SOA (RSOA) are showing great promise for use in evolving optical communication networks. They can be used as a general gain element, but also have many other functional applications including modulation, switching, and wavelength conversion. Semiconductor amplifiers have been the subject of much research, especially in WDM PONs [39]-[44], [46]-[48]. Their major advantages include:

- low fabrication cost, small size, easy integration, wide bandwidth, fast response, and wavelength transparency;
- SOAs used at the ONU side can accomplish both modulation and amplification functions;
- intensity noise can be suppressed by the gain compression effect of the gain-saturated SOA (useful in various next generation PON scenarios);
- in SCM schemes, the unnecessary residual downlink at each ONU is suppressed by the high pass filter (HPF) effect of RSOA; and

- the modulation speed of commercially available devices can reach up to 5 Gb/s in wide wavelength bands in the range of 50-100 nm [39].

3.2.1. SOA and Reflective SOA Basics

Semiconductor optical amplifiers are essentially laser diodes, without end mirrors, which have fiber attached to both ends [49]. They amplify any optical signal that comes from either fiber and transmit an amplified version of the signal out of the second fiber. A schematic diagram of an SOA is shown in Figure 3.1 as well as commercial SOAs and RSOAs in different packages. The device is driven by an electrical current. The active region in the device imparts gain, via stimulated emission, to an input signal. The output signal is accompanied by noise. This additive noise, also called amplified spontaneous emission (ASE), is produced by the amplification process.

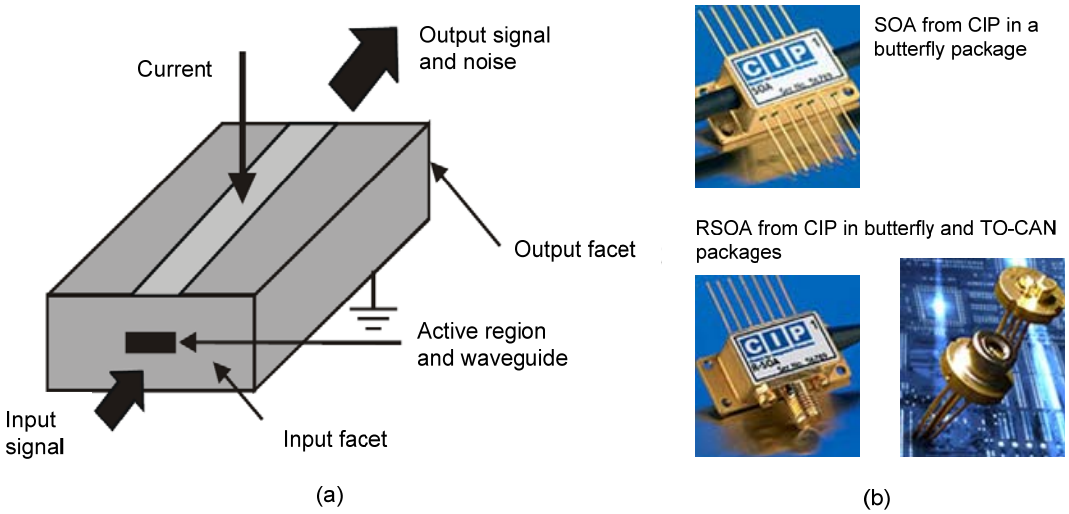

Figure 3.1. (a) Basic architecture of an SOA, (b) commercial SOAs and RSOAs in butterfly and TO-CAN packages [http://www.ciphotonics.com].

Typically SOAs are constructed into small packages, and they work for 1310 nm and 1550 nm systems. In addition, they can be bidirectional, making the reduced size of the device an advantage over erbium-doped fiber amplifiers (EDFAs). However, the drawbacks of SOAs as compared to EDFAs include high-coupling loss, polarization dependence, and a higher noise figure.

Recent designs include anti-reflective coatings, tilted waveguide and window regions to eliminate end-face reflection almost perfectly. This effectively prevents the amplifier from acting as a laser. By simply replacing one of the facets by a perfectly reflecting mirror the SOA is transformed to an RSOA. To perform as an external modulator, the current is modulated so that the RSOA reflects the light coming from the fiber into it again for transmitting a '1' and blocks the reflection for a '0'. Similar modulation is achievable with an SOA, in transmission rather than in reflection. An RSOA senses the signal that arrives to it by a voltage variation in its terminals, and modulates the signal in amplitude through the control current, exactly as in an SOA.

One of the attractive RSOAs available in the market is the SOA-RL-OEC-1550[1] from CIP (Center for Integrated Photonics). This RSOA has very low front facet reflectivity ($<10^{-5}$), and is ideal as a reflective, colorless amplifying modulator in WDM PON schemes. Key specifications include a small signal gain of 20 dB typical over a wavelength range from 1530 to 1570 nm, gain ripple of 0.5 dB, polarization dependent gain of 1.5 dB, and a modulation data rate of up to 1.5 Gb/s (other specifications can be found in the datasheet available online at the CIP website).

3.2.2. Saturation Regime and Noise Cleaning Principles

The gain saturation in semiconductor amplifiers is caused by the carrier-density depletion and fast phenomena such as carrier transport in multiple layers and intra-band carrier dynamics in the device [50]. In the saturation regime the output power is almost constant regardless of the input power; the gain is high and constant in the linear region and then starts to decrease as the input power is further increased.

It is well known that a semiconductor amplifier operated well into gain saturation can significantly reduce the intensity noise due to the so-called "amplitude squeezing" effect. This squeezing effect cancels the photon bunching of the chaotic light by limiting excess photon generation [51], [52]. The other mechanism contributing to the noise cleaning in

[1] http://www.ciphotonics.com

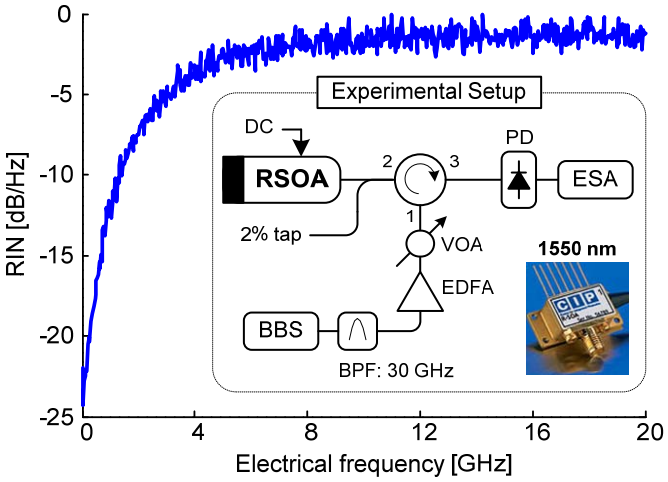

Figure 3.2. Typical RIN measurement for the SOA-RL-OEC-1550 (BBS: broadband source, BPF: band pass filter, DC: direct current, EDFA: erbium-doped fiber amplifier, ESA: electrical spectrum analyzer, PD: photodiode, VOA: variable optical attenuator).

SOAs and RSOAs is their high-pass filtering (HPF) effect which can suppress low frequency noises. This HPF effect is due to the self-gain modulation [44]. A typical relative intensity noise (RIN) measurement for the SOA-RL-OEC-1550 is shown in Figure 3.2. The experimental setup used for the characterization is also illustrated. A broadband source (BBS) and a 30 GHz wide band pass filter (BPF) were used to be consistent with the results presented in Chapter 5. The center wavelength of the BPF was tuned to 1550 nm and the variable optical attenuator was adjusted to make sure that the RSOA is deeply saturated. The depth of the HPF effect depends on the amount of gain saturation and the cut-off is governed by the carrier lifetime. Because the carrier lifetime in RSOAs is shorter than in SOAs due to the higher internal photon density caused by their double pass gain, we expect more HPF effect in RSOAs and thus more noise reduction compared to SOAs.

Using SOAs to achieve noise cleaning in incoherent SS-WDM systems has been studied extensively by different research groups [53]-[56]. Different schemes have been proposed and successfully demonstrated, including the use of an SOA in conversion at the receiver side. It was also reported that filtering a noise-cleaned signal degrades the performance. However, using wide filters can mitigate to a certain extent this degradation, at the expense of the spectral efficiency. In [19], Mathlouthi *et al.*, recently proposed a balanced

receiver for SS-WDM systems that avoids filtering and therefore preserves the noise cleaning when gain-saturated SOAs are used at the transmitter side. In Chapter 6, we present a new dense SS-WDM PON architecture over the legacy infrastructure, using this novel receiver together with a proposed self-seeded RSOA transmitter.

Less research has been conducted for the use of gain-saturated SOAs in SAC-OCDMA systems [57], [58]. In [57], McCoy *et al.*, proposed to use one SOA per frequency bin to achieve noise cleaning in SAC-OCDMA systems. This solution is not cost effective and was not examined in the laboratory. Recently, noise cleaning in SAC-OCDMA systems was reported using one SOA per user [58]. The low complexity receiver reported in [59] was used in the experiment to avoid filtering the desired user at the receiver side.

3.3. OCDMA for Future PONs

Optical CDMA networks are now receiving more and more attention because they combine the large bandwidth of the fiber medium with the flexibility of the CDMA technique to achieve high-speed connectivity [15], [60]. The essence of OCDMA is that multiple users can share the whole bandwidth simultaneously. In such systems, each user is assigned a unique code from a set of codes having good auto-correlation and cross-correlation properties [61]-[63]. Each transmitter imprints a particular code onto the bit sequence to be sent. At the receiver side, a matched filter is used to distinguish the desired user from others, and the data is recovered.

Since OCDMA allows high spectrum utilization efficiency, simple network control, and improved security, it is considered a promising technology for optical access networks and a good solution for next generation PONs [64]-[66]. Optical CDMA also allows asynchronous transmission, completely decentralized and uncoordinated transmissions among users. Furthermore, the soft capacity of CDMA systems permits growing the client base beyond the nominal maximum capacity (while accepting some quality of service degradation) without extensive upgrades to the infrastructure.

Among different OCDMA flavors, SAC-OCDMA deserves close attention because of its ability to suppress the multiple-access interference (MAI) using balanced detection [67]-[70]. Furthermore, the most obvious choice of the optical source in SAC-OCDMA is an incoherent broadband source which is inexpensive compared to coherent light sources, and provides comparable performance [71]. For these reasons, and others to be introduced in the next pages, in this thesis we only examine SAC-OCDMA as an OCDMA PON solution. Challenges remain, as the performance of SAC-OCDMA is degraded by the intensity fluctuations arising from the beating between different spectral components, which we call intensity noise or simply beat noise [69]-[72].

3.3.1. Principle of Frequency Encoding in OCDMA Systems

Zacarrin and Kavehrad first described and demonstrated the idea of frequency encoding in OCDMA, in other words SAC-OCDMA [67], [68]. The block diagram of their proposed system is shown in Figure 3.3. At the transmitter side, a spectral amplitude encoder is used to selectively block or transmit certain frequency components according to the spreading code. At the receiver side, a balanced receiver filters the incoming signal with the same spectral amplitude filter used at the transmitter as well as its complementary filter. For an unmatched transmitter, half of the transmitted spectral components will match the direct filter and the other half will match the complementary filter (In the case of m-sequence or Hadamard codes). Since the output of the balanced receiver represents the difference between the two photodetector outputs, unmatched

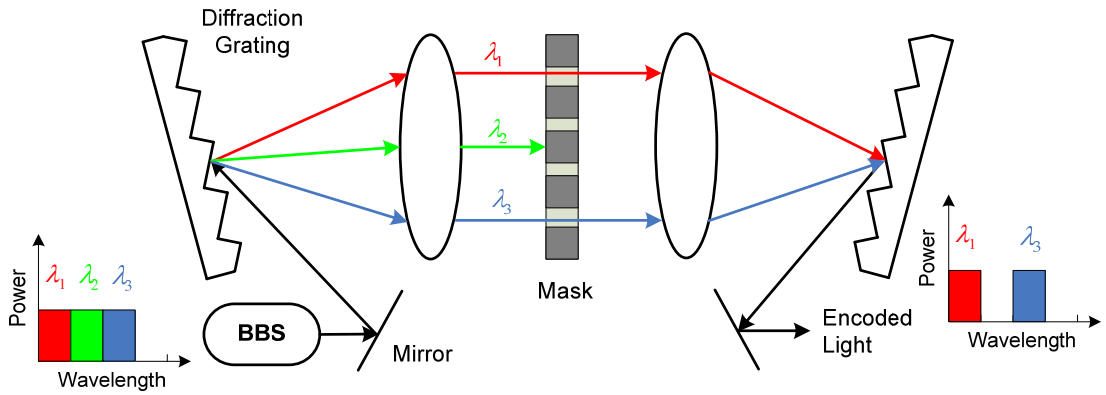

Figure 3.3. Basic idea of spectral amplitude coding for OCDMA [67].

channels will be cancelled, while the matched channel is detected.

To avoid the use of the bulk optics system proposed in [67], and to provide the advantage of a low cost reconfigurable all-optic encoder/decoder, fiber Bragg gratings (FBGs) have been proposed as encoders/decoders for SAC-OCDMA. The reflection and transmission responses (amplitude and phase) of the FBGs depend on their design [73]. In 2001, a SAC-OCDMA system using two linear arrays of chirped FBGs working in reflection was proposed and studied via simulations [62]. Later on, a SAC-OCDMA system using reflective superimposed FBGs was developed and experimentally demonstrated for up to four simultaneous users transmitting at 622 Mb/s [69], [74]. The gratings were written at the same location in the fiber to avoid delays between the different reflected frequency components. The first gratings were written stronger, as they were partially erased by the other gratings during the writing process [69]. To avoid the writing problems associated with the superimposed FBGs as well as the complexity of other systems, chirped FBGs working in transmission were proposed and successfully demonstrated in [70].

3.3.2. Code Selection and MAC Layer Considerations

Central to any successful CDMA system, whether electrical or optical, is the choice of the high rate sequences, namely, the signature sequences, on which the information data bits of different users is mapped. In CDMA, many asynchronous users occupy the same channel simultaneously. A desired user's receiver must be able to extract its signature sequence in the presence of other users' signature sequences. Therefore, a set of signature sequences that are distinguishable from time shifted versions of themselves and for which any two such signature sequences are easily distinguishable from each other is needed. Among the different codes used for SAC-OCDMA, balanced incomplete block design (BIBD) codes are characterized by a unity cross-correlation between codes and they offer a larger cardinality than the modified quadratic congruence (MQC) codes [63]. Further, BIBD codes are parameterized by a power of a prime number which offers a smoother range of values than a prime number alone as for MQC codes.

The media access control (MAC) layer is of an important concern as it can be exploited in a complementary way with the physical layer to enhance the performance of OCDMA systems [75]. A good MAC protocol ensures efficient and fair access to the medium while being simple. Most research in the field of OCDMA has focused either on the physical layer [64]-[71], or on the optical link layer [76]-[78]. The impact of these protocols on practical OCDMA systems has yet to be investigated (to our knowledge). In [79] we presented our contribution to the joint physical and MAC layers analysis of a real SAC-OCDMA system. We simulated the system throughput and the average packet delay of a SAC-OCDMA system that was recently demonstrated in [70]. Both the slotted ALOHA-CDMA and the round robin receiver/transmitter (R^3T) protocols were considered [76], [78]. The performance of SAC-OCDMA systems can be improved by implementing a simple MAC protocol, even with a poor BER and without using a FEC.

3.4. RSOA-Based ONUs for WDM PONs

Putting aside for now the SAC-OCDMA option for PONs, we consider WDM solutions next. Incorporating WDM in a PON allows increased bit rate per subscriber as compared to the standard PON which uses a single-wavelength architecture [12]-[14]. However, the network complexity and its subsequent cost have been the most critical issues for the practical deployment. To overcome this problem, it has been proposed to implement WDM PONs using centralized light sources (CLS) architecture where the light sources are placed at the OLT side [39]-[44], [46]-[48]. Coherent laser sources can be used, but their cost is high due to stability requirements. A single broadband source can supply multiple channels by slicing the spectrum of that source. Using spectrum-sliced incoherent light sources such as light emitting diodes (LEDs) and ASE sources reduces cost [80], [81]. However, spectrum-slicing has limited system margin due to the large slicing loss and low output power of LEDs. This problem could be relaxed to some extent by using high-power LEDs and sensitive receivers. Using SOAs or RSOAs as incoherent ASE sources at the ONU side is another interesting solution as they provide amplification while maintaining colorless operation. Another drawback of spectrum-slicing technology

is the large amount of intensity noise arising from incoherent sources, which significantly limits the bit rate and the maximum distance [82].

In this section we have selected representative recent publications that convey the state of research into WDM and SS-WDM PONs using mainly RSOAs at the ONU side. We also present a recent solution to enhance the performance of such systems by using a remotely pumped erbium-doped fiber amplifier (EDFA), to allow for more splitting losses to support more users using TDM over WDM [83]. Finally we present a promising alternative to centralized light sources, self-seeded RSOA-based transmitters [84]-[87].

3.4.1. Colorless ONU Operation

A key element in access networks is the ONU design. For FTTH success, ONUs need to be simple as well as robust, flexible, and inexpensive. The translation of these concepts into technical requirements is that ONUs need to be wavelength independent by avoiding the use of distributed feed-back (DFB) lasers and thus preventing their stabilization at the customer side. In order to match these requirements, colorless ONUs are a potential solution for WDM PONs, in particular, RSOA-based ONUs [46], [47].

Several techniques have been investigated to obtain colorless ONUs. The simplest is to use tunable lasers as transmitters. The wavelength is simply tuned at the installation. Nevertheless tunable lasers are too expensive up to now for FTTH access networks. An interesting alternative is to use a broadband source and the spectrum-slicing technique. Superluminescent LEDs are interesting because they emit a high output power, their center wavelength and bandwidth are easily manipulated, and they are relatively low cost. The modulation speed can reach up to 1 Gb/s, but the transmission distance is limited due to dispersion and slicing loss [39].

For higher data rates the remote modulation technique is preferred. The principle of remote modulation is to send an optical carrier from the central office and to modulate this continuous wave (CW) wavelength at the ONU with upstream data, to be sent back to the OLT. Different components can be used as a modulator, in order to support different bit rates. For bit rates up to 1.25 Gb/s, injection locked Fabry-Perot (FP) lasers

are well adapted with the use of an incoherent broadband source at the OLT [88]. For higher data rates (up to 5 Gb/s) RSOAs are better adapted. The gain of the RSOA allows higher power budget; the optical injected power can be as low as -20 dBm, and they have a low polarization-dependent gain [39].

Other techniques have also been proposed and evaluated. The use of different modulation formats for the uplink and downlink is also an interesting solution, as will be discussed in Section 3.5. However, this solution typically requires additional components, and therefore the cost may not be appropriate for FTTH systems. In Section 3.5, we also consider the remodulation and data erasure solutions using saturated SOAs. Currently, these solutions require high input powers (to saturate the SOAs) which are not suitable for WDM PON [90], [91]. The use of a centralized supercontinuum source to generate CW signals is also interesting in terms of spectral bandwidth and for its coherent nature but optical amplification is needed [89].

3.4.2. Remotely Pumped EDFAs

Despite the advantages we have already mentioned for RSOA-based ONUs, they need to be injected/seeded with enough power from the centralized source to guarantee error free operation for the uplink. Increasing the WDM PON physical reach or its capacity using TDM imposes more losses. Using high power light sources at the OLT or amplification is not a good solution because of the nonlinear effects associated with high power levels. Furthermore, using an EDFA between the OLT and ONUs violates the passive nature of a PON and requires a supply of electricity within the optical distribution network (ODN).

Recently, remotely pumped EDFAs have been proposed to enhance the performance of RSOA-based hybrid WDM/TDM PONs [83]. A 1480 nm laser diode (LD) is used at the OLT to pump the remote EDFA, and only an erbium-doped fiber (EDF) is located between the transmission fiber and the RN as shown in Figure 3.4. The remotely pumped EDFA operates as a bidirectional amplifier for both the CW seed light sources for upstream signals and the modulated upstream signals. L-band downstream signals obtain negligible gain due to the short length of EDF. In their experiment DFB lasers were used

for the seed light sources as well as for the downstream, and the RSOAs were directly modulated at 1.25 Gb/s. Without a remotely pumped EDFA, the seed power reaching the ONUs is too low so that bit error rate (BER) floors around 10^{-5} appear for the upstream signals for only 4 TDM splits. Using the remotely pumped EDFA error free transmission is easily achieved for 16 TDM splits.

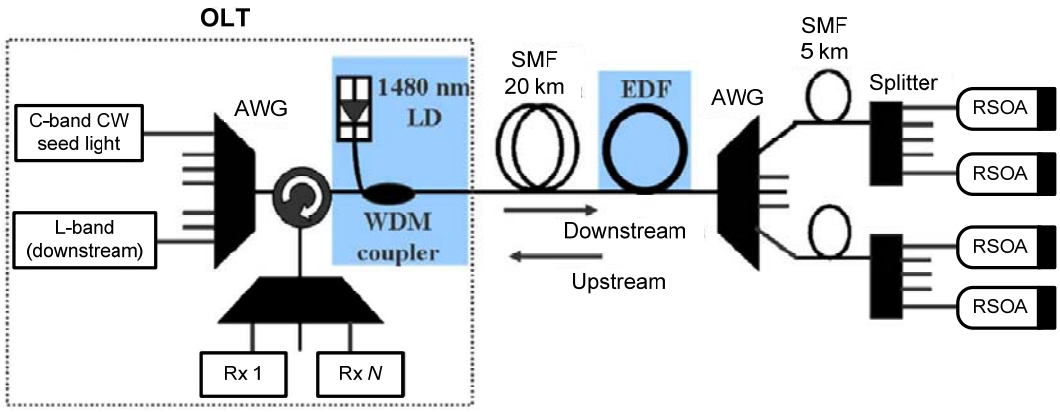

Figure 3.4. RSOA-based hybrid WDM/TDM PON with remotely pumped EDFA [83].

Using a remotely pumped EDFA for the RSOA-based hybrid WDM/TDM PON is an excellent candidate for next generation access networks. Error free 1.25 Gb/s uplink transmissions are feasible over a total reach of 25 km for 512 ONUs with 32 WDM channels and 16 TDM splits [83]. However sharing 1.25 Gb/s between 16 users reduces the average user bit rate per user to roughly 80 Mb/s.

3.4.3. Self-Seeded RSOA Transmitters

In order to further reduce cost we can eliminate the centralized light source at the central office, by using self-seeded RSOA-based transmitters [84]-[87]. The principle of self-seeding is to concentrate the ASE output power of the RSOA into a specific band without the need for an external seed source. Directly filtering the output ASE of the RSOA is not efficient from a power perspective as shown in Figure 3.5a. For a reliable transmission, an EDFA followed by another BPF are required to boost the power. Alternately, self-seeded RSOA transmitters (see Figure 3.5b) are powerful because of the self-injection.

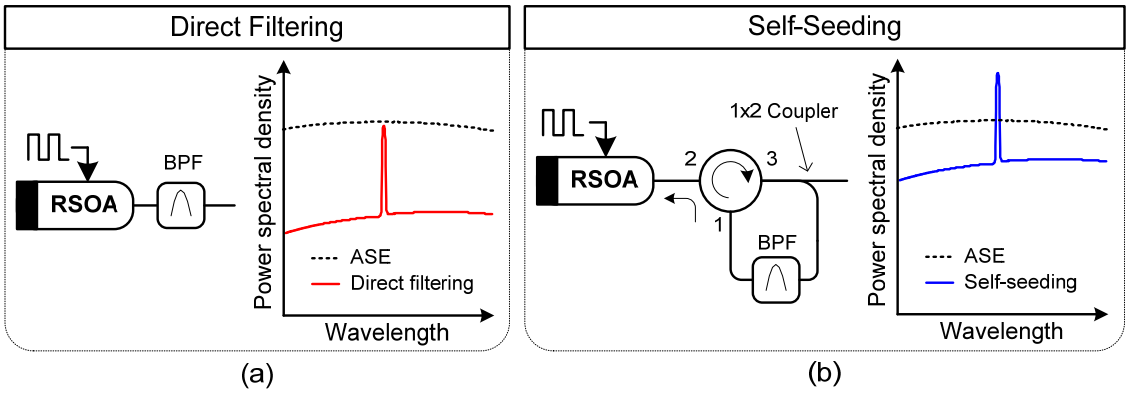

Figure 3.5. RSOA-based SS-WDM transmitters: (a) direct filtering, (b) self-seeding.

The output ASE from the RSOA is filtered and then re-injected back to the RSOA for amplification and possibly modulation. Re-injecting the RSOA with a certain color favors the gain/output of the RSOA to that specific wavelength, therefore the out of band ASE is lowered and the desired channel is amplified.

E. Wong, *et al.*, recently proposed remotely self-seeded RSOA ONU transmitters by placing a reflective filter at the RN [84], [85]. The slicing is achieved using the AWGs at the RN, the light is then partially reflected back to each ONU again through the AWGs. Although this architecture seems to be promising as it provides colorless ONU operation, it suffers from high roundtrip insertion losses, resulting in low seeding power that consequently limits the uplink performance. An EDFA is thus needed at the RN which violates the passive nature of a PON. To overcome the problems associated with remote self-seeding, local self-seeding was proposed by placing a wavelength specific reflector at each ONU [86], [87]. The ONUs become wavelength dependent 'colored', unless tunable filters are used.

In Chapter 5 and Chapter 6, we propose a self-seeded RSOA transmitter, and a *p*% reflective FBG-based self-seeded RSOA transmitter, respectively. We study the wavelength coverage of these transmitters over a 40 nm band. We further exploit the noise cleaning effect and address the challenges in combining self-seeding with noise cleaning by optimizing our proposed transmitter. We successfully demonstrate both local and remote self-seeding without the need of any amplification as was the case in [86], [87]. Therefore, the remotely self-seeded RSOA transmitter we proposed can provide

colorless ONU operation while preserving benefits from both high power and noise cleaning effects.

3.5. WDM PONs over Single-Feeder Architectures

Two possibilities exist for the physical topology of an ODN: single-feeder and two-feeder architectures. In a single-feeder architecture the upstream and downstream are sent over the same optical fiber, whereas in a two-feeder architecture two separate fiber feeders are used for the uplink and downlink signals. When the same wavelength is used for both uplink and downlink, single-feeder architectures are more sensitive to back reflections and reflections caused by Rayleigh backscattering than two-feeder architectures. In current PON installations a single feeder is installed between the OLT and the RN [1]. Installing additional feeders is not cost effective when upgrading TDM to WDM PONs. Sending both the uplink and downlink over the same fiber at the same wavelength represents a design challenge. We present here possible solutions for PONs to achieve full duplex communication using the same wavelength over the same feeder.

3.5.1. Downstream Remodulation Techniques

To efficiently exploit available resources, downstream signals can be reused for uplink transmission through data rewrite and remodulation techniques using SOAs or RSOAs [40], [92]. The downstream signal source is "recycled" for the upstream, thus eliminating the need for CW light sources at the OLT and reducing the cost and complexity. However the received power at the ONU must be sufficient to drive the SOA or the RSOA (used for rewriting) into the gain saturation region for data erasure and remodulation [90], [91].

In [40], F. Payoux *et al.* proposed a hybrid WDM-TDM PON architecture using RSOA based ONUs. Downstream and upstream transmissions at 1.25 Gb/s were successfully demonstrated over a 15 km link. Both single-feeder and two-feeder architectures were tested. The downstream signals were generated with directly modulated DFB lasers. At the ONU 20% of the received optical power was detected with an avalanche photodiode (APD) and 80% injected to the RSOA to be re-used for the upstream. A higher extinction

ratio was used for the upstream modulation, essentially masking the downstream data. The performance of the uplink over a single-feeder architecture was limited by Rayleigh backscattering. The effect of such reflections on the performance of both the uplink and downlink signals is mathematically analyzed and experimentally confirmed in [93]-[95].

3.5.2. Subcarrier Multiplexing and Different Modulation Formats

In order to benefit from a single-feeder architecture and to avoid problems associated with data remodulation and Rayleigh backscattering, different solutions including SCM techniques and wide spectrum modulation techniques were proposed [42]-[44], [46].

In order to further increase the capacity of WDM PONs, solutions including TDM and SCM were proposed. J. Kang *et al.* measured the modulation characteristics of a hybrid WDM-SCM PON using an RSOA as a modulator [43], [44]. Downlink transmission was accomplished using directly modulated DFB laser diodes (LDs) at 622 Mb/s. The WDM channels were spaced by 100 GHz. At the ONU side, the downlink signal was split for detection and remodulation. The 100 Mb/s uplink signal was up-converted using a mixer and a local oscillator at 900 MHz. According to their measurements, the proposed scheme required no amplifiers, as the RSOA provided enough gain to guarantee power margin for both uplink and downlink. Error free transmission was achieved for back-to-back and 10 km links.

A similar WDM PON architecture using radio frequency (RF) multiplexing was proposed and successfully demonstrated by C. Arellano *et al.* in [46]. Upstream and downstream signals were multiplexed on different RF carriers. A bit rate of 155 Mb/s was chosen to be able to accommodate upstream and downstream data in the RSOA electrical bandwidth (1.2 GHz). The results showed that the effect of Rayleigh backscattering is greatly reduced whenever the upstream and downstream data are transmitted on different RF bands.

Using frequency shift keying (FSK) for the downlink and amplitude shift keying (ASK) for the uplink has been reported in [46]. In this approach the OLT generates an FSK downstream data, at 1 Gb/s for this experiment. At the ONU before detection, a tunable

band pass filter (BPF) converts the FSK modulation into intensity modulation by suppressing the transmission frequency corresponding to the zero data. As the FSK signal is constant in amplitude, the upstream data can be ASK modulated by an RSOA with minor distortion.

Although error free operation can be achieved in single-feeder WDM PONs, this requires the use of SCM or different modulation techniques, adding to complexity and cost. In this thesis, we will exploit the principle of data erasure and rewrite [90], [91], not to manipulate a centralized source, but rather for the generation of a self-seeded RSOA transmitter for WDM PONs over single-feeder architectures. In Chapter 6 we propose using different wavelengths for the uplink and downlink and based on that, we calculate the maximum PON capacity. Using SCM would double the capacity, at the expense of the network cost and complexity.

3.6. Migration Path from TDM to WDM PONs

A WDM-based PON provides scalability compared to TDM because it can support multiple wavelengths over the same fiber infrastructure. Furthermore, WDM is inherently transparent to the channel bit rate, and does not suffer power-splitting losses as in TDM PONs. Having discussed recently proposed solutions for WDM PONs with their design challenges, we briefly cover in this section the migration path from the legacy TDM PONs to the next generation WDM PONs. Both the physical architecture and the MAC layer are considered.

3.6.1. Architectural Considerations

For operators who have invested in PON infrastructures, it is cost effective to reuse the optical splitters in the outside plant in future updates. WDM PON architectures based on AWGs are therefore reserved for green field (*i.e.*, new housing developments) deployments where no splitters were yet installed. The reason why WDM PONs offer more scalability than TDM PONs is due to the use of AWGs at the RN instead of the passive splitters. The typical insertion loss of an AWG (around 5 dB regardless of the

number of channels) is far less than that of the optical splitter, which has an excess loss of around 0.5 dB in addition to the 1:*N* splitting loss. However, AWGs need to be thermally stabilized since the RN is located in a harsh temperature environment varying from -40°C to +85°C.

Evolution from GPON architecture can be either by the overlay of multiple point to point connections or by the multiplexing of several TDM PONs with WDM to decrease the number of OLTs and aggregate more users on a single PON. For few connections, lasers with specific wavelengths can be used. However, as the number of connections increases, the system requires colorless ONUs to remain at a reasonable cost [39]. In Chapter 6, we present an innovative way of upgrading existing PONs to SS-WDM PONs over the legacy passive splitter-based infrastructure without using AWGs.

3.6.2. MAC Layer Considerations

In a hybrid TDM over WDM PON, by assigning a wavelength to each PON group (a group of ONUs connected to the same splitter), the MAC protocol of existing TDM PONs can be used, as there is no interaction between wavelengths [12]. This is a practical and simple approach in the initial stage of TDM/WDM PON implementation, and this protocol transparency property is regarded as one of its merits. But this scheme is not bandwidth efficient, especially when some wavelengths are overloaded while others are not. If wavelengths are shared among all ONUs, then the total throughput may be increased significantly. For this purpose, a new wavelength control protocol, which helps setting up the communication between the OLT and ONUs, is needed [12]. In addition to the basic communication protocol, a new dynamic bandwidth allocation (DBA) algorithm that assigns not only time slots but also wavelengths to each ONU is also needed [14], [96].

3.7. Conclusions

Having provided a focused literature review, we draw conclusions and select the technologies that better fit (per our assessment) next generation PONs. We justify our

selection in terms of performance, reasonable complexity and cost. Both OCDMA and WDM solutions are addressed in Chapter 4 and Chapter 6, respectively. Recall that in this thesis we propose solutions for upgrading the existing TDM PONs over the legacy infrastructure; therefore, our solutions are based on single-feeder PON architectures with passive splitter-based remote nodes.

3.7.1. OCDMA for Future PONs

Regarding OCDMA and looking at the different solutions we presented in this chapter, we believe that SAC-OCDMA would be the appropriate candidate for future OCDMA FTTH networks. This is mostly attributed to its incoherent nature when an inexpensive BBS is used, and to its ability to cancel MAI. We use BIBD codes as the user signatures because of their superiority over the other codes [63]. Compared to the solutions reported in [45] and [66] for phase encoded OCDMA, in Chapter 4 we use the system reported in [70] where an EDF based source is used instead of mode-locked lasers, and chirped FBGs working in transmission instead of super-structured FBGs in reflection. The use of an incoherent BBS makes our solution more cost effective for PONs. The use of FBGs working in transmission eliminates the need for circulators making the ONU design cheaper and more compact. Inspired by centralized light sources architectures for WDM PONs, we propose in the following chapter using a similar architecture for SAC-OCDMA PONs. We further study the relative merits of local sources versus centralized light sources architectures.

3.7.2. WDM for Future PONs

Concerning WDM for next generation PONs, more choices are available because of the vast amount of research in that area and the maturity of WDM technology compared to OCDMA. Among the different WDM technologies, SS-WDM, *i.e.*, incoherent WDM would be preferred for future PONs due to cost issues. The use of incoherent sources reduces the system complexity by eliminating the need for highly stabilized laser diodes. However, as the bit rate increases and/or the WDM slices become narrower (*i.e.*, smaller optical bandwidth), SS-WDM performance will be limited by the intensity noise. For

typical 1.25 Gb/s bit rate in a symmetrical PON, a sufficiently wide optical bandwidth would guarantee acceptable performance. However, the optical bandwidth expansion could lead to dispersion problems. Therefore, for the same bit rate, a tradeoff exists between the intensity noise and the dispersion. Saturated SOAs or RSOAs can help reduce significantly the intensity noise [54]-[56], while the relatively short distances in a PON (typically, 20 km) makes the dispersion effect tolerable. For example, in Chapter 5, we will see that the propagating over a 20 km feeder at 1.25 Gb/s is feasible without dispersion compensation for a 55 GHz wide channel. This channel width is significantly narrower than typical SS-WDM solutions.

Among the different WDM solutions we presented in this chapter, self-seeded RSOA based transmitters seem to be attractive for SS-WDM PONs. Not only because they eliminate the need for centralized light sources and/or remote amplification, but because they are powerful enough to overcome the losses within the ODN, when passive-splitters are used at the RN. In Chapter 5, we will study the wavelength coverage of these transmitters, and for the first time to our knowledge we will exploit their potential for noise cleaning. In Chapter 6, and based on our previous results, we will propose a novel FBG based self-seeded RSOA transmitter that combines both self-seeding with noise cleaning. We will also discuss the PON architectural aspects, the migration path from TDM to dense SS-WDM, and we will exploit the possibility of remote self-seeding for colorless ONU operation. Since we will be considering the legacy PON infrastructure, different wavelengths might be used for full duplex communication or SCM techniques.

Chapter 4

Experimental Demonstration of a SAC-OCDMA PON: Local versus Centralized Sources

[1] Z. A. El-Sahn, B. J. Shastri, M. Zeng, N. Kheder, D. V. Plant, and L. A. Rusch, "Experimental demonstration of a SAC-OCDMA PON with burst-mode reception: local versus centralized sources," *IEEE J. Lightwave Technology*, vol. 26, no. 10, pp. 1192-1203, June 2008, [16].

Abstract

In this paper, we demonstrate experimentally the uplink of a 7×622 Mb/s incoherent spectral amplitude coded optical code-division multiple access (SAC-OCDMA) passive optical network (PON) with burst-mode reception. We consider two network architectures: local sources (LS) at each optical network unit (ONU) versus a single source located at the central office. We examine both architectures over a 20-km optical link, as well as a reference back-to-back configuration. Our architectures can adopt two-feeder and single-feeder topologies; however, we only test the two-feeder topology and therefore the effect of Rayleigh backscattering is neglected. We also study the relative merits (cost and performance) of local sources versus centralized architectures. A penalty of less than 2 dB between the LS and the centralized light sources (CLS) architectures was measured at a bit error rate (BER) of 10^{-9} under certain assumptions on the relative power of the sources. The power budget in the CLS architectures is more critical than in the LS architectures; extra splitting and propagation losses exist as the uplink travels through the network back and forth. Doubling the number of users while maintaining the same distance and source power in LS architectures imposes 3-dB additional losses, whereas for CLS architectures, there are 6-dB extra losses. CLS architectures can overcome these penalties using amplification at the central office. Alternately, central office amplification can be used to more than double the number of users in LS SAC-OCDMA PONs. A standalone (no global clock) burst-mode receiver with clock and data recovery (CDR), clock and phase alignment (CPA), and Reed-Solomon RS(255,239) forward-error correction (FEC) decoder is demonstrated. A penalty of less than 0.25 dB due to the nonideal sampling of the CDR is reported. The receiver also provides an instantaneous phase acquisition time for any phase step between consecutive packets, and a good immunity to silence periods. A coding gain of more than 2.5 dB was reported for a single-user system, and BER floors were completely eliminated. Error free transmission (BER < 10^{-9}) for a fully loaded PON was achieved for the LS architecture as well as the CLS architecture. Continuous and bursty upstream traffic were tested. Due to the CPA algorithm, even with zero preamble bits we report a zero packet loss ratio (PLR) for up to

four simultaneous users in case of bursty traffic, and more than two orders of magnitude improvement in the PLR for fully loaded PON systems.

4.1. Introduction

Passive optical networks (PONs) are recognized as an economic and future solution to alleviate the bandwidth bottleneck in the access network [2], [5], [6], and [8]. A PON typically has a physical tree topology with an optical line terminal (OLT) located at the root and optical network units (ONUs) connected to the branches. Existing PON standards are based on time division multiplexing (TDM) and can serve up to 32 or 64 users at an aggregate bit rate of 1.25 Gbps [2]. In order to handle future bandwidth demands, many researchers considered wavelength division multiplexing (WDM) to increase the capacity of these existing PONs [13], [46], [47], and [80]. However, some limitations to WDM PONs market penetration exist. Adoption of WDM PONs requires upgrading the infrastructure from passive splitters to passive wavelength routers. The use of coherent laser sources in such PONs adds to the cost and complexity of the system, requiring external circuits for laser stabilization. Other solutions which combine sub-carrier multiplexing (SCM) to WDM were proposed to make use of the same wavelength for both uplink and downlink [43], [44]. In this case more electrical circuits containing with local oscillators and mixers are required. Using TDM over WDM PONs helps increase the capacity further, but requires synchronization [40].

Optical code-division multiple-access (OCDMA) combines the large bandwidth of the fiber medium with the flexibility of the CDMA technique to achieve high-speed connectivity [15]. A promising approach for upgrading existing PONs, or for next generation PONs, is the use of OCDMA with its simple ONU and OLT configurations requiring no synchronization [45], [70], and [66]. PON infrastructures (*i.e.*, passive splitters) need not to be upgraded to adopt OCDMA. Other attractive features of OCDMA include all-optical processing, truly asynchronous transmission, bandwidth efficiency, soft capacity on demand, protocol transparency, simplified network control, and flexibility on controlling the quality of service (QoS) [15], [66].

In this paper we focus on incoherent spectral amplitude-coded optical code-division multiple-access (SAC-OCDMA) as a solution for PONs, because of its ability to cancel multiple access interference (MAI), and to permit the use of low speed electronics operating at the bit rate [70], [97]. Furthermore, advances in writing fiber Bragg gratings (FBGs) make possible the design of low cost and compact passive encoders/decoders well adapted to PONs [70], [98]. In our work we examine several PON physical architectures, namely, the use of local sources at each ONU versus the use of a single light source housed at the central office. An inexpensive incoherent light source is placed either at each ONU or at the OLT, for the local sources (LS) architecture or the centralized light sources (CLS) architecture, respectively. In order to manage uplink (from users to OLT) and downlink (from OLT to users) traffic, we consider both two-feeder and single-feeder approaches [40].

Much research into OCDMA focuses on optical design, while assuming the availability of high-speed electronics [15], [45], [70], and [66]. Emerging research is concerned with the electronic design of receivers for optical multi-access networks, featuring post-processing functionalities [99], [100]. Previous electronic receivers were reported in the literature for fast-frequency hop (FFH) OCDMA and PON systems [21], [101]. FFH-OCDMA (or λ-t OCDMA) requires electronics that operate at the chip rate rather than the data rate. SAC-OCDMA has the advantage of operating at the data rate, and enjoys excellent MAI rejection with balanced detection. In this paper we demonstrate experimentally burst-mode reception of an incoherent SAC-OCDMA PON uplink supporting seven asynchronous users at 622 Mbps (FFH results were at 155 Mbps data rate). Our receiver has no global clock (*i.e.*, synchronization), instead exploiting a commercial SONET clock-and-data recovery (CDR). Reed-Solomon RS(255,239) forward-error correction (FEC) is also implemented on a field programmable gate array (FPGA). The receiver features clock-and-phase alignment (CPA) and includes a custom bit error rate tester (BERT) implemented on the FPGA.

Different PON architectures are tested experimentally, and bit error rate (BER) and packet loss ratio (PLR) are measured. The immunity of the CDR in terms of consecutive identical digits (CID) is also measured. We simulate the BER with FEC in order to

validate our measurements. We quantify the increase in soft capacity via FEC, while working with a nonideal recovered clock that provides realistic, achievable sampling. We also present and analyze the cost and power budget (uplink direction) of both LS and CLS SAC-OCDMA PON architectures.

The rest of this paper is organized as follows: Section 4.2 is concerned with the SAC-OCDMA PON physical topologies. We present and compare different OCDMA PON architectures including LS versus CLS architectures, and two-feeder versus single-feeder architectures. Section 4.3 is devoted to the description of the burst-mode receiver functionalities. The operation of the CDR, CPA, FEC, and the FPGA-based BERT are outlined there. Our experimental setup, as well as the results, are presented and discussed in Section 4.4. In Section 4.5, we consider the performance and cost tradeoffs of the LS versus the CLS solution for SAC-OCDMA PONs. Finally, the paper is summarized and concluded in Section 4.6.

4.2. Proposed SAC-OCDMA PON Architectures

Tree architectures are widely used for fiber-to-the-home (FTTH), or the so called “last mile” market. Such networks referred to as PONs employ only passive components (couplers, circulators, etc.) in the optical distribution network (ODN) and at the remote node (RN), and they have low installation and management costs. Different PON architectures have been proposed by different research groups [13], [40], [43], [44], [46], [47], and [80], including both two-feeder and single-feeder architectures to multiplex uplink and downlink traffic. In two-feeder architectures, uplink and downlink traffic is sent independently on separate feeders; a single-feeder architecture carries both uplink and downlink on one fiber. Although single-feeder topologies reduce infrastructure and maintenance costs, they suffer from Rayleigh backscattering if the same wavelength is used for upstream and downstream. Two-feeder architectures give the flexibility to use the same wavelength band for upstream and downstream, making the design easier. Although our OCDMA PON architectures offer the flexibility of adopting both two-feeder and single-feeder architectures, we test only the two-feeder architecture for

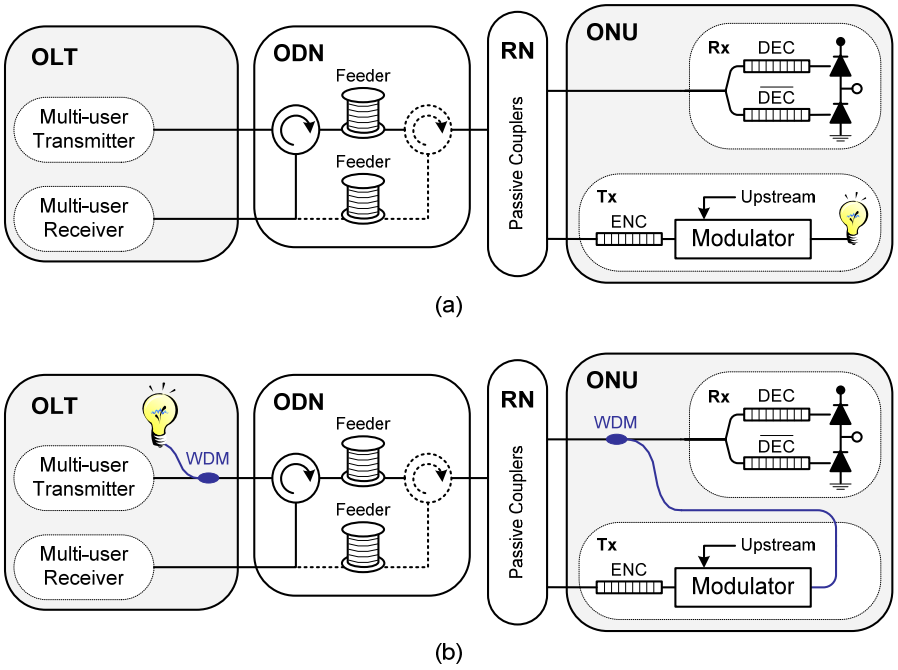

Figure 4.1. SAC-OCDMA PON physical architecture: (a) LS architecture, (b) CLS architecture.

experimental convenience. The effects of Rayleigh backscattering, which are reduced in such architectures, are then not addressed.

In this paper, we propose four different architectures for SAC-OCDMA PONs as illustrated in Figure 4.1; both LS architectures [Figure 4.1(a)] and CLS architectures [Figure 4.1(b)] can exist with two-feeder and single-feeder topologies (shown within the ODN). We analyze both architectures with each feeder topology in terms of power budget, but we experimentally test only the two-feeder topology. Although our architectures provide full-duplex communications, we focus on the design of the ONU side, as it is one of the most challenging factors in PON design [2], [5], [6], [8], and [21]. More specifically, we focus on the design of the ONU transmitter (uplink transmitter). The optimum receiver for a SAC-OCDMA PON at both the OLT and ONU is the conventional balanced receiver because of its ability to suppress first-order MAI. The structure of such a receiver for the ONU is given in Figure 4.1, including a 1×2 coupler, a decoder (DEC), a complementary decoder ($\overline{\text{DEC}}$) , and a balanced photodiode (PD). Fiber Bragg gratings working in transmission are used as the encoders/decoders because

of their good group delay performance, which is vital in SAC-based OCDMA systems [70]. Figure 4.1(a) shows the proposed LS SAC-OCDMA PON; in that case, an inexpensive directly modulated light emitting diode (LED) or a broadband erbium-based source is externally modulated and located at each ONU. On the other hand, the proposed CLS SAC-OCDMA PON, shown in Figure 4.1(b), places a single powerful source at the OLT with remote external modulation of that source at each ONU. In CLS architecture, coarse WDM filters are needed at the OLT and ONU, as shown in Figure 4.1(b), to separate the continuous wave light for the uplink from the modulated downlink. Such filters can be replaced by passive couplers if the same wavelength band is used for both downlink and uplink. The RN, the ODN, and the OLT multiuser transmitter/receiver are similar for the two architectures. The RN consists of passive combiners and splitters, as in existing TDM PONs, so there is no need to upgrade the PON infrastructure; for WDM PONs, the couplers must be replaced by arrayed waveguide gratings (AWGs). The RN serves as a connection between the ONUs and the ODN. Users are connected to the RN through short length fibers (~1 km) called distribution drop fibers. The ODN, composed of feeder fibers (~20 km) and passive optical circulators, can adopt a two-feeder (the second feeder with its corresponding circulator shown in dotted in Figure 4.1) or a single-feeder architecture. At the OLT, a multiuser transceiver is used to communicate with all the users in both directions. The OLT should contain optical amplifiers to compensate for the losses through the network and also for the combining and splitting losses of the multiuser transmitter and receiver when implemented all optically (the same design as ONUs in Figure 4.1). Note that electronic implementation of OLT transceivers could help reduce the loss budget significantly by eliminating the optical couplers. Furthermore, all preprocessing and postprocessing functionalities could be easily handled in electronics.

The uplink power budget of the proposed PON architectures in Figure 4.1 is mainly affected by the RN and the ODN adopted. In LS architectures [see Figure 4.1(a)], the uplink signal travels only in one direction, from the ONU to the OLT. For N ONUs (corresponding to a 1:N splitting ratio), we have $10\log(N)$ dB splitting losses, in addition to the propagation losses through one feeder and the insertion losses of a three-port circulator. These observations are valid for both the two-feeder and the single-feeder topology. In the CLS architecture, shown in Figure 4.1(b), for uplink, the unmodulated

source travels from the OLT to the ONU and after modulation returns to the OLT. Therefore, a CLS PON experiences twice the ODN and RN losses (splitting losses + propagation losses + insertion losses) as a similar LS PON, again whether the two-feeder or the single-feeder topology is used. We will discuss in Section V the performance and cost tradeoffs of the LS versus the CLS solution.

4.3. SAC-OCDMA Burst-Mode Receiver

According to the PON standards, a continuous downlink in the wavelength band of 1480-1500 nm carries TDM data, or OCDMA encoded data in our case, from the OLT towards multiple ONUs. A burst-mode link in the 1310-nm window collects all ONUs upstream traffic toward the OLT as variable-length packets at the same rate. Because of the bursty nature of the upstream, the OLT receives packets from active ONUs with different amplitude levels and phases. In class B PONs, the average signal level may vary 21 dB in the worst case from packet to packet [21]. These packets are of variable length and are interleaved with a guard time of only four bytes as specified by the physical medium-dependent (PMD) layer [21], [25].

A typical burst-mode uplink signal that complies with PON standards is used as a test signal in our experiments and is shown in Figure 4.2(a). Packet 1 serves as a dummy packet to force the burst-mode CDR to lock to a certain phase (ϕ_1) before the arrival of packet 2. A silence period including m CIDs and a phase step $\Delta\varphi$ is inserted between the two packets. This idle period also represents the asynchronous nature of OCDMA due to the random phase step $-2\pi \leq \Delta\varphi \leq +2\pi$ between the two packets. The PLR measurements and their corresponding BER measurements are performed only on packet 2, which consists of preamble bits, 20 delimiter bits, 2^{15}-1 payload bits, and 48 comma bits. The preamble and the delimiter bits correspond to the physical layer upstream burst-mode overhead at 622 Mb/s, as specified by the ITU-T G.984.2 standard [25]. The preamble bits are used to perform phase recovery. The delimiter is a unique pattern indicating the start of the packet to perform byte synchronization. Similarly, the comma is a unique pattern to indicate the end of the payload. The payload is simply a 2^{15}-1 pseudorandom

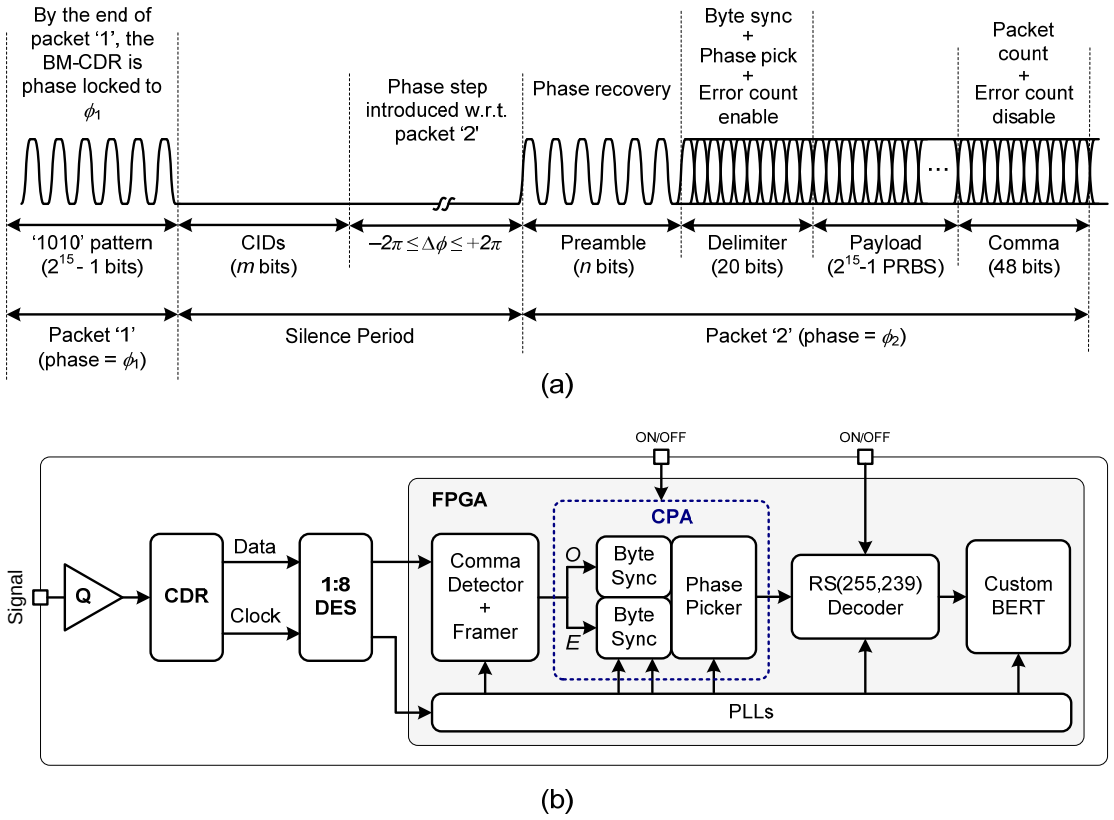

Figure 4.2. (a) Typical burst-mode uplink test signal used to test the phase acquisition time of the clock phase aligner, (b) block diagram of the OLT burst-mode receiver for SAC-OCDMA PONs (DES: deserializer, Sync: synchronizer).

binary sequence (PRBS). The BER and PLR are measured for the payload bits only. The lock acquisition time corresponds to the number of bits (n) in front of the delimiter in order to get a zero PLR for over 3 min at 622 Mb/s ($>10^6$ packets received, *i.e.*, PLR$<10^{-6}$), a BER$<10^{-10}$, and for any phase step ($-2\pi \le \Delta\varphi \le +2\pi$) between consecutive packets [100]. We will demonstrate that even at $n = 0$, *i.e.*, no preamble bits, our phase picker gives excellent results. To generate alternating packets with adjustable phase, as in Figure 4.2(a), we combined two programmable ports from the HP80000 pattern generator shown in Figure 4.3 using a radio frequency (RF) power combiner. The phase steps between the consecutive packets can be set anywhere between ±2 ns on a 2 ps resolution, corresponding to a ±1.25 unit interval (UI) at 622 Mb/s. Note that 1 UI corresponds to 1-bit period.

4.3.1. Building Block Diagrams

The main building blocks of the SAC-OCDMA burst-mode receiver we designed are illustrated in Figure 4.2(b). The receiver includes a multirate SONET CDR from Analog Devices (Part #ADN2819), a 1:8 deserializer from Maxim-IC (Part #MAX3885), and a CPA module and a FEC RS(255,239) decoder implemented on a Virtex II Pro FPGA from Xilinx. Our receiver without the CPA is therefore similar to that in [101], but without the return-to-zero (RZ) to nonreturn-to-zero (NRZ) converter needed for FFH-OCDMA. The receiver also avoids the use of an 8:1 serializer (used with FFH-OCDMA) to up convert the frequency. The quantizer (*Q*) is used before the CDR to threshold the incoming signal to filter out intensity noise and other channel impairments. The threshold is manually adjusted to sample in the middle of the eye opening to obtain the optimum BER. The multirate CDR then recovers the clock and data from the incoming signal. The receiver is operated at either 622 or 666.43 Mb/s depending on whether the FEC module is OFF or ON, respectively. The CDR is followed by a 1:8 deserializer (DES) that reduces the frequency of the recovered clock and data to a frequency that can be processed by the digital logic. Afterwards, a framer, a comma detector, a CPA (including a phase picker and byte synchronizers), phase locked loops (PLLs), an RS(255,239) decoder, and a custom BERT are implemented on an FPGA. Note that a computer is used to control the output of the pattern generator and to communicate with the FPGA on the receiver (Figure 4.3). Automatic detection of the payload is implemented on the FPGA through a comma detector and a framer, which are responsible for detecting the beginning (delimiter bits) and the end (comma bits) of the packets, respectively, as in [101]. The CPA module makes use of the phase picking algorithm in [100] and the CDR operating at 2× oversampling. The CPA is turned ON for the PLR measurements with phase acquisition; otherwise, it is bypassed. The CPA is then followed by the RS decoder and the FPGA-based BERT.

4.3.2. Burst-Mode Receiver Functionalities

The idea behind the CPA is based on the simple, fast, and effective algorithm in [100]. Since the CDR samples the data twice per bit, the odd samples and even samples (*O* and

E, respectively in Figure 4.2b), sampled on the alternate (odd and even) clock rising edges (t_{odd} and t_{even} in Figure 4.12) are identical. The odd samples are forwarded to path *O* and the even samples to path *E*. The byte synchronizer is responsible for detecting the delimiter. It makes use of a payload detection algorithm to look for a preprogrammed delimiter. The idea behind the phase picking algorithm is to replicate the byte synchronizer twice in an attempt to detect the delimiter on either the odd and/or even samples of the data respectively. That is, regardless of any phase step, *i.e.*, $-2\pi \leq \Delta\varphi \leq +2\pi$, between consecutive packets, there will be at least one clock edge (either t_{odd} or t_{even}) that will yield an accurate sample. The phase picker then uses feedback from the byte synchronizers to select the correct path from the two possibilities. For further illustration, we refer the reader to Figure 4.12, where the CDR output for the 2× over sampling mode at specific three possible phase differences between consecutive packets is shown.

The realigned data is sent to the RS(255,239) decoder which is turned on for BER measurements with FEC, otherwise it is bypassed (Figure 4.2b). The RS decoder is an IP core from the Xilinx LogiCORE portfolio. The FPGA-based BERT designed in [100] is implemented to selectively perform BER and PLR measurements on only the payload of the packets. The BERT compares the incoming data with an internally generated 2^{15}-1 PRBS. This eliminates the need to up convert the frequency back to 622 Mbps or 666.43 Mbps using an 8:1 serializer after the FPGA, and avoids the use of a commercial BERT. Note that conventional BERTs require a continuous alignment between the incoming pattern and the reference pattern, and milliseconds to acquire synchronization. The phase step response of the burst-mode CDR can make conventional BERTs lose pattern synchronization at the beginning of every packet while the sampling clock is being recovered by the CDR. The custom BERT does not require fixed synchronization between the incoming pattern and the reference pattern of the error detector. Synchronization happens instantaneously at the beginning of every packet, therefore enabling PLR measurements on discontinuous, bursty data.

4.4. Experimental Setup and Results

4.4.1. Experimental Setup

The experimental setup illustrated in Figure 4.3 is used to test the uplink of the LS and CLS SAC-OCDMA PON architectures shown in Figure 4.1, using only the two-feeder topology. A single incoherent broadband source (BBS) is filtered around 1542.5 nm using two cascaded FBG band-pass filters providing a 9.6 nm band, and serves to test both the CLS and LS architectures. An NRZ 2^{15}-1 PRBS is input to a single polarization independent electro-absorption modulator (EAM) that, in conjunction with appropriate decorrelating delay lines, represents independent data streams each modulated externally at a distinct ONU. For the CLS architecture, the single powerful BBS is sent over the 20 km CLS/downlink feeder and is then split by the first 1×8 coupler representing the RN. For the LS architecture, the 20 km single mode fiber (SMF-28) is not present and the first 1×8 coupler is not part of the network, but rather an experimental trick to emulate eight separate, low power incoherent sources. The balance of the setup is interpreted as seven ONUs each with a distinct CDMA encoder, followed by the second 1×8 coupler representing the RN and a 20 km SMF for the uplink in the two-feeder architecture. We

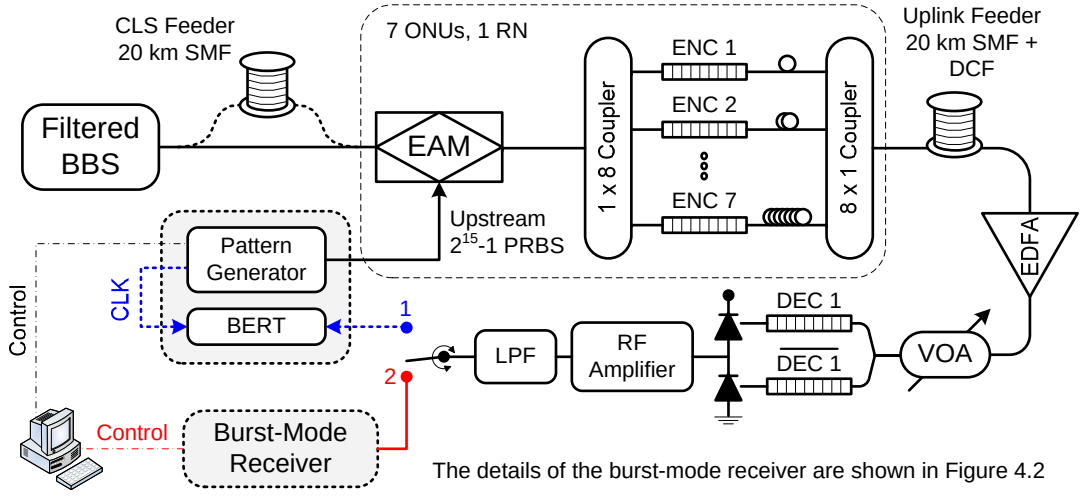

Figure 4.3. Experimental setup for a 7×622 Mbps SAC-OCDMA PON uplink (BERT: BER tester, CLK: clock, DEC: decoder, and ENC: encoder).

did not use the circulators and the WDM filter in Figure 4.1, as we were only testing the uplink; these components would only contribute to insertion losses.

At the OLT an appropriate dispersion compensation fiber (DCF) is used, and the signal is amplified by an erbium-doped fiber amplifier (EDFA) and detected in a balanced receiver. A variable optical attenuator (VOA) serves to control the received power level. A balanced detection scheme similar to that in Figure 4.1 is then used to decode user 1. To ensure good detection and MAI cancellation, the optical lengths of the two branches of the receiver are perfectly adjusted; furthermore, the power at both arms due to MAI is controlled using another VOA (not shown in Figure 4.3) that accounts also for the splitting ratio of the 1×2 coupler as in [70]. After decoding, each arm goes into one of the two separate inputs of an 800-MHz balanced photodiode from New Focus (model 1617). The electrical signal is then amplified (MITEQ, 0.01–500 MHz) and low-pass filtered by a 4^{th} order Bessel-Thomson filter (Picosecond, 467 MHz) to remove the out-of-band high-frequency electrical noise. Such a filter reduces intensity noise from the incoherent broadband source [70], while keeping inter-symbol interference to a minimum. Measurements are then performed with either a global clock, or through our OCDMA burst-mode receiver, corresponding to switch position 1 or 2, respectively. The desired information rate per user is 622 Mbps; an RS(255,239) code introducing 15/14 overhead leads to an aggregate bit rate of 666.43 Mbps. The spectral coding is achieved by FBGs working in transmission; balanced incomplete block design (BIBD) codes with length 7 and weight 3 are used as in [70].

4.4.2. Results and Discussions

In this subsection we present the system performance in terms of BER, PLR and the CID immunity for the back-to-back configuration (without fiber link), and the LS and the CLS SAC-OCDMA PON architectures. The experimental results are presented in Figure 4.4 to Figure 4.11, except for Figure 4.8 which shows simulation versus measurement results. We present also the power and link budget for the different architectures that were tested. BER measurements are reported for continuous upstream traffic, while PLR is reported for packet data, based on the burst-mode BERT results. PLR measurements use bursty

traffic (similar to that in Figure 4.2a) with packets of 2^{15}-1 bits length and zero preamble length; use of a preamble would improve PLR, but at the cost of reduced throughput. Today's PON standards provide for a maximum preamble length of 28 bits [25], to allow the receiver enough time to recover the clock, adjust the phase, and control the gain. The operation of the CDR and its ability to provide a clock signal with a 2× oversampling which is used by the phase picking algorithm, is explained in Figure 4.12 through a set of measured eye diagrams.

In Figure 4.4 we present the BER versus power for the back-to-back configuration. The horizontal axis represents the useful power, *i.e.*, the received power from the desired user. Curves are presented for a single user system up to a fully loaded system of seven users. Ignoring for a moment the solid curves with filled markers (FEC results), we focus our attention on the set of curves for the global clock (dashed) and for the CDR module (solid + unfilled markers). Starting from a single user we see a classic waterfall curve; as we go to a fully charged system of seven users BER floors begin to appear, starting from five

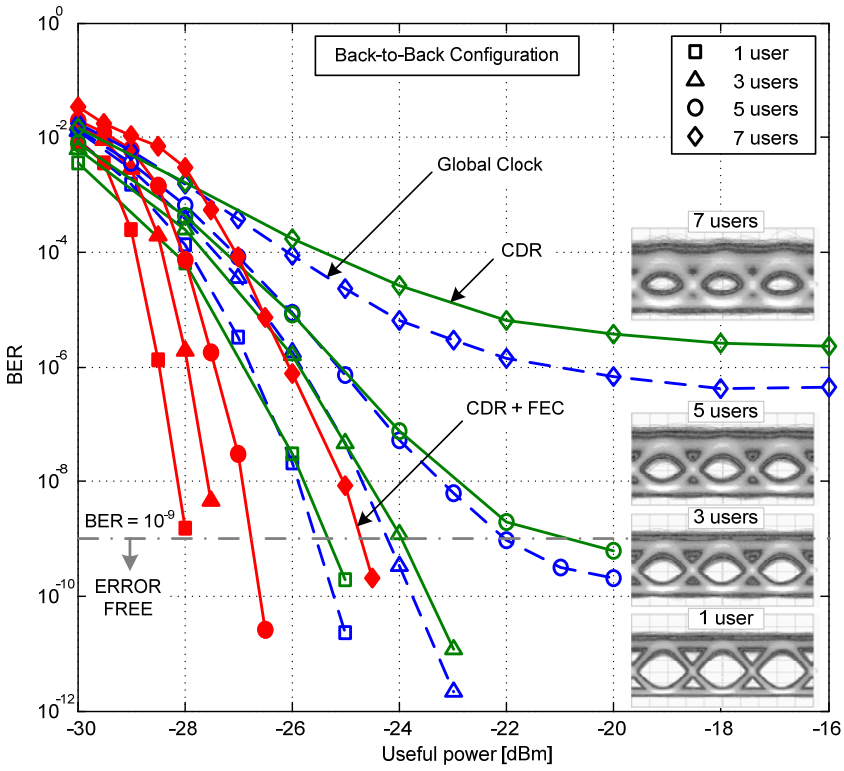

Figure 4.4. BER vs. useful power for back-to-back configuration (Dashed lines for global clock; solid lines and unfilled markers for CDR; solid lines and filled markers for CDR with FEC).

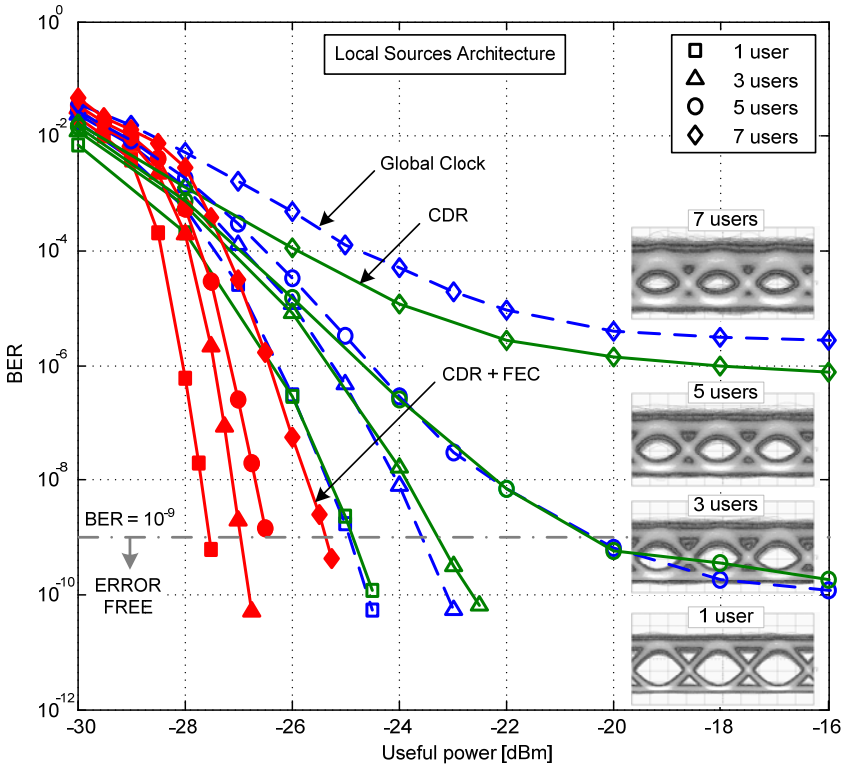

Figure 4.5. BER vs. useful power for LS architecture (Dashed lines for global clock; solid lines and unfilled markers for CDR; solid lines and filled markers for CDR with FEC).

users. The penalty when using the CDR unit is not significant (less than 0.25 dB), as we can see by the proximity of the CDR and global clock curves. When adding the FEC to the CDR operation, we see that all BER floors disappear and we return to the classic waterfall close to the single user performance. Eye diagrams measured at -18 dBm are included as insets in Figure 4.4. The single-user eye diagram is very open, while the fully loaded system with seven users has a severely closed eye. Despite the eye closure, the FEC allows us to return to error free performance.

Similar curves for the LS and CLS PON architectures are presented in Figure 4.5 and Figure 4.6, respectively. The same trends are observed, except for the case of seven users for the LS PON architecture. In that case, we note a slight improvement in the performance with the CDR compared to the global clock measurement, despite the nonideal sampling of the CDR. This improvement is related to the threshold adjustment, as in [101]. At small power levels we were able to manually control the decision threshold (using a DC power supply) to great accuracy for the CDR measurements, while

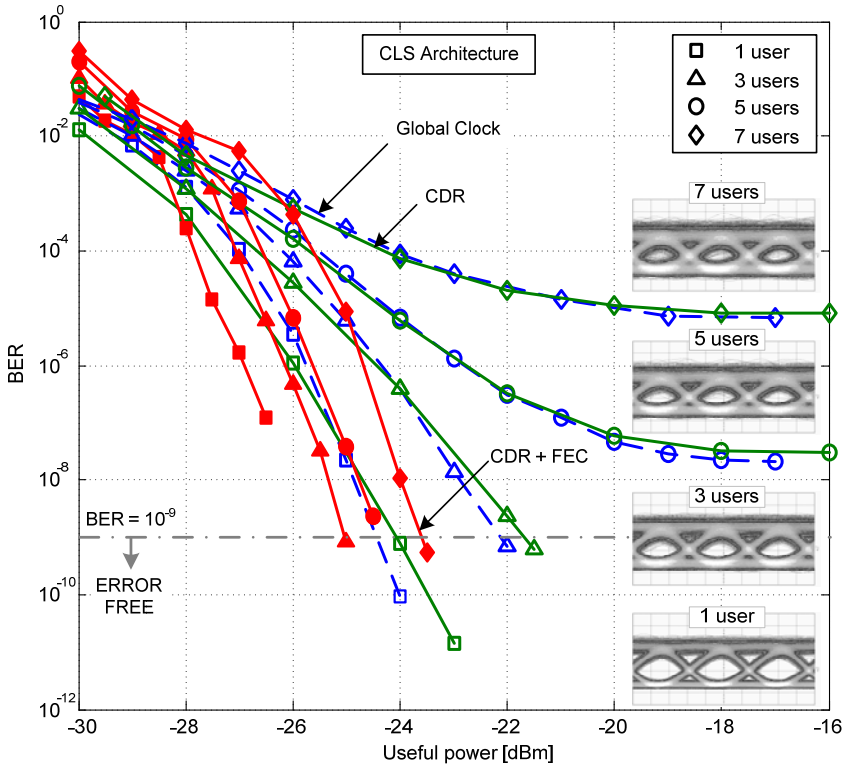

Figure 4.6. BER vs. useful power for CLS architecture (Dashed lines for global clock; solid lines and unfilled markers for CDR; solid lines and filled markers for CDR with FEC).

we were limited by the automated decision threshold in the commercial BERT for global clock measurements. The manual optimization explains the slight improvement in the performance when using the recovered clock especially at lower power levels; this explains the crossings of the global clock curves with the CDR curves at around -26 dBm for the three measurement configurations in Figure 4.4 to Figure 4.6.

For easier comparison of the back-to-back configuration and the two PON architectures, we plot in Figure 4.7 the single user and fully loaded (seven users) systems BER curves. We consider the performance using our burst-mode receiver when the FEC module is OFF (curves with unfilled markers), and when it is ON (curves with filled markers). A coding gain of more than 2.5 dB (measured at BER = 10^{-9}) is observed for a single user for the three architectures. Furthermore, the penalty from a back-to-back configuration to the LS PON is negligible (less than 0.25 dB), as well as the one from a LS PON to the CLS PON architecture. Results are consistent with that in [70] for a back-to-back configuration and a 20 km communication link. For the seven users case, we see clearly

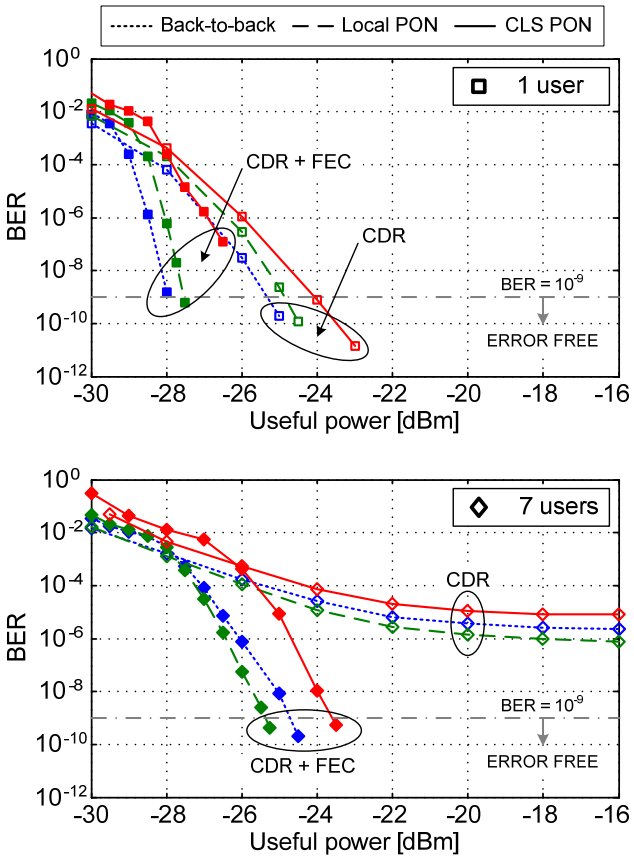

Figure 4.7. BER vs. useful power for a single user and fully-loaded systems (Dotted lines for back-to-back; dashed lines for LS architecture; solid lines for CLS architecture).

all BER floors are eliminated by the FEC. Operating at a relatively low power (-23 dBm received power) we obtain error free transmission (BER << 10^{-9}) for the three architectures. Therefore, we were able to demonstrate for the first time to our knowledge an error free 7×622 Mbps uplink of an incoherent SAC-OCDMA PON (LS and CLS architectures were tested) using a standalone burst-mode receiver with CDR and FEC.

Finally, in Figure 4.7 we can compare the performance of LS and CLS architectures under our assumption of an 8:1 ratio of the relative power of the centralized to the local sources. A penalty of less than 2 dB was measured for LS at a bit error rate (BER) of 10^{-9} when FEC and CDR were in use. Recall that this penalty is for the particular instance of a network of eight users, and an 8:1 ratio of relative power. We will discuss later how to generalize these results.

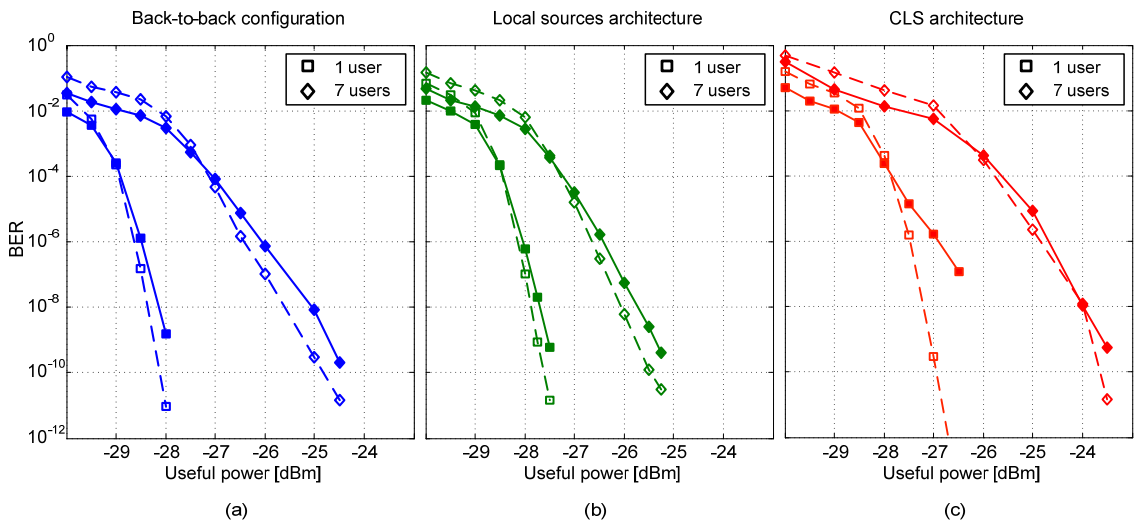

Figure 4.8. Simulated and measured BER vs. useful power for different configurations (Dashed lines for simulated BER; solid lines for measurements).

Simulation versus measurement of the BER using FEC for the three different configurations is shown in Figure 4.8. Let P_B be the measured BER without FEC in Figure 4.4, Figure 4.5, and Figure 4.6 for the various scenarios. Organizing the bits in symbols of m bits yields an equivalent symbol error rate of

$$P_S = 1 - (1 - P_B)^m \qquad (4.1)$$

The RS(255,239) FEC uses 8 bit symbols and, in a memoryless channel, can correct up to t = 8 symbol errors per frame (239 uncoded symbols), yielding a symbol error rate after FEC of [102]

$$P_{S_{FEC}} \approx \frac{1}{2^m - 1} \sum_{j=t+1}^{2^m-1} j \binom{2^m - 1}{j} P_S^j (1 - P_S)^{2^m - 1 - j} \qquad (4.2)$$

Again assuming a memoryless channel, the bit error rate P_{B_FEC} is about one half this symbol error rate, as we are using orthogonal signaling (on-off keying), [102]. We plot the memoryless channel prediction for P_{B_FEC} and our measurement in Figure 4.8. There is one order of magnitude mismatch between simulation and measurements; our predictions are too optimistic. This is more likely due to the memory added to the channel through the BBS (intensity noise), the CDR, and other components.

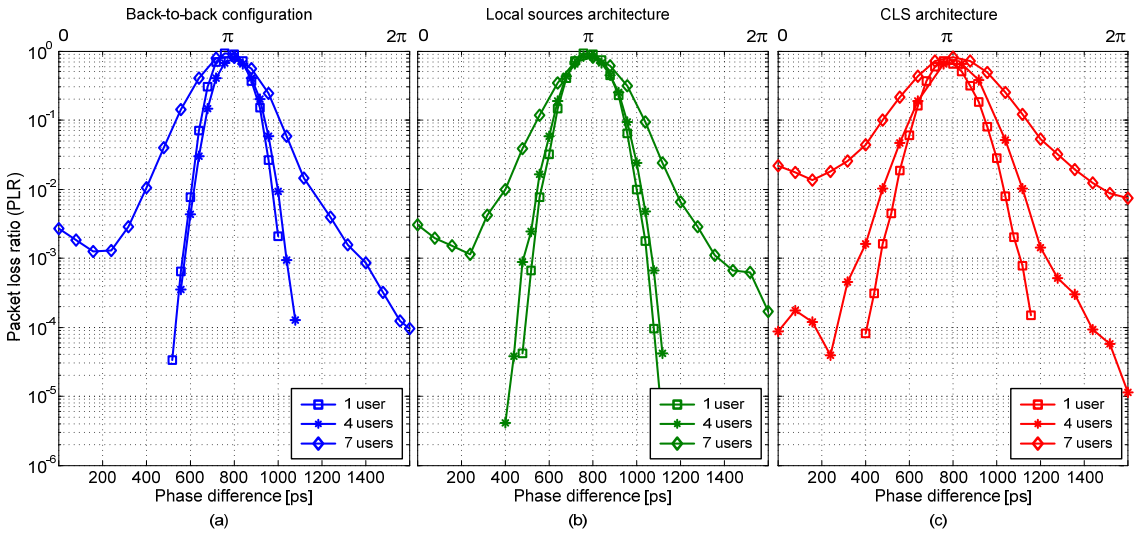

Figure 4.9. PLR vs. phase difference without CPA for different number of users: (a) back-to-back configuration, (b) LS architecture, (c) CLS architecture.

In Figure 4.9 we plot the PLR versus the phase difference between packets for the three configurations under test when using the SONET CDR without the phase picking algorithm. The power level was kept at -18 dBm for these and all subsequent measurements. Bursty traffic identical to that in Figure 4.2 with zero preamble bits is generated for all users. We will demonstrate that our phase picker does not require any preamble bits for phase acquisition. We consider that all packets are correctly received when PLR<10^{-6}, corresponding to a BER<10^{-10}. We have restricted the horizontal axis to values from 0 to 1600 ps, corresponding to 0 to 2π phase difference at the desired bit rate (~622 Mbps). We did not consider the interval from -2π to 0, because it gives theoretically the same performance as the positive interval [100]. We observe bell-shape curves for PLR centered around 800 ps; 800 ps corresponds to a phase shift of π radians, *i.e.*, the worst case. Jitter would have led to the worst case phase (π rad) being displaced from 800 ps, hence we conclude that jitter is not significant in our measurements. At relatively small phase shifts (near 0 or 2π rad), we note that for a single user system we can easily achieve zero PLR with the CPA module disabled, because the CDR is almost sampling at the middle of each bit (refer to Figure 4.12 for the conventional CDR output when the phase shift is 0 rad). By comparing the curves on the same subplot, *i.e.*, for each configuration, we note the degradation in performance passing from a single user system

to a fully loaded network of seven users. There is also a penalty when passing from the back-to-back configuration to the LS PON and then to the CLS PON, when comparing curves on different subplots. The degradation in the PLR can be explained by the corresponding degradation in the BER. As the BER performance degrades, there is a higher chance of having erroneous bits in the packet delimiter. With the delimiter not being correctly detected, a packet is declared lost, hence contributing to the packet loss count.

In order to show the improvement that can be achieved using the CPA functionality of our SAC-OCDMA burst-mode receiver, we have plotted in Figure 4.10 the worst case PLR, *i.e.*, the maximum PLR value that occurs at π phase shift, against the number of users for the three configurations, with and without CPA. In the case of CDR without CPA, the worst case PLR is near 1 (see Figure 4.9), as it corresponds to the receiver sampling at the edge of the eye diagram. In contrast, the phase picking algorithm samples each bit twice, within the eye, and significantly enhances the performance. With the CPA no packets are for lost up to four users for the three different architectures (PLR<10^{-6}).

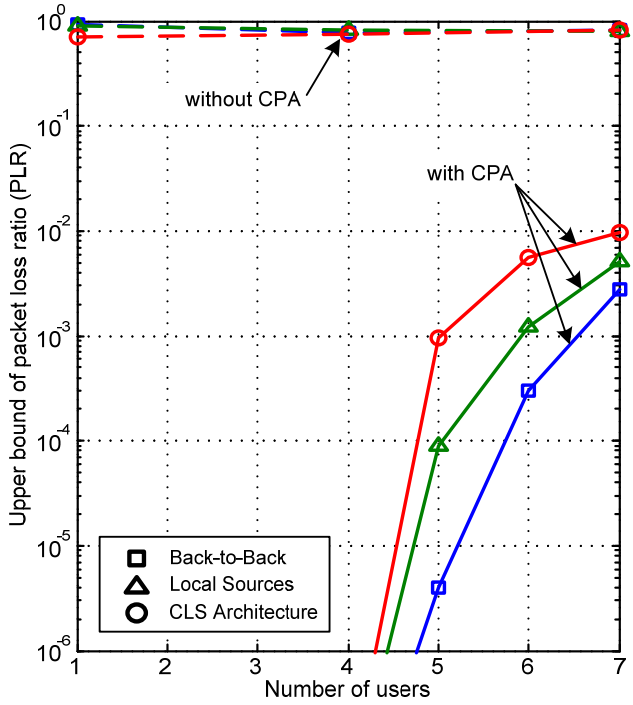

Figure 4.10. PLR vs. number of users for different PON architectures (Dashed lines for the system without CPA; solid lines for the system with CPA).

Increasing the number of users beyond four deteriorates the BER and thus the PLR. For a fully loaded PON of seven users, the CPA algorithm can improve the performance by more than two orders of magnitudes.

The immunity of the CDR to silence periods is examined in terms of the CID length in Figure 4.11, showing the PLR for the single user case for the back-to-back configuration, and the LS and CLS architectures. Recall that the useful power is still kept at -18 dBm and that the packets do not contain any preamble bits. The maximum length of CIDs can reach roughly 400, 600, and 800 bits for the CLS, LS, and the back-to-back configurations, respectively. A maximum of 200 bits of CIDs would guarantee zero packet loss for the three configurations; therefore our SAC-OCDMA burst-mode receiver meets all existing PON standards.

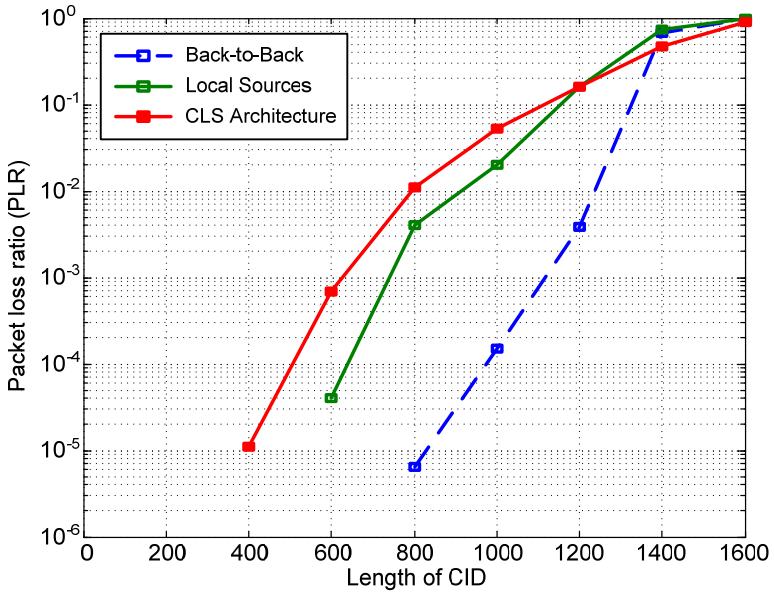

Figure 4.11. PLR vs. length of CID for different PON architectures.

Figure 4.12 shows the response of the CDR to bursty traffic, as well as the 2× oversampling mode of the CDR and the CPA operation. Three specific phase differences between packets are considered: (a) no phase difference $\Delta\varphi = 0$ rad (0 ps), (b) $\Delta\varphi = \pi/2$ rads (400 ps), and (c) $\Delta\varphi = \pi$ rads (800 ps). Whereas $\Delta\varphi = \pi$ rads (800 ps) represents a worst case phase step for the CDR operated at the bit rate, $\Delta\varphi = \pi/2$ rads

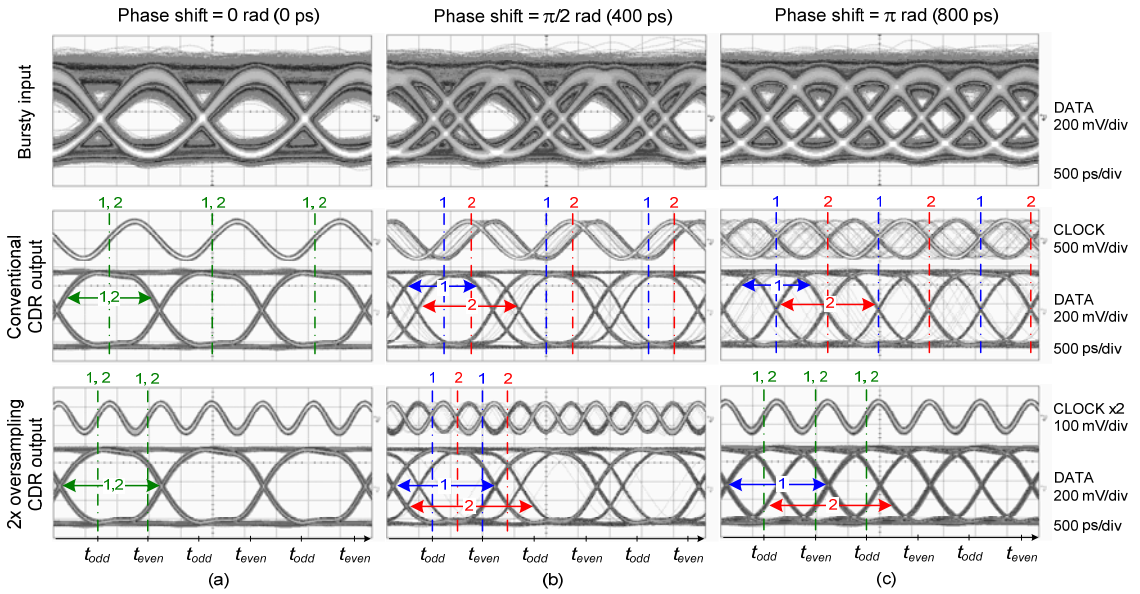

Figure 4.12. Response of the CDR to bursty traffic (packets with different phases): (a) no phase difference, (b) π/2 phase difference, (c) π phase difference.

(400 ps) phase step is the worst case scenario for the over sampling CDR at 2× the bit rate. The 2× oversampling mode produces two samples per bit which helps the CPA algorithm locking to the correct phase of the incoming packet. To understand how the CPA works, consider the case when there is no phase step ($\Delta\varphi = 0$ rads); path *O* correctly samples the incoming pattern (see t_{odd} in Figure 4.12a). For phase step $\Delta\varphi = \pi/2$ rads (400 ps), path *E* will sample the bits on or close to the transitions after the phase step. In this situation, the byte synchronizer of path *E* will likely not detect the delimiter at the beginning of the packet. On the other hand, the byte synchronizer of path *O* will have no problems detecting the delimiter (see t_{odd} in Figure 4.12b). The phase picker controller monitors the state of the two byte synchronizers and selects the correct path accordingly (path *O* in this particular case). Once the selection is made, it cannot be overwritten until the comma is detected, indicating the end of the packet. This process repeats itself at the beginning of every packet. The result is that the CPA achieves instantaneous phase acquisition (0 bit) for any phase step (±2π rads). That is, no preamble bits at the beginning of the packet are necessary.

4.5. Impact of PON Size on Local Sources versus CLS PON Architectures

In this section we examine the relative merits (cost and performance) of local sources versus centralized architectures. The power budget of a PON is an important parameter in the design, as it helps FTTH service providers to select the appropriate light sources and the convenient receivers for their network. The power budget is mainly determined from the PON physical architecture. The uplink power budget of the CLS architecture ($P_{Budget,CLS}$) is related to that of the LS architecture ($P_{Budget,LS}$) by the following equation:

$$P_{Budget,CLS} = 10\log\left(\frac{P_{CLS}}{P_{LS}}\right) - 10\log N - \alpha_F D + P_{Budget,LS} \qquad (4.3)$$

where, P_{CLS} and P_{LS} are the source power for CLS and LS architectures, respectively, N is the number of splits (or number of ONUs), α_F is the fiber attenuation in dB/km, and D is the feeder length in km. The first term in (4.3) represents the gain in relative power that can be achieved in CLS architectures; we expect P_{CLS} to be much greater than P_{LS}. The second and third terms represent the extra splitting losses and additional fiber attenuation in CLS architectures, respectively. In CLS architectures an EDFA can be used at the central office to increase the margin by compensating the extra losses terms in (4.3). Using a semiconductor optical amplifier (SOA) or a reflective SOA at ONU for modulation instead of the EAM reduces the amplification requirements in both architectures [40], [43], [44], [46], and [47]. Placing a gain saturated SOA at the central office can further reduce the intensity noise of BBS as in spectrum-sliced WDM PONs [56]. The possibility of integration of the external modulators (using silicon) can be advantageous from the cost point of view [103]. The selection of a powerful light source for CLS PONs also increases the power budget as in (4.3). The cumulative cost of light sources in LS architectures is N times the cost of a single local source, and this should be compared to the cost of the single high power source for the CLS solutions. Using powerful directly modulated LEDs at 622 Mbps could tilt costs in favor of LS architectures by eliminating the need for modulators. However, these super-luminescent

Table 4.1. Uplink power budget and link loss for both PON architectures.

		LS	LS (Effective)	CLS
Source Power [dBm]		2.83	-6.62	2.83
Loss [dB]	**RN Splitting**	**18.88**	**9.43**	**18.88**
	ODN Feeders	**3.95**	**3.95**	**8.07**
	Modulation	12.20	12.20	14.51
	Encoding	3.99	3.99	3.99
	DCF	2.41	2.41	2.41
	Decoding	6.42	6.42	6.42
	Total Loss	**47.85**	**38.40**	**51.28**
Amplification [dB]		36.56	36.56	40.84
Received Power [dBm]		-8.46	-8.46	-7.61

LEDs have cost comparable to that of the BBS we used, and they require temperature control.

Table 4.1 details the uplink power budget and optical losses in our experimental realization of the two SAC-OCDMA PON architectures. In the column marked LS (effective) we give the values when interpreting the combination of the BBS and the first 1×8 splitter (see Figure 4.3) as eight independent sources for each of the ONUs. Effectively, the total losses in the LS configuration was approximately 39 dB (excluding 9 dB losses through the 1×8 splitter incurred for experimental convenience), whereas the total losses in a similar CLS PON was roughly 52 dB. The 13 dB difference is the contribution of the extra 9 dB losses of the 1×8 coupler on the CLS first passing through RN before modulation, and the extra 4 dB losses for the unmodulated light traversing 20 km of SMF. For our experiment, examining the final two columns of Table 4.1, $P_{Budget,CLS}$= -48.45 dBm (excluding amplification), $P_{Budget,LS}$= -45.02 dBm (excluding amplification). Note that P_{CLS} /P_{LS} was chosen to offset the RN losses of 10logN dB, so the only remaining difference was the additional fiber losses.

The second 8×1 coupler in Figure 4.1a represents the splitting loss at the RN. From Table 4.1, the RN splitting losses represent the major source of losses, and would be higher for larger PONs with 1:32 or 1:64 splitting ratio. Fiber losses are the combinations of propagation losses (20 km and 40 km of SMF-28 for LS and CLS architectures,

respectively), and a 2.41 dB loss DCF. The modulation losses for the CLS PON is greater than that of the local sources, as the input power to the modulator is lower (see Figure 4.3); the light travels a 20 km feeder before it reaches the ONU. Encoding and decoding losses are related to the design of the codes and FBGs, namely, the code weight and the reflectivity of each frequency bin. The decoding losses shown in Table 4.1 include also a 3.5 dB loss of the 1×2 coupler at the balanced receiver. Modulation and encoding/decoding losses should remain almost the same for larger PONs. Because the EDFAs are not gain clamped, we note that the gain varies from one configuration to the other depending on the corresponding EDFA input power. The maximum received power levels for both architectures are illustrated in Table 4.1; recall that at -23 dBm we achieve error free operation for the two PON architectures. Practically, the gain of the EDFAs, as well as the source power, must be sufficient to overcome the losses and the limited sensitivity of the receiver. Using avalanche photodetectors (APD), for example, increases the link margin.

Extrapolating our results for larger PONs using (4.3), we note that in CLS architectures the loss budget goes up with the square of the number of splits, instead of being proportional to the number of splits for the LS solution. In other words, doubling the number of users in a LS architecture imposes an additional 3 dB loss, whereas for CLS PONs there is a 6 dB extra loss. The same relationship holds when increasing the PON physical reach. However, as discussed earlier this extra loss can be compensated using amplification at the OLT, or SOAs at the ONUs, without increasing the cost significantly.

4.6. Summary and Conclusions

We proposed and experimentally demonstrated different incoherent SAC-OCDMA PON physical architectures using a standalone burst-mode receiver at the OLT side. Local sources and centralized sources architectures have been examined. For experimental convenience, we examined only the two-feeder architecture; therefore, the effects of Rayleigh back-scattering are not addressed. Continuous and bursty upstream traffic for seven asynchronous users at 622 Mbps were considered for the BER and the PLR

measurements, respectively. We performed measurements at a bit rate of 666.43 Mbps when using FEC to account for its overhead. Furthermore, we analyzed the power budget and the relative merits of LS versus CLS architectures. A small penalty of 2 dB added to the CLS with respect to the LS architecture was measured at a BER of 10^{-9}. We presented a simple power budget equation relating CLS to LS architectures. Using that equation we can extrapolate our results to larger SAC-OCDMA PONs. We showed that CLS architectures experience double the ODN and RN losses of similar LS PONs, whether the two-feeder or single-feeder topology is used. Doubling the number of users imposes an additional 3 dB loss in LS architectures, whereas doing the same for CLS architectures imposes an extra 6 dB loss. CLS architectures can overcome these penalties using amplification at the central office, or even SOAs at the ONUs for modulation. Alternately, central office amplification can be used to more than double the number of users in LS SAC-OCDMA PONs. The selection of appropriate light sources for both architectures also plays an important role in the power budget, and can help increase the link margin.

The OLT receiver we designed features automatic detection of payload, clock-and-data recovery, instantaneous (0 preamble bit) phase acquisition for any phase step, and FEC with a RS(255,239) decoder. Furthermore, the receiver significantly reduced the intensity noise of the BBS, and other impairments, by quantizing (refer to the output of the CDR in Figure 4.12). We have also shown that the penalty added by the global clock due to the nonideal sampling is negligible. Error free transmission (uplink) was achieved for a fully loaded system of seven users for LS and CLS architectures. A coding gain of more than 2.5 dB at BER = 10^{-9} was reported and BER floors for five users (only for the CLS PON) and seven users were eliminated with FEC. The FEC had one order of magnitude worse performance than that predicted for a memoryless channel.

When using the CPA we have reported a zero PLR for up to four simultaneous users (for any phase difference between packets), and more than two orders of magnitude improvement for a fully loaded system (compared to using only the CDR without CPA) for the worst phase shift between packets. Our burst-mode SAC-OCDMA receiver proved to have a good immunity to silence periods in the sense that it can support several

hundreds of CIDs at 622 Mbps; therefore it is suitable for PON applications because the standards restrict the maximum CIDs to only 72 bits [21], [25].

Chapter 5

On the Performance of Self-Seeded RSOA-Based Transmitters for SS-WDM PONs

5.1. Introduction

Having now looked at our SAC-OCDMA solution for next generation PONs, we consider in this chapter, and in the following one, our proposed dense SS-WDM solution for upgrading the existing TDM PONs. Despite the good results we obtained for SAC-OCDMA, the power budget was critical and therefore OLT amplification was required even for LS architectures. Putting aside the splitting losses at the RN, the use of an

external modulator, together with the encoding and decoding operations contributed to more than 20 dB of losses. Furthermore, the 10 nm optical bandwidth used imposed the use of a DCF at the central office which adds more loss and increases cost. SS-WDM can support the same number of users as SAC-OCDMA for the same number of frequency bins; therefore, there is no advantage for SAC-OCDMA over SS-WDM in terms of capacity. Moreover, writing FBGs for SS-WDM is simpler, and narrower slices can be obtained, which makes SS-WDM more attractive in terms of spectral efficiency and bandwidth usage.

Recall that RSOA-based ONUs achieve both amplification and modulation without the need of additional/external devices [46], [47], relaxing the constraints on the power budget when the legacy PON infrastructure is exploited. Moreover, noise cleaning effects can be achieved when operating the RSOAs in the saturation regime [54]-[56]. Despite these advantages, the direct slicing of the ASE output of the RSOAs is not efficient from a power budget perspective, the power is simply too low and reliable communication is not possible without amplification.

Recently self-seeded RSOA-based transmitters have been proposed for WDM and SS-WDM PONs as discussed earlier in Chapter 3. Such transmitters are powerful enough to obviate the need for centralized seed sources and remotely pumped EDFAs. In the following chapter, we benefit from these high-power RSOA-based transmitters alongside with a recently proposed balanced receiver [19], to propose an innovative way of migration from TDM to dense SS-WDM, over the passive splitter and single-feeder based PON infrastructure.

We first study in this chapter the performance of self-seeded RSOA transmitters in terms of their wavelength coverage in the C-band. For this purpose we use a simple embodiment of the self-seeded RSOA transmitter using a circulator and a tunable filter. A more effective and lower cost implementation is presented in Chapter 6. Our use of a tunable filter in this chapter will allow us to easily tune over the 40 nm C-band, to test the efficiency of self-seeding dependence on the wavelength. For the first time to our knowledge, we try to assess the noise cleaning effect that can be achieved while using a

self-seeded RSOA. We experimentally demonstrate that self-seeded RSOA transmitters provide noise cleaning. The effect of filtering at the RN through AWGs in traditional SS-WDM PONs is also addressed. This chapter represents a motivation and an introduction to Chapter 6, where we try to better understand the challenges in combining self-seeding with noise cleaning, and the use of the balanced receiver that preserves the noise cleaning. In Chapter 6, we will also examine the possibility of colorless ONU operation through remote self-seeding, and address the architectural aspects, the power budget and the spectral efficiency issues.

5.2. A Proof of Concept Self-Seeded RSOA Transmitter

In this section, we experimentally demonstrate a simple yet flexible embodiment of a self-seeded RSOA transmitter as a proof of concept. We measure the BER in a back-to-back configuration, as well as over a 20 km PON link with and without dispersion compensation. To assess noise cleaning, we consider both the degenerate[1] receiver (DR), *i.e.*, one without a channel select filter (CSF), and the conventional receiver (CR) with a CSF. Recall that in a traditional SS-WDM PON, the AWG at the RN acts as a CSF, and therefore the performance is expected to be similar to that with the CR.

5.2.1. Principle of Data Erasure and Rewrite Operations

Before we go through the experimental demonstration of our self-seeded RSOA transmitter, we first discuss the principle of data erasure and rewrite operations as they are key elements for a successful self-seeded RSOA transmitter. The basic mechanism for data erasure is the gain compression of the saturated RSOA when the input signal has low extinction ratio (ER). Figure 5.1 shows the typical input-output characteristic of a SOA/RSOA; the amplifier output power saturates as the input power increases. Since the SOA/RSOA is operated in the saturation regime for data erasure, the difference between the mark and space levels is considerably reduced at the output of the amplifier, thus the

[1] This receiver has ideal noise cleaning, but is incompatible with WDM as there is no channel selection, hence the name degenerate.

input signal modulation is effectively erased. The unsuppressed input modulation is considered a source of noise and is referred to in this chapter as the residual output modulation.

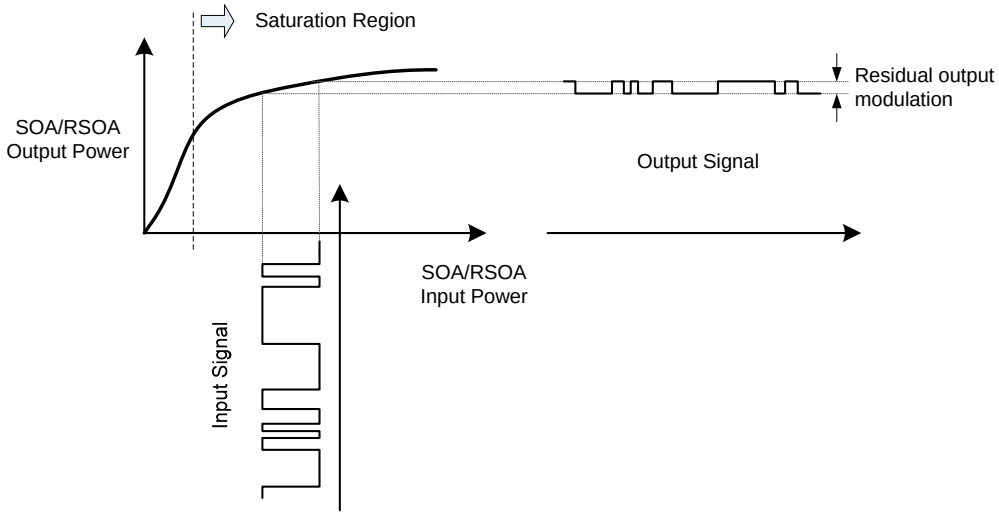

Figure 5.1. Principle of data erasure operation using a saturated optical amplifier.

For the same input modulation depth, increasing the input power drives the amplifier more into the saturation region improving the efficiency of the erasure operation by reducing the residual output modulation. In downstream remodulation techniques, already described in Chapter 3, the SOA/RSOA at the ONU is modulated with a higher ER upstream signal to be able to 'hide' the downstream residual output modulation. In our case, *i.e.*, the case of a self-seeded RSOA transmitter, the same signal is 'recycled'; therefore the ER should be optimized to tradeoff data erasure versus data rewrite for reliable communications. In other words, the ER should be kept low to favor data erasure, but should be increased at the same time for efficient rewrite operation.

5.2.2. Transmitter Architecture

Our proposed proof of concept self-seeded RSOA transmitter is shown in Figure 5.2a as a part of the experimental setup. The transmitter consists of a 3-port circulator, a tunable 30 GHz wide TB9 grating filter from JDS Uniphase and a 1×2 coupler. The bandwidth of the filter is wide enough to avoid lasing effects. The RSOA is self-seeded with a filtered

version of its ASE, while directly modulating its current. The current is modulated at 1.25 Gb/s with a low extinction ratio (ER) to favor erasure and remodulation inside the feedback look [90], [91]. Clearly a high ER facilitates detection; therefore there exists an optimum ER that permits both remodulation and reliable detection. A non-return-to-zero (NRZ) 2^7-1 pseudo-random binary sequence (PRBS) is used, in order to have a signal similar to the 8B/10B encoding of Gigabit Ethernet [40]. We found experimentally that a bias of 3.5 V and a 2 V peak-to-peak variation gave no apparent jitter and provided the correct trade-off on the ER. Using a 50/50 coupler and under these biasing conditions, the re-injected power was -4 dBm enough for saturating the RSOA we used (SOA-RL-OEC-1550 from CIP). The temperature of the RSOA is kept constant at 20°C throughout the experiment.

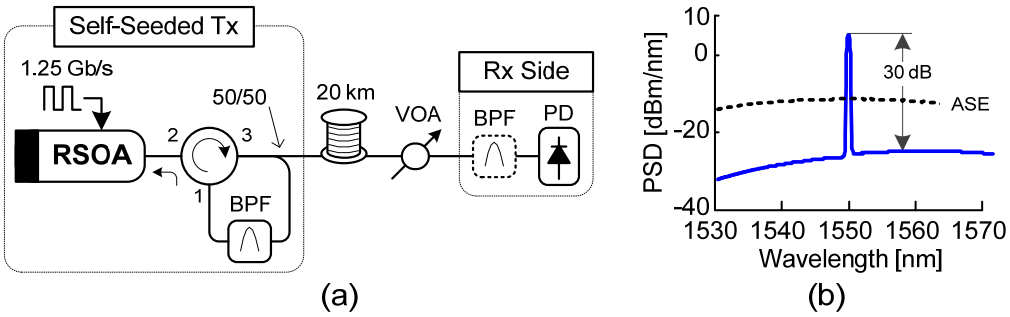

Figure 5.2. Proof of concept self-seeded RSOA transmitter: (a) experimental setup, (b) power spectral density (ASE: amplified spontaneous emission, BPF: band pass filter, PD: photodiode, PSD: power spectral density, Rx: receiver, Tx: transmitter, VOA: variable optical attenuator).

The power spectral density (PSD) at the output of the transmitter when the TB9 filter is tuned to 1550 nm is shown in Figure 5.2b. The output ASE from the RSOA before the 1×2 coupler is also plotted for comparison; the total ASE power at that point was 4 dBm. Re-injecting the RSOA with a certain color concentrates the ASE power of the RSOA into that specific waveband increasing the in-band power, *i.e.*, the power efficiency. Completely uncorrelated light becomes partially correlated, imparting noise cleaning effects. Our transmitter provides 30 dB of out of band ASE suppression, and 1 dBm of output power. Traditional slicing that simply filters the output ASE from the RSOA (the results are not shown), has output power of -21 dBm. Note that the output of our transmitter is 55 GHz due to the bandwidth enlargement of the RSOA [49].

The experimental setup in Figure 5.2a shows also the receiver side, where a photodiode[1] (PD) is used without any CSF for the DR, and a 30 GHz wide BPF (before the photodiode) similar to the one at the transmitter acting as a CSF for the CR.

5.2.3. BER Performance

Figure 5.3 shows the BER for a single-user system versus the received power in two configurations; 1) back-to-back, and 2) a 20 km feeder with standard single-mode fiber (SMF-28). The back-to-back configuration is tested with and without a CSF. The feeder configuration has no CSF, but is tested with and without the use of dispersion compensation fiber (DCF). An RF amplifier (JDS Driver H301-2310) and a 4th order 933 MHz Bessel-Thomson filter are used after photodetection. Error free transmission (BER<10^{-10}) is achieved for both configurations. Eye diagrams at -12 dBm of optical received power are also shown as insets.

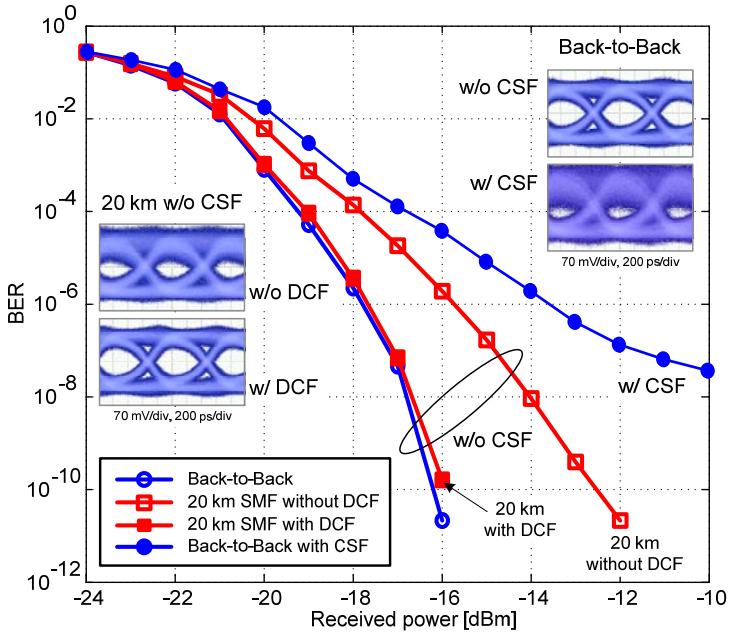

Figure 5.3. BER versus the received power at 1.25 Gb/s for a 55 GHz SS-WDM channel centered at 1550 nm, with and without a 30 GHz wide CSF.

[1] The photodiode we used in this experiment is the Agilent 11982A.

Compared to performance when no CSF is used, *i.e.*, the degenerate receiver (DR), a power penalty (measured at a BER of 10^{-10}) less than 0.25 dB is noticed for propagation over a compensated 20 km link. When no dispersion compensation is used there is a 3 dB penalty, yet the sensitivity is still less than -12 dBm at a BER of 10^{-10}.

A BER floor at ~10^{-8} appears when using a CSF (30 GHz wide) for the back-to-back configuration. This is expected due to the post-filtering effect. Since the RSOA is operated in the saturation regime, we benefit from its noise cleaning effects, but reduced due to post-filtering. It is clear from the corresponding eye diagram that the effect of noise cleaning is severely curtailed when using a narrowband CSF [54].

For error free operation with a CSF, a forward-error correcting (FEC) code is therefore needed. Another alternative is to use a wider CSF, but this would be at the expense of the spectral efficiency and the bandwidth usage [19]. In Chapter 6, we use a 100 GHz wide CSF, and we get almost the same BER floor for a 25 GHz wide SS-WDM channel at 1.25 Gb/s, which means less degradation in the performance[1].

5.3. Wavelength Coverage

The wavelength coverage of a transmitter is an important parameter that determines the network scalability. A colorless ONU should be transparent to all wavelength channels, so that all users have almost the same performance. Although RSOAs are now available for both the C-band and L-band, we focus here only on the C-band as we are using the SOA-RL-OEC-1550 from CIP.

5.3.1. BER Performance over a 40 nm Band

The wavelength coverage of our self-seeded RSOA transmitter from 1530 nm to 1570 nm is shown in Figure 5.4a in terms of the back-to-back BER performance with no CSF; the

[1] In an SS-WDM system the performance is limited by the intensity noise. The signal-to-noise ratio (SNR) is proportional to the optical bandwidth and inversely proportional to the electrical bandwidth [74]. For the same bit rate (1.25 Gb/s in our case), decreasing the optical bandwidth (from 55 GHz to 25 GHz in our case) degrades the performance even with the DR.

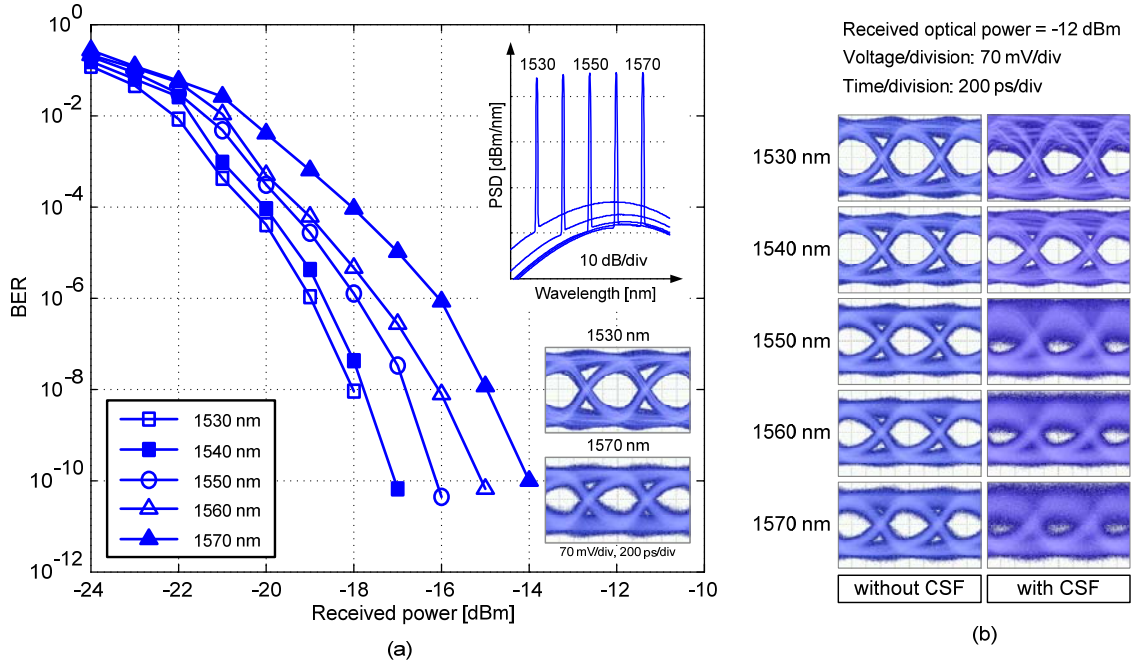

Figure 5.4. Wavelength dependence of BER for our self-seeded RSOA transmitter: (a) back-to-back BER performance at 1.25 Gb/s over a 40 nm band around 1550 nm, without a CSF, (b) back-to-back eye diagrams showing the effect of using a 30 GHz wide CSF identical to the slicing filter.

inset shows the corresponding PSD. The out of band ASE rejection varies from 27 dB to 33 dB from 1530 nm, to 1570 nm, respectively. Although our transmitter can operate from 1530 nm to 1570 nm with less than 1.5 dB power variation, there is more than 3 dB power penalty over this 40 nm band. We found that the noise cleaning in the RSOA is wavelength dependent (details are shown in the next subsection). Eye diagrams at -12 dBm for 1530 nm and 1570 nm are shown as an inset of Figure 5.4a. The tuning range of our 30 GHz filter could not exceed 1575 nm.

The AWG at the RN of a traditional SS-WDM PON acts as a CSF and therefore degrades the performance when gain saturated RSOAs are used. This effect is shown in Figure 5.4b for the different wavelengths. Eye diagrams measured at -12 dBm for the back-to-back configuration without a CSF corresponding to the BER in Figure 5.4a are shown, as well as the corresponding eye diagrams when using a CSF. At 1530 nm despite the CSF, we obtain error free transmission at -15 dBm (results are shown in Figure 5.5) and therefore a FEC is not needed.

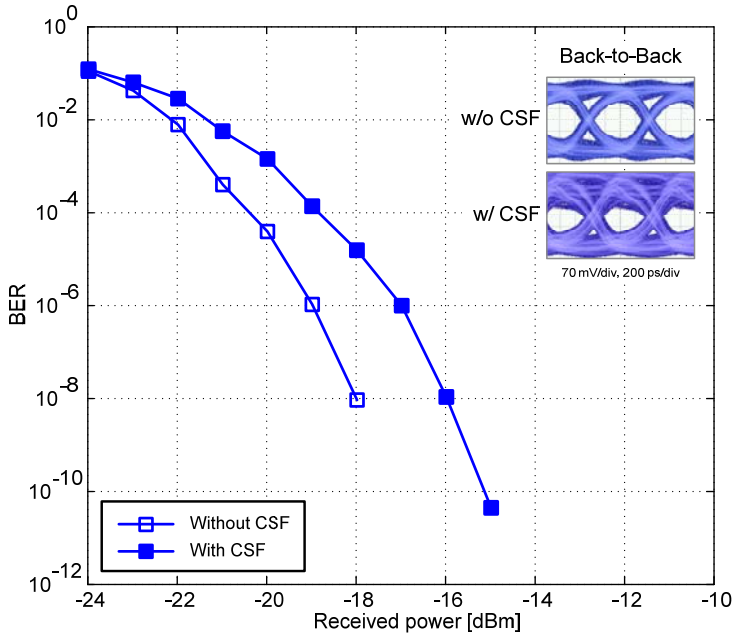

Figure 5.5. Back-to-back BER performance at 1530 nm with and without a 30 GHz wide CSF.

When a BER floor is present (as in Figure 5.3, for the back-to-back case without a CSF), many possibilities exist to exploit our high power RSOA transmitter in WDM PONs, using forward error correction to compensate for the degradation introduced by filtering at the RN. A FEC eliminates the BER floors and provides additional margin that can be used to add TDM users or increase the PON reach.

An interesting solution to avoid filtering exploits the existing TDM PONs RN consisting of passive splitters only. A balanced receiver [19] could retain our transmitter's noise cleaning. While some degradation is incurred relative to curves for the DR (Figure 5.3), the performance is much better than the CR. This is the subject of Chapter 6.

5.3.2. Noise Cleaning and Wavelength Dependence

In Figure 5.4 we see BER performance that gradually degrades when passing from 1530 to 1570 nm. This behavior can be explained by examining the wavelength dependence of key noise cleaning parameters, *i.e.*, the gain saturation curves and the relative intensity noise (RIN) characteristics of the RSOA. A typical RIN measurement at 1550 nm is reported in Figure 3.2. The cut-off frequency of the HPF effect is the same for

wavelengths from 1530 to 1570 nm, so this frequency is not wavelength dependent. The depth of the HPF is related to the level of gain saturation and we will see that this is not the same for all wavelengths.

The experimental setup used for the input/output power characterization, i.e., the gain saturation, is shown in Figure 5.6a. For convenience, 30 GHz band pass filters identical to the one in Figure 5.2a are used. Band pass filter 1 filters the ASE from a broadband source (BBS) and determines the wavelength of the input signal to the RSOA. An EDFA is used to boost the power and a VOA controls the input power to the RSOA, measured through a 2% tap. At the output another filter (BPF 2) is used to remove the ASE before measuring the power at port 3 of the circulator. The RSOA output power is calculated by accounting for the insertion losses of the circulator and the insertion loss of BPF 2.

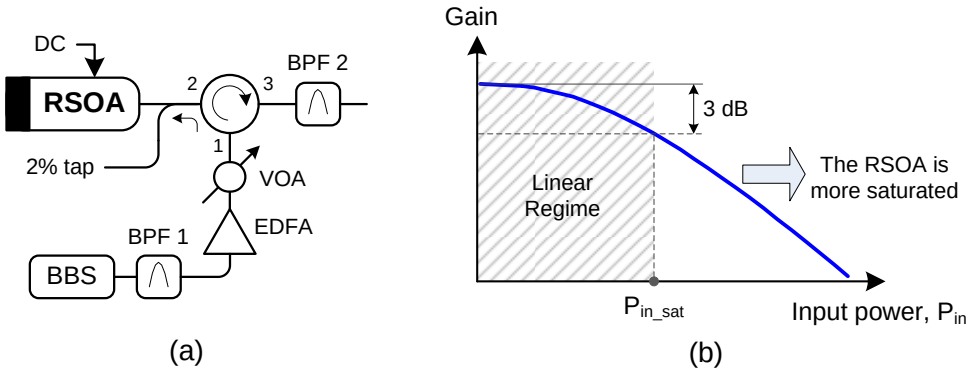

Figure 5.6. Input/output characteristics of the RSOA: (a) experimental setup, (b) typical gain versus input power curve. (BBS: broadband source, BPF: band pass filter, DC: direct current, EDFA: erbium-doped fiber amplifier, P_{in}: input power, P_{in_sat}: input saturation power, VOA: variable optical attenuator).

Figure 5.6b illustrates a typical gain curve for an RSOA showing the regions for both linear and saturation regimes. The gain of the RSOA is normally plotted against the input power. In the linear regime the gain is almost constant regardless of the input power. As the power is further increased the gain of the RSOA decreases (tends to zero) and the output of the RSOA is saturated (the output power remains the same even when the input power is increased). The input saturation power is defined as the input power where the output is 3 dB down from the small signal gain of the RSOA. Increasing the power beyond that level improves the performance of noise cleaning, as the RSOA is more

saturated and exhibits a deeper HPF effect. The ratio between the RSOA input power and the input saturation power determines the degree of saturation of the RSOA, and therefore it is a good metric for the noise cleaning effect.

The RSOA input saturation power is plotted against the wavelength in Figure 5.7 (square markers and left y-axis). We note a 1.25 dB variation in the input saturation power along the 40 nm band, with the minimum being around -19 dBm at 1550 nm. Although the optimum noise cleaning performance is expected to be around 1550 nm (for the same input power), we report the best BER performance at 1530 nm (see Figure 5.4a); the BER degrades with increasing wavelength. This is explained in Figure 5.7 by the degree of saturation as a function of the wavelength; there is a 3 dB difference over the 40 nm band in favor of the lower wavelengths. In our experiment (see Figure 5.2a) the RSOA input power varied slightly with wavelength because of the wavelength dependence of the RSOA gain (recall the 1.5 dB power variation over the 40 nm band) and the insertion loss of the JDS filter.

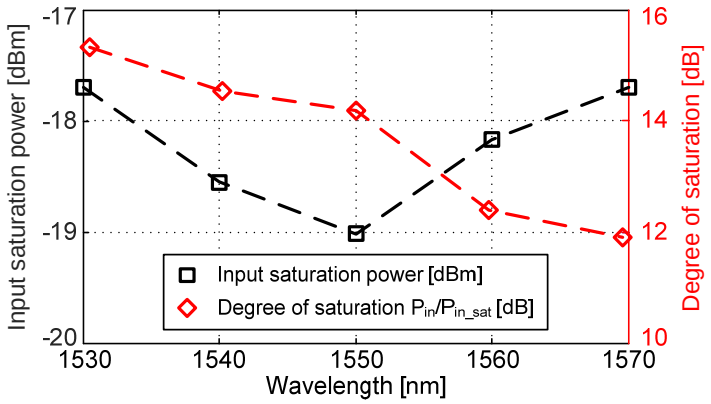

Figure 5.7. RSOA input saturation power and the degree of saturation versus wavelength.

In Figure 5.8 we plot the input power versus output power in linear scale (in mW) of the SOA-RL-OEC-1550 for various wavelengths. As an example, we show the average RSOA input power (for the 1550 nm case) and the input modulation depth. Biasing the RSOA at 3.5 V with a 2 V peak-to-peak modulation provided initially a 7.3 dB modulation depth at the input of the RSOA regardless of the wavelength under test. Due

to the gain squeezing of the RSOA, the signal is compressed when the amplifier is saturated, *i.e.*, the input modulation is almost erased, before being remodulated.

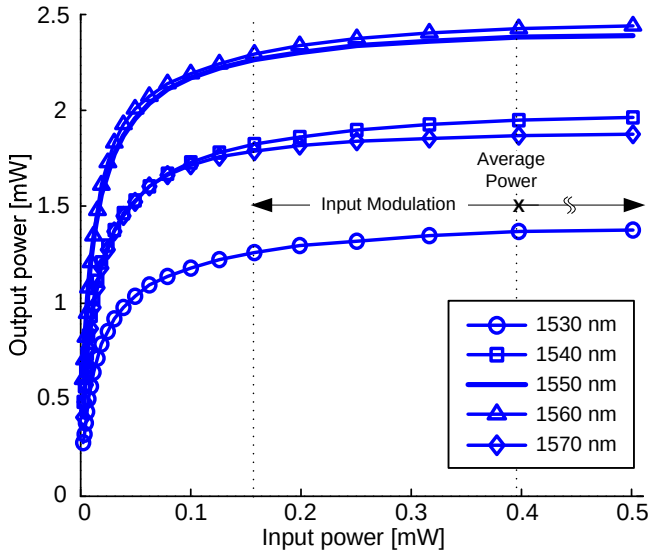

Figure 5.8. RSOA input/output power measurements for different wavelengths.

The efficiency of the data rewrite operation also explains the wavelength dependence of the BER performance. In Figure 5.9 we plot the residual output modulation as a function of the wavelength, the degree of saturation (Figure 5.7) is also plotted for convenience. Knowing the RSOA input power as well as the input modulation depth, the residual output modulation can be calculated from Figure 5.8 (in log scale). The efficiency of the data rewrite operation is higher at shorter wavelengths as the RSOA is more saturated. At

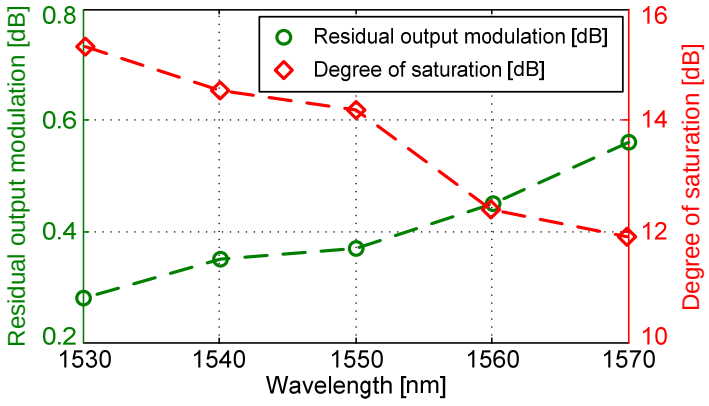

Figure 5.9 Residual output modulation and the degree of saturation versus wavelength.

1530 nm, the residual output modulation is 0.25 dB compared to 0.55 dB for 1570 nm, *i.e.*, the remodulation efficiency of the RSOA is better for shorter wavelengths.

5.4. Summary and Conclusions

In this Chapter we demonstrated a proof of concept self-seeded RSOA-based transmitter for dense SS-WDM PONs via a simple but flexible embodiment. The RSOA performs both modulation and amplification; up to 1 dBm of power is transmitted within a 55 GHz slice at 1.25 Gb/s. Error free transmission is achieved over a 20 km PON link without dispersion compensation using a degenerate receiver. The extinction ratio is optimized to favor both data erasure and reliable detection. Our transmitter exploits the entire C-band with a 3 dB penalty between 1530 nm and 1570 nm.

Further, since the RSOA is operated in the saturation regime to favor data erasure and remodulation, we can exploit possible noise cleaning effects due to the gain squeezing and the high-pass filtering effect of the RSOA. However, the performance was degraded when using a conventional WDM receiver with a CSF prior to the detection, due to the post-filtering effect.

In this chapter, we investigated the wavelength dependence of the noise cleaning effect and identified the challenges in combining self-seeding with noise cleaning. Recall that the main purpose of our self-seeded RSOA transmitter (using a circulator and a tunable filter) was only for a proof of concept demonstration and for studying the wavelength dependence of such transmitters over the C-band. In other words, the transmitter was not ‘optimized’ for noise cleaning.

In the following chapter, we migrate from the simple structure used in this chapter to a more efficient and a higher yielding setup. We propose a novel self-seeded RSOA transmitter using a *p*% reflective FBG [18]. The reflectivity is optimized to maximize the output power and the noise cleaning effect simultaneously. In addition to the degenerate receiver and the conventional receiver, we use a balanced WDM receiver recently proposed by Mathlouthi *et al.*, [19]. This novel receiver outperforms conventional WDM

receivers and can maintain the noise cleaning effect to a certain extent. Moreover, the migration path from TDM to dense SS-WDM, the architectural considerations, the power budget, and the network capacity are considered. We will further consider denser SS-WDM and go from 55 GHz to 25 GHz wide channels.

Chapter 6

Dense SS-WDM over Legacy PONs: Smooth Upgrade of Existing FTTH Networks

[1] Z. A. El-Sahn, W. Mathlouthi, H. Fathallah, S. LaRochelle, and L. A. Rusch, "Dense SS-WDM over legacy PONs: Smooth upgrade of existing FTTH networks," accepted in *IEEE J. Lightwave Technology*, February 2010, [18].

Abstract

We propose a hybrid passive optical network (PON) architecture supporting time-division multiplexing (TDM) and dense spectrum-sliced wavelength-division multiplexing (SS-WDM) over the legacy PON infrastructure. We use a fiber Bragg grating (FBG)-based self-seeded reflective semiconductor optical amplifier (RSOA) transmitter in conjunction with a recently proposed balanced receiver (BR); identical transceiver pairs are placed at the central office and customer side. Self-seeded RSOAs obviate the need for centralized sources, providing a high power, directly modulated source. Intensity noise mitigation of this thermal source is investigated by operating the RSOA in saturation and employing the recently proposed BR. We study the optimal reflectivity for seeding that balances signal power and noise cleaning to achieve the best bit error rate (BER) possible; channel widths are comparable with dense WDM when using coherent sources.

We experimentally demonstrate a symmetrical 1.25 Gb/s dense SS-WDM transmission over the legacy PON infrastructure using our optimized self-seeded RSOA transmitter and the BR. Using a reflective (18 ± 2%) FBG for self-seeding, we achieve up to 4.5 dBm of output power within a 25 GHz channel. Error free transmission (BER < 10^{-10}) is achieved over a 20 km feeder. We investigate the possibility of ONU colorless operation. The power budget allows 32 users (64 users with reasonable OLT amplification) to be supported over the existing PON infrastructure. Simulations show capacity increases to 128 users when a Reed-Solomon RS(255,239) forward error correcting code is used.

6.1. Introduction

Dense spectrum-sliced wavelength-division multiplexing (SS-WDM) is an attractive solution for increasing the capacity of future fiber-to-the-home (FTTH) access networks. Such systems benefit from the same advantages as WDM, while employing low cost incoherent light sources [104]. Currently, the capacity of existing FTTH passive optical networks (PONs) is under 100 Mb/s per client, as users share the aggregate bit rate using

time-division multiplexing (TDM) [2]. Bandwidth hungry applications such as broadband Internet access, high-speed file transfer, remote storage, video services with high-definition TV quality, high-quality online multi-party video gaming, etc, are driving the service providers to migrate from standard TDM-based PONs to high capacity future PONs [4], [5] with symmetric up and down stream bandwidths [105], and increased bit rate per user.

WDM increases the capacity of legacy PONs by assigning different wavelengths for different optical network units (ONUs), *i.e.*, different subscriber [14]. However, deploying WDM in existing PONs requires in most cases that the existing passive splitters at the remote nodes (RNs) be replaced with arrayed waveguide gratings (AWGs), as well as upgrading *all* optical line terminal (OLT) equipment and ONUs. OLT and ONU upgrades can be made on a per subscriber basis for our hybrid TDM/WDM solution allowing a gradual rollout of high bit rate clients [14]. The use of reflective semiconductor optical amplifiers (RSOAs) as incoherent sources lowers cost, but they suffer from severe intensity noise, forcing a tradeoff between the spectral efficiency and the bit rate [106].

6.1.1. Related Work

There are two separate research areas regarding WDM PONs that exploit RSOAs that are relevant to this work. One addresses the use of self-seeded RSOAs as ONU light sources, the other studies semiconductor optical amplifiers (SOAs) as noise cleaning devices. In this subsection we give a brief overview of this related work, and in the next subsection we outline our novel combination of these two separate and distinct research thrusts.

RSOAs have been widely proposed as inexpensive wavelength independent or ‘colorless’ ONU transmitters in WDM and SS-WDM PONs using centralized light sources [46], [48]. Given that the RSOAs can serve as incoherent light sources, researches have examined the possibility of eliminating the centralized source. In other words, instead of amplifying/modulating a signal originating at the central office, the RSOA modulates its own thermal emissions. To concentrate all available light into a particular WDM

waveband, and thus increase power, RSOAs can be self-seeding [84]-[87]. In such systems, the passive filtering device at the RN concentrates the ASE emission of the RSOA into one band, feeding back the light in that band only to the RSOA. The RSOA continues to amplify this band until no ASE appears outside the band. Please note that such systems require the legacy PON infrastructure be upgraded to AWGs at the RN.

When using thermal source for spectrum sliced WDM, intensity noise limits overall performance and incurs error floors. A rich body of research has examined the use of the nonlinear dynamics of SOAs to mitigate this intensity noise [107]. When no channel selection filter is used, the so called degenerate case for WDM, the noise suppression is remarkable. Unfortunately receiver side filtering using a conventional channel select filter finds the intensity noise returning in force. Typically wide filtering at the receiver can find a compromise between spectral efficiency and noise cleaning. Recently, Mathlouthi, *et al.*, [19] proposed a balanced receiver (BR) for dense SS-WDM systems that preserves significant noise cleaning so that dense WDM channel spacing can be achieved even with thermal sources.

6.1.2. Our Contribution

Previous studies used in-line SOAs to suppress the intensity noise of a separate thermal source, and did not involve the use of RSOAs in a combined role of thermal source and noise mitigation device. We confirmed that a self-seeded RSOA signal exhibits a significant reduction in intensity noise, comparable to centralized thermal sources that are amplified by the RSOA. We investigated the use of the recently proposed balanced receiver and confirmed that noise mitigation is preserved in the case of self-seeded RSOAs, as has been observed with in-line SOAs. In this paper we report on two aspects of the combination of self-seeding with balanced detection: 1) the optimization of spectral efficiency, and 2) the architectural impact for PONs.

We propose a self-seeded transmitter that uses a partially reflective (p%) fiber Bragg grating (FBG) directly following the RSOA. Optimizing power output for self-seeding requires that some light be shunted to seeding, while the balance of light exits the FBG as

the output signal. Optimizing noise cleaning requires that the SOA or RSOA operate in deep saturation. High FBG reflectivity guarantees that the RSOA is deeply saturated, thus improving noise suppression, although decreasing output power. Lower FBG reflectivity increases output power, but reduces noise suppression. We optimize the FBG reflectivity to balance these effects and minimize the bit error rate (BER).

The BER is a function not only of the FBG reflectivity, but also the filtering strategy used at the receiver. We consider three strategies: the degenerate[1] receiver (DR) without a channel select filter (CSF), the conventional receiver (CR) with a CSF, and the balanced receiver (BR) from [19] employing a notched filter in one receiver arm to achieve channel selection. We show experimentally that when using a self-seeded RSOA as a source, the BR outperforms the CR, and indeed, the BR performance approaches the DR performance. These results confirm that noise mitigation is preserved in the RSOA/BR architecture.

Our use of a p% reflective FBG for self-seeding contrasts with [84]-[87] where a totally reflective grating and 1×2 coupler combine to achieve 50% effective reflectivity. No attempt was made in those studies to examine the noise mitigation, and therefore no optimization of the reflectivity.

Our combination of self-seeded RSOA transmitter (Tx) with partial notch filtering at the receiver (Rx) has an interesting impact on the PON architecture. The use of passive filtering in the RN would essentially imply "receiver side" filtering that would negate the noise cleaning advantages, unless that filtering was extremely wide (very spectrally inefficient). The combined RSOA/BR strategy is therefore best targeted as an innovative method for gradually upgrading existing PONs from TDM to SS-WDM with no modification to the passive splitter RN. Legacy users remain on the main PON wavelength band, while SS-WDM users could be placed in another band or in the enhancement band (when not used for video).

The RSOA/BR combination offers tight wavelength packing (dense WDM), and

[1] This receiver has ideal noise cleaning, but is incompatible with WDM as there is no channel selection, hence the name degenerate.

therefore a viable means of rolling out a large number of higher paying, higher performance clients, without incurring the expense of upgrading the RN to stabilized AWGs, and upgrading all ONUs. The RSOA also affords a less expensive, more compact, and more powerful transmitter, compared to the traditional SS-WDM transmitter in [19]. We examine as well the possibility of remote self-seeding when placing the FBGs at the RN, to reduce ONU cost.

6.1.3. Multi-Channel Operation

The reader will note that all experimental results presented are for single user systems and no examination is made of system crosstalk. The spectral efficiency of our solution is implied by the ratio of bit rate and width of the FBG slicing filter. All single user systems assume a channel select filter that is the same bandwidth as the slicing filter. We examine dense WDM spacing (~30GHz) and bit rates of 1.25 Gb/s.

Cross-talk is an important factor when using wide filtering at the receiver to maintain noise cleaning. Depending on the channel width chosen the cross-talk or intensity noise could be the dominant noise source. When using balanced detection, however, the cross-talk was shown to have no discernable impact on performance [19]. Given the lack of equipment for multichannel operation, and the previously demonstrated robustness of BR to cross-talk, we focused our attention on the single channel experimental validation. Our contribution is finding the optimum balance of output power vs. noise mitigation via the p% factor.

While cross-talk is negligible in this study, the use of a multi-channel system will invoke significant splitting losses. We use our single channel measurements to analyze the power budget in multi-channel systems. We investigate the capacity of our proposed system both spectrally as well as via power budget.

The rest of this paper is organized as follows; after the introduction, we discuss in Section 6.2 the impact on PON architecture when using self-seeded RSOA transmitters. We focus on our proposed transmitter and discuss the challenges in combining noise cleaning with self-seeding and the optimization of the FBG reflectivity. In Section 6.3 we present how

TDM PONs can be migrated to dense SS-WDM PONs. Our experimental results are presented and discussed in details in Section 6.4. Technological and architectural considerations are highlighted in Section 6.5, as are performance and cost issues. A demonstration of remote self-seeding and a discussion of other requirements for colorless ONUs appears in Section 6.6. We summarize and conclude in Section 6.7.

6.2. Self-Seeded RSOAs: Impact on PON Architecture

The availability of inexpensive RSOAs is enabling next generation multiple wavelength PONs. The direct slicing (filtering) of the RSOA amplified spontaneous emission (ASE) for SS-WDM systems is impractical as it is not power efficient. Therefore, a centralized light source (placed at the OLT) is distributed to the ONU [19], [40], [46], [48], [56], and [91]. RSOAs at the ONU directly modulate the distributed source for the uplink, thus providing amplification while avoiding external modulators. In this configuration, the ONU transmitter is not wavelength-specific, hence relaxing the wavelength management on the customer side of the access network [48]. If the RSOA is operated in saturation it can also provide noise cleaning of the incoherent source, via the same mechanisms as do semiconductor optical amplifiers (SOAs) [56].

Several architectures exist for centralized sources. One solution uses a centralized continuous wave (CW) broadband, incoherent source at the OLT; the light is sliced by the AWGs at the RN and injected to an RSOA (or SOA) for uplink modulation. Another solution uses re-modulation techniques, injecting the RSOA with a low extinction ratio (ER) downlink signal to be re-modulated with higher ER upstream data to “recycle” the downstream data signal [40], [91]. Remotely pumped erbium-doped fiber amplifiers (EDFAs) have also been proposed to enhance the performance of RSOA-based hybrid WDM PONs, where a pump laser is located at the OLT and only erbium-doped fibers deployed near the RN [83].

In the following we discuss how self-seeding of RSOAs can obviate the need for a centralized source. Power levels are high, and noise cleaning will be exploited to a great degree by use of a recently proposed receiver. The combination of these novel

transmitters and receivers will enable dense channel spacing even with thermal (RSOA) sources. Most importantly, these upgrades can be achieved over the installed PON infrastructure as we will see in Section 6.3. The cost of these advantages is creating wavelength dependent ONUs; possible extensions to colorless operation will be examined in Section 6.6.

6.2.1. Proposed Self-Seeded RSOA-Based Transmitter

Recently, self-seeded RSOA-based ONU transmitters were proposed [84]-[87] whose launch power is sufficient to eliminate the need of a centralized light source at the OLT and remotely pumped EDFAs. In [85] remote self-seeding was proposed using a reflective filter at the AWG-based RN, however an EDFA was required at the RN (making the network no longer passive) to overcome round trip losses and to ensure sufficient power is re-injected to the RSOA. To overcome such problems, local self-seeded RSOA transmitters were proposed in [86] and [87] where a 100% reflective FBG placed at the ONU is used for self-seeding.

Our first goal is to confirm self-seeded operation of the RSOA using a commercially available optical filter (the tunable 30 GHz wide TB9 grating filter from JDS Uniphase in the upper setup of Figure 6.1a). Next we will examine optimization of the FBG reflectivity (p%) at the ONU as shown in the lower setup of Figure 6.1a. Instead of maximizing launched power as was done in the past, we will optimize bit error rate. Due to the nonlinear interaction in the RSOA (see the next subsection on noise cleaning), maximizing the launched power does not minimize the BER when using a receiver designed to exploit noise cleaning to its fullest potential.

The RSOA is self-seeded with a filtered version of its ASE, while directly modulating its current with a low extinction ratio (ER) to favor erasure and remodulation inside the feedback loop [40], [91]. Clearly high ER facilitates detection; therefore there exists an optimum ER that permits both remodulation and reliable detection. We employ a non-return-to-zero (NRZ) 2^7-1 pseudo random binary sequence (PRBS), in order to have a signal similar to the 8B/10B encoding of Gigabit Ethernet [40]. We found experimentally

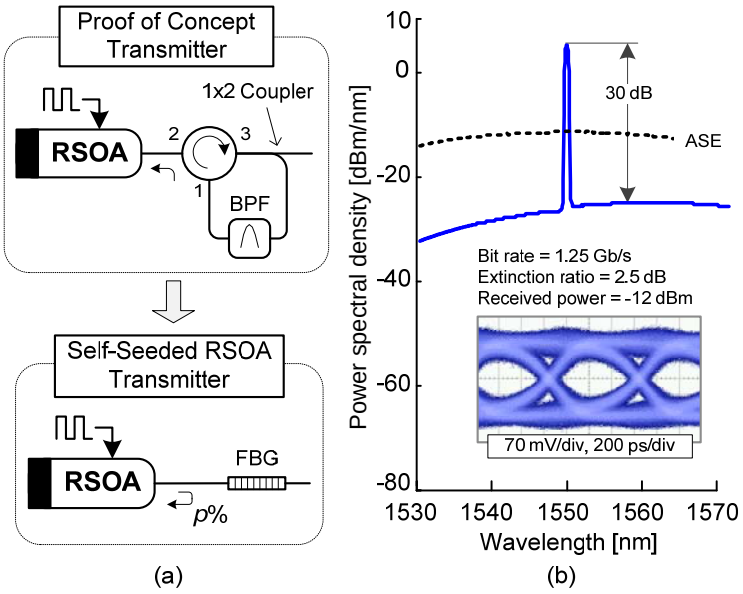

Figure 6.1. (a) The proposed self-seeded RSOA transmitter using a reflective FBG as well as an alternate configuration for proof of concept, (b) Power spectral density for a 55 GHz channel at 1550 nm.

that a bias of 3.5 V and a 2 V peak-to-peak variation gave no apparent jitter and provided the correct tradeoff on the ER. Using a 50/50 coupler and under these biasing conditions, the re-injected power was -4 dBm enough for saturating the RSOA we used (SOA-R-OEC-1550 from CIP).

The power spectral density (PSD) at the output of our proof of concept transmitter is plotted in Figure 6.1b when the TB9 filter is tuned to 1550 nm. The spectrum is enlarged after passing through the RSOA so that the 3 dB bandwidth is now 55 GHz. The output ASE from the RSOA before the 1×2 coupler is also plotted for comparison; the total ASE power at that point was 4 dBm. The transmitter provides 30 dB of out of band ASE suppression and 1 dBm of output power. Traditional slicing of the RSOA ASE (not shown), yields out of band ASE suppression of 38 dB and output power of -21 dBm. Self-seeding concentrates the ASE power of the RSOA into a specific band increasing the in-band power, *i.e.*, the power efficiency.

A back-to-back eye diagram at 1.25 Gb/s and -12 dBm of photo-detected power is shown as an inset of Figure 6.1b, when no CSF is used before detection, *i.e.*, for the DR. The clean eye is due to both the saturation effects in the RSOA that leads to noise cleaning of

incoherent light, and the use of the DR that preserves noise cleaning (by obviating optical filtering). Completely uncorrelated light becomes partially correlated, imparting noise cleaning effects. Not only are self-seeded RSOA outputs greater power, they also have low intensity noise. Unfortunately much of the noise cleaning effect is lost when using a channel select filter [54], [56], such as the typical use of an AWG in the RN.

6.2.2. Noise Cleaning in SS-WDM Using a Balanced Receiver

In order for the noise cleaning to carry through to reception, optical filtering should be avoided as reported in [54]. Recently, Mathlouthi, *et al.*, proposed and demonstrated a balanced receiver for SS-WDM systems that preserves much of the noise cleaning achieved by semiconductor optical amplifiers even in dense WDM channel spacing [19]. The upper arm of this receiver is an all-pass filter and the lower arm is a notch filter centered on the desired channel, as shown in part in Figure 6.2. An FBG operating in transmission serves as a notch filter; the coupling ratio of the 1×2 coupler is carefully selected to ensure balancing thus reducing channel cross-talk. The bandwidth of the notch filter is designed to be larger than that of the self-seeding FBG to allow a certain detuning between the transmitter and receiver due to possible temperature variations at the ONU

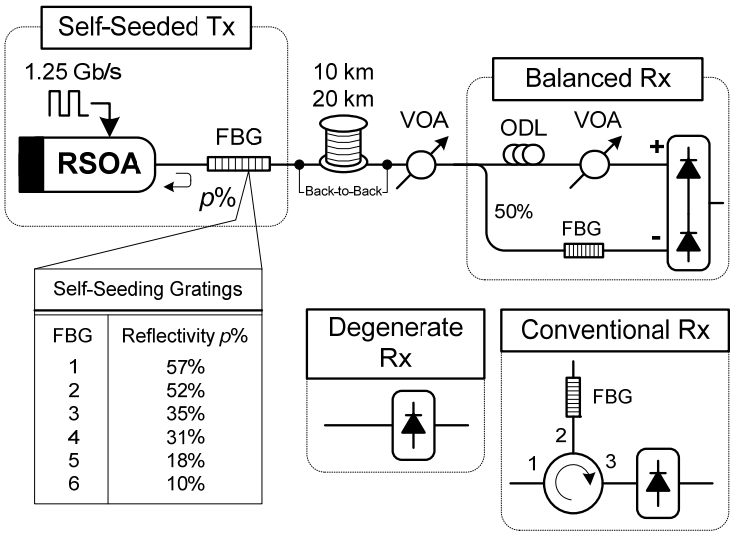

Figure 6.2. Experimental setup showing our self-seeded RSOA transmitter with the three receiver structures under test and a table with the FBGs used for self-seeding (ODL: optical delay line, VOA: variable optical attenuator).

side. While two photodetectors are used in this solution, the cost of the receiver is not significantly higher than that of standard SS-WDM systems.

Recall that filtering a noise-cleaned signal deteriorates its performance. If the channel select filter (CSF) bandwidth is wide enough compared to the WDM slice width, the performance can still be acceptable [54], [56], however the channel spacing will be high, reducing the spectral efficiency. Dense SS-WDM using self-seeded RSOA transmitters can be efficiently achieved using instead the BR. In our proposal the FBG used at the transmitter is less than 20% reflective (as will be seen in Section 6.4.3), therefore it is not a classical filter; the post-filtering effect was observed for a single pass through a filter with100% transmissivity. In our case the dynamics are much more complex. The filter is building up the output signal using feedback, working with the RSOA dynamics to achieve (not destroy) noise cleaning. Passive post filtering after our FBG does destroy this self-seeded noise cleaning as it does in other systems using SOAs for intensity noise cleaning.

Note that previous demonstrations of this recently proposed balanced receiver for noise cleaning used SOAs and external modulation. Our proposal is the first examination and optimization, to our knowledge, of noise cleaning on a self-seeded RSOA. Our RSOA-based transmitter greatly reduces the complexity and cost over the architecture in [19] as the RSOA performs modulation, amplification and noise cleaning at the same time.

An FBG with partial reflectivity is the key to minimizing the bit error rate by trading off noise cleaning versus transmitter output power. For optimal noise cleaning, the RSOA should be deeply saturated requiring a certain amount of power be fed-back to the RSOA, and therefore affecting the output power. Therefore we fix the channel (slice) width of the FBG in Figure 6.1a, and vary reflectivity (values are shown in Figure 6.2) to achieve various levels of saturation. Reflectivity greater than the optimum decreases the output power, without sufficiently enhancing the noise cleaning. Based on our original experimentation with the JDS tunable filter (and knowing the transmitter output power and the RSOA seed power), we set the FBG bandwidth to 37.5 ± 2.5 GHz, and fabricated six chirped FBGs with reflectivities ranging from 57% to 10%; the group delay

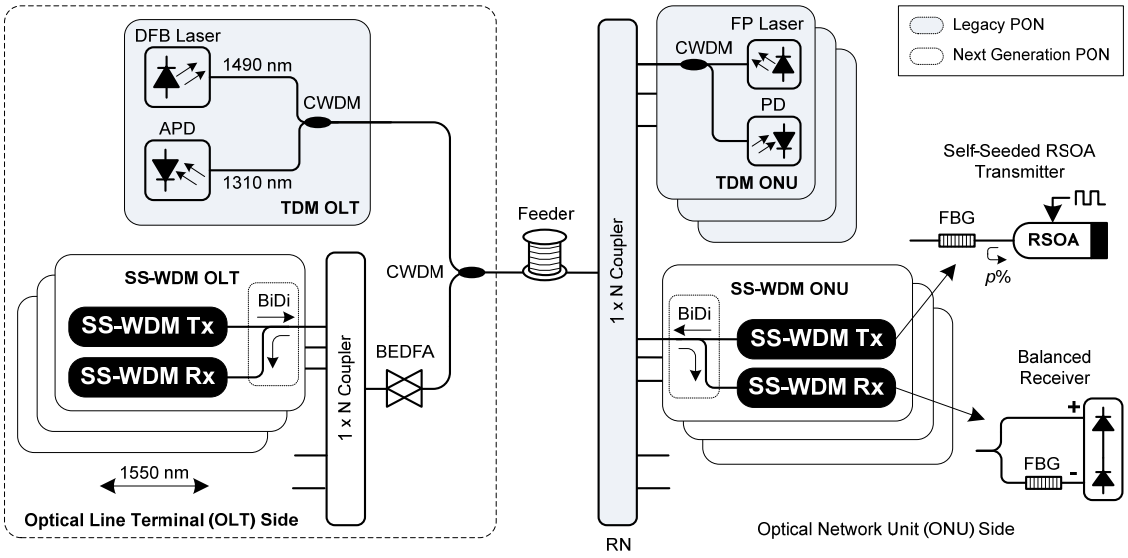

Figure 6.3. Hybrid dense SS-WDM PON and TDM PON over the existing PON infrastructure (APD: avalanche photodiode, BEDFA: bidirectional EDFA, BiDi: bidirectional, CDWM: coarse WDM, DFB: distributed feed-back, FBG: fiber Bragg grating, FP: Fabry-Perot, PD: photodiode, Rx: receiver, Tx: transmitter).

response was controlled to avoid dispersion-like problems. In Section 6.4 we find the optimal reflectivity experimentally. To implement the BR adapted to our choice of self-seeding FBG, we fabricate a 100 GHz wide FBG to serve as a notch filter for the BR and a CSF for the CR when operated in transmission and in reflection, respectively.

6.3. Dense SS-WDM over the Existing PON Infrastructure

In this section we take the opportunity to discuss how the transmitter and receiver pair we propose can be exploited over the existing PON infrastructure. Typically, a PON has a physical tree topology with the OLT located at the root and the subscribers connected to the leaf nodes of the tree through a passive coupler, as depicted in the shaded portion of Figure 6.3. Existing PONs are TDM-based; a single transceiver is located at the OLT and serves N legacy ONUs. A coarse WDM (CWDM) filter is used at both terminals to separate the up-stream (1310 nm) and downstream (1490 nm) traffic) [2]. The 1550 nm band is normally reserved for video distribution in the PON standards. While the PON standards specify a maximum feeder length of 20 km and a maximum split ratio of 1:64

for gigabit PON (GPON), in practice the maximum reach of 20 km and a PON split of 1:32 cannot be achieved simultaneously [108].

Figure 6.3 **s**hows also the necessary upgrades at the OLT and ONUs to support dense SS-WDM in the 1550 nm band within the legacy passive splitter-based infrastructure. At the central office a coupler similar to the one already installed at the RN is added, and a bidirectional erbium-doped fiber amplifier (BEDFA) is used to compensate for the added coupling losses. The coupler and the BEDFA can be easily integrated into a lossless coupler using an erbium-doped waveguide amplifier. CWDM filters are used at the OLT to separate the three wavebands. Bidirectional (BiDi) modules (also called wavelength couplers) are used to separate uplink and downlink.

Identical dense SS-WDM transceiver pairs are used from both network sides for new clients that will exploit the high data rates achievable by introducing multiple wavelengths. Each transceiver is equipped with a self-seeded RSOA-based transmitter identical to the one in Figure 6.1a, and the BR [19] seen in Figure 6.3. Subcarrier multiplexing (SCM) can be used to separate the uplink and downlink traffic for full duplex communication when the same wavelength is used in both directions [43]. The architecture is flexible enough to allow other techniques to be used for full duplex operation. The entire C-band can be exploited due to the availability of RSOAs with bandwidths as large as 40 nm.

Currently, the modulation speed of RSOAs is limited up to 2.5 Gb/s by current technologies, which is sufficient for FTTH access networks. For field deployments, polarization independent RSOAs in TO-CAN packaging are commercially available at very competitive pricing (already in small quantities the cost is a few hundreds of dollars), making our solution a potentially cost-effective upgrade for existing PONs. Compared to traditional SS-WDM PONs, our architecture offers reduced PON capital expenses (CAPEX) as it exploits current generation equipment, and mature inexpensive splitters. Challenges remains for splitting loss in scaling the network (compared to AWG-based PONs) and is discussed in Section 6.5. The possibility of colorless ONU operation is discussed in Section 6.6.

6.4. Experimental Results and Discussions

In this section, we experimentally study the performance of our proposed self-seeded RSOA transmitter with the BR as well as the CR and DR. We find the optimum value of the reflectivity of the self-seeding FBG in order to benefit from both self-seeding and noise cleaning.

The DR enjoys all noise cleaning advantages, while the BR does better than other filtering scheme, but still suffers from reduced noise cleaning, even in the single user case. An im-portant conclusion from [19] is that the BR does not expe-rience any further performance loss when adjacent channels are present, *i.e.*, loss in noise cleaning dominates the perfor-mance, not adjacent channel crosstalk. For this reason we confine our experimentation to the single user case. Note that per [19], the crosstalk penalty (7 channels) was negligible even at 10 Gb/s for 30 GHz channels spaced by 100 GHz (our tested channel allocation).

As the RSOA is deeply saturated (to benefit from noise cleaning), it acts as a high pass filter and reduces the effect of Rayleigh backscattering, reflection interferences, and ASE. Therefore, the effect of Rayleigh backscattering and such in-band crosstalk is negligible.

6.4.1. Experimental Setup and FBG Characterization

Figure 6.2 **s**hows the experimental setup used to evaluate the optimum value of the reflectivity of the self-seeding FBG. In addition to the BR, the DR and CR are examined as a reference. The RSOA is directly modulated at 1.25 Gb/s with an NRZ 2^7-1 PRBS. The bias is kept at 3.5 V and the signal peak-to-peak variation at 2 V for optimum data erasure and remodulation; RSOA temperature is maintained at 20^{o}C.

At the transmitter side we use our proposed self-seeded RSOA transmitter with six different FBGs as listed in inset table of Figure 6.2. Standard single mode fiber (SMF-28) of 10 or 20 km is used to represent the PON feeder; no dispersion compensation is used. Since the RN contributes only to splitting losses, we forgo a 1×N coupler; in Section 6.5, we calculate power budget and maximum supported splitting ratio.

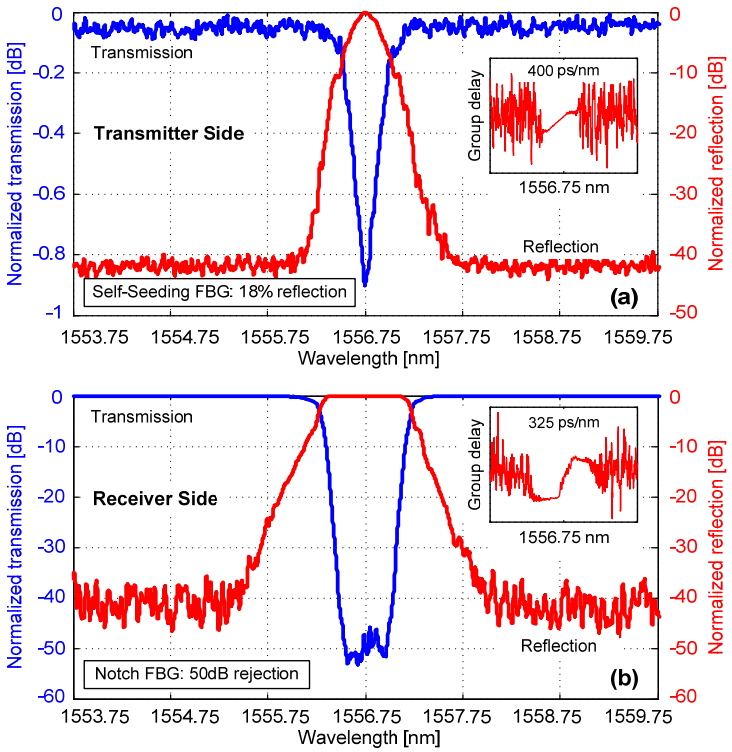

Figure 6.4. Characterization of the 18% self-seeding FBG used at the transmitter and the FBG used with both the BR and the CR.

At the receiver side a variable optical attenuator (VOA) is used to control the received power for the BER measurements. For the BR a 3 dB coupler is used as in [19]; at the lower arm a notch filter implemented using an FBG working in transmission is used. A variable optical delay line (ODL) is used in the upper arm and is adjusted to maintain good synchronization between the signals at both arms. Another VOA minimizes cross-talk by assuring that the out of band signals (including ASE) are exactly canceled by balanced detection.

The DR is simply a photodiode (PD) without any CSF, whereas the CR uses a circulator and the same notch filter FBG as the BR, but now operated in reflection as a CSF. An 800 MHz balanced PD from New Focus is used for all three receiver types. The PD is followed by an RF amplifier (JDS H301-2310) and a 4^{th} order 933 MHz Bessel-Thomson low-pass filter (LPF) to suppress out of band noise.

All FBGs are mounted on stretchers and their wavelength is tuned to 1556.75 nm with ± 0.05 nm precision. In Figure 6.4 we plot the normalized transmission and reflection

response of the 18% reflective self-seeding FBG (Figure 6.4a) as well as the notch filter FBG (Figure 6.4b). All the gratings were designed having a Gaussian profile in reflection. The self-seeding FBG 5 is exactly 35 GHz wide in reflection, whereas the notch filter FBG is 100 GHz wide in reflection and has 50 dB of rejection. The group delay responses of both FBGs are shown in the insets.

The 100 GHz wide FBG at the receiver is considered as a wide CR and does not degrade the performance considerably compared to a CR with a CSF having a bandwidth equal to that of the SS-WDM channel [19], [54]. This represents the best compromise of spectral efficiency and noise cleaning for a standard channel select filter, *i.e.*, optimal bandwidth. This identical width is used for the BR notch filter. While this leads to some compromise on spectral efficiency, the BR will still see much better noise cleaning than the CR. The relatively wide channel spacing allows for a certain wavelength drift due to possible temperature variations when the FBGs at the ONUs are not packaged using a temperature compensating package [109], especially when the ONUs are located outdoor.

6.4.2. Characterization of the Proposed Transmitter

All six FBGs listed in Figure 6.2 were tested, however, we only present results for FBG 3, FBG 4, FBG 5, and FBG 6 as FBG 1 and FBG 2 have reflectivities far from the optimum. The output PSDs (exiting the self-seeded transmitter) are plotted in Figure 6.5. Judging strictly by output power, decreasing the reflectivity of the FBG from 35% to 10% increases the output power from 3 dBm to 5 dBm. The output ASE from the RSOA without self-seeding is also plotted in dotted lines. FBG 5 (p = 18%) gives the optimum performance in terms of the out of band ASE rejection; the optical signal-to-noise ratio (OSNR) is increased by 4 dB as compared with FBG 6, while output power is only decreased by 0.5 dB, less output power than FBG 6. The seed power for FBG 5 is -6 dBm, enough to saturate the RSOA and improve noise cleaning. Note the output frequency band and 3-dB bandwidth of 25 GHz due to the transmission response (Figure 6.4) of the FBGs. In the case of the JDS filter implementation, the filter transmission response is flat over all wavelengths leading to bandwidth expansion due to nonlinear effects in the RSOA.

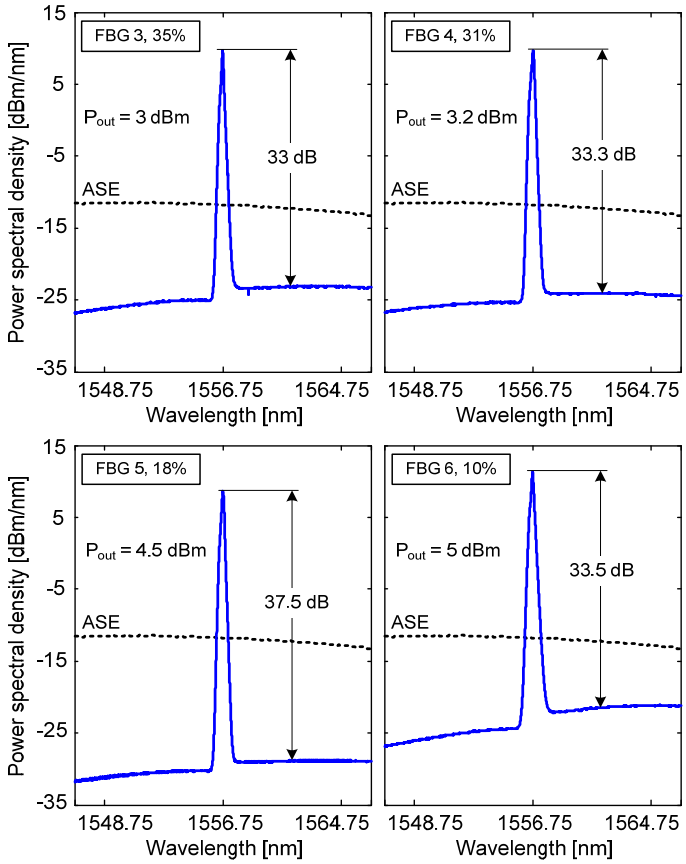

Figure 6.5. Power spectral density at the output of our proposed self-seeded RSOA transmitter for FBGs with 35%, 31%, 18%, and 10% reflectivities, compared to the output ASE from the RSOA without self-seeding.

6.4.3. Optimization of the BER Performance

Ultimately we wish to optimize bit error rate performance rather than output power or output OSNR. We conduct back-to-back transmission experiments for each reflectivity and measure bit error rates for each of the three receivers under evaluation, reported in Figure 6.6. The horizontal axis represents the photo-detected power, *i.e.*, the power at the PD and not at the receiver input. The degenerate receiver (no receiver side filtering, circle markers) shows the best performance and serves as a benchmark. FBG 5 at 18% gives the best performance among the reflectivities tested. The same trend can be observed for the set of curves for the BR (square markers) with the optimum performance for 18% reflectivity. This demonstrates the tradeoff between noise cleaning and self-seeding already discussed. As the CR (triangle markers) suffers a significant loss in noise

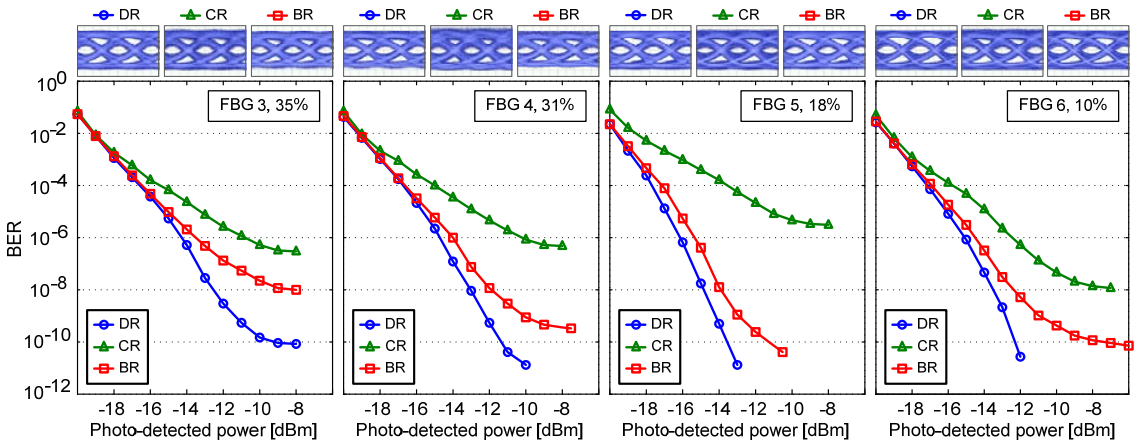

Figure 6.6. Back-to-back BER performance corresponding to the same FBGs in Figure 6.4 when using the three receiver options (BR: balanced receiver, CR: conventional receiver, DR: degenerate receiver).

cleaning advantage [54], the trade-off between crosstalk and noise cleaning is different for this receiver, with a minimum for FBG 6 (p = 10%). The BR outperforms the CR as already demonstrated in [19] and approaches the performance of the DR for optimal FBG reflectivity. Eye diagrams at -12 dBm are also provided.

Having established an optimum reflectivity exists between 31% and 10%, we next examine the sensitivity of the optimality in the neighborhood of 18%. We fabricated two additional FBGs with 13% and 23% reflectivities and tested them with the BR. In Figure 6.7 we plot the sensitivity versus the FBG reflectivity at BER 10^{-9} and 10^{-10}. The back-to-back BER measurements as well as the corresponding eye diagrams at -12 dBm photo-detected power are shown as an inset. We conclude that the optimum reflectivity would be 18% ± 2%. This optimum is not unique; it depends on the characteristics of the RSOA and the channel 3 dB bandwidth. The key idea is to get the good amount of seed power that optimizes the self-seeding and noise cleaning simultaneously. Note that while our results based on both OSNR and BER optimality coincided in this experiment (both were maximized by FBG 5 at 18%) this is not always the case as noise statistics for noise cleaning are in general highly non-Gaussian [19].

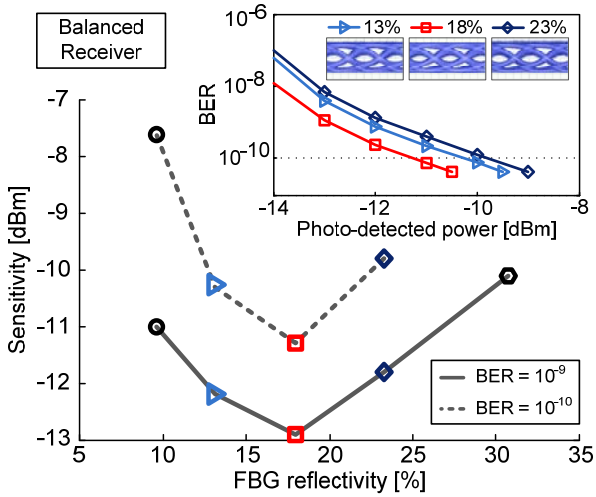

Figure 6.7. Sensitivity vs. FBG reflectivity for the BR.

6.4.4. Uplink/Downlink Transmission

We next move from back-to-back to propagation experiments using FBG 5. The self-seeded RSOA transmitter is modulated at 1.25 Gb/s across symmetrical 10 km and 20 km PON links, with the BR at the receiver side, per Figure 6.2. The BER performance is shown in Figure 6.8, where we plot the BER measurements (unfilled markers) for a 10 km (circle markers) and a 20 km (square markers) feeder. A dispersion penalty of 2.3 dB is discernable for the 10 km case when comparing with back-to-back measurements; at 20 km the penalty is an additional 3 dB due to additional fiber attenuation and dispersion. Error free (BER below 10^{-10}) performance is achieved for both feeder lengths. Eye diagrams at -12 dBm are shown as an inset. We also plot simulations (filled markers) of forward error correction (FEC) performance based on the measured BER without FEC. Reed-Solomon RS(255,239) coding was assumed, as well as a memoryless channel and orthogonal signaling. In this case, the symbol error P_{S_FEC} rate after FEC is related to the symbol error rate before without FEC (P_S) by

$$P_{S\_FEC} \approx \frac{1}{2^m - 1} \sum_{j=t+1}^{2^m-1} j \binom{2^m - 1}{j} {P_S}^j (1 - P_S)^{2^m - 1 - j}$$

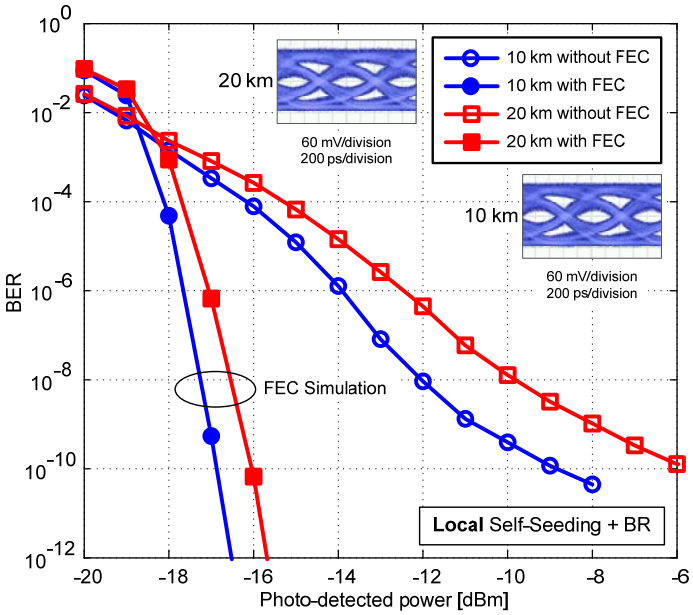

Figure 6.8. BER performance at 1.25 Gb/s with local self-seeding and BR.

where m = 8 bits/symbol and t = 8 is the number of symbols errors that can be corrected per frame [102]. The symbol error rate P_S is related to the measured BER (P_B) by

$$P_S = 1 - (1 - P_B)^m$$

We anticipate a coding gain of 7.8 dB and 10 dB for the 10 km and 20 km cases, respectively.

6.5. Power Budget and Spectral Efficiency

Exploiting the legacy infrastructure requires that our SS-WDM channels have sufficient power to overcome the significant splitting losses incumbent in this architecture. Self-seeding improves the power margin, while noise cleaning and FEC improves performance (and spectral efficiency). With BER experiments and FEC simulations, we calculate the power budget for the proposed PON architecture in Figure 6.3.

The BEDFA only compensates the losses of the 1×N coupler at the OLT, *i.e.*, the BEDFA and the coupler act together as an integrated lossless coupler. The total losses L from the

transmitter output to the receiver input for both uplink and downlink directions can be given by

$$L = 2L_{BiDi} + L_{CWDM} + \alpha_F D + 10\log N$$

where L_{BiDi} and L_{CWDM} represent the insertion losses of the bidirectional modules and the CWDM filter, respectively. We adopt typically values $L_{BiDi} = L_{CWDM} = 0.5$ dB. The third term represents the propagation losses, where $\alpha_F = 0.2$ dB/km is the fiber attenuation around 1550 nm, and D is the length of the feeder plus the distribution drop fiber (DDF) in kilometers. The last term gives the splitting losses at the RN, where N is the number of splits, or the number of ONUs per OLT. In our analysis we consider a symmetric PON running at 1.25 Gb/s, a 2 km DDF, and a 10 or 20 km feeder without dispersion compensation.

From Figure 6.8 we calculate the receiver sensitivity at 10^{-10} BER; 3 dB is added to the photo-detected power to account for the 1×2 coupler, so sensitivity is calculated at the input of the BR. Given the 4.5 dBm transmitter output power we compute the available power budget and therefore, the maximum PON capacity. The results are presented in the first two rows of Table 6.1; please note that the remote self-seeding results will be discussed in the next section.

In our experiment we used a JDS H301-2310 as an RF amplifier after the PD. From the BER measurements we note that the receiver sensitivity is poor due to the 11 dB noise figure (NF) of that amplifier. Per [110], the NF of the RF amplifier at the receiver affects the sensitivity linearly. While we would have preferred running experiments with a low noise amplifier, none was available in the laboratory. To achieve a more realistic power budget, we repeat our calculations using specifications from the MITEQ AM-1300 low noise amplifier with only 1.6 dB NF. The receiver sensitivity is enhanced by 9.4 dB relative to our JDS driver, as is the available power budget. Table 6.1 **s**hows in the first four columns results for the JDS driver, and in the final four columns results if the MITEQ amplifier was used instead.

Table 6.1. The maximum capacity of our proposed next generation PON (N/A: not applicable, NF: noise figure).

		JDS Driver H301-2310 (NF = 11 dB)				**MITEQ Amplifier AM-1300 (NF = 1.6 dB)**			
		without FEC		with FEC		without FEC		with FEC	
		Maximum Split: *N*	Margin [dB]	Maximum Split: *N*	Margin [dB]	Maximum Split: *N*	Margin [dB]	Maximum Split: *N*	Margin [dB]
Local Self-Seeding	10 km	4	0.6	16	2.4	**32**	**1**	**128**	**2.8**
	20 km	-	1.6	8	2.6	**8**	**2**	**128**	**0**
Remote Self-Seeding	10 km	-	5.1	16	1.4	**16**	**2.5**	**128**	**1.8**
	20 km	N/A	N/A	8	1.6	**N/A**	**N/A**	**64**	**2**

Up to 32 users can be supported over a 10 km PON with self-seeded RSOA transmitters without FEC (a 1 dB link margin is remains). Over a 20 km feeder, 8 users can be supported with local self-seeding with 2 dB of link margin. Using FEC, up to 128 users can be supported. Another possibility would be to exploit the gain of the BEDFA at the central office so that up to 32 or even 64 users are supported without using a FEC. The total losses even for 1:64 splitting ratio and for a feeder length of 20 km, fall within Class B PONs where the total loss should range between 10 and 25 dB [2].

From a power budget perspective, a typical SS-WDM PON using AWGs at the RN experiences lower losses than our proposed SS-WDM PON architecture (the AWG typical insertion loss is only 5 dB). Further, the losses do not scale up with the number of users in the network. However using an AWG based RN imposes an upgrade of all users on the PON and no gradual roll-out. AWGs also make tight spacing of channels problematic if the advantages of noise cleaning are to be maintained. Our use of the BR allows dense channels, increasing spectral efficiency and bandwidth usage. When an AWG is used, the filtering effect occurs before the receiver, hence reduced noise cleaning gain with tight frequency spacing.

6.6. Remote Self-Seeding and Possibility of a Colorless ONU Transmitter

Reduced inventory cost is often advocated to support colorless PON architectures. The

proposed architecture requires two FBGs (one for self seeding and one for notch filtering) whose wavelength sets the wavelength deployed at the client, *i.e.*, colored. To make the setup colorless requires the FBGs to be tunable. One solution would be to exploit a set-and-forget optical filter, *i.e.*, a tunable FBG. To achieve low loss and wide spectral tunability, our approach uses reflective FBGs with strain tuning. Tuning of FBG filters over more than 100 nm has been demonstrated [111]. Another possibility exploits remote self-seeding by placing the self-seeding FBG at the RN so that the ONU transmitter is colorless. We investigate this solution, with the caveat that it will only address a colorless transmitter and not a colorless receiver. A tunable FBG is still required at the receiver for colorless reception.

Remote self-seeding places the self-seeding FBGs at the RN so that the ONU transmitters become colorless. These FBGs are transparent to the downlink which is sent over another wavelength band. Placing the self-seeding gratings at the RN makes the design of the ONUs simpler, more compact, and lowers ONU cost. At the RN the FBGs would be exposed to greater temperature variations, but could be thermally isolated using a passive temperature-compensating package [109].

The experimental setup for the ONU remote self-seeding with a 2 km distribution drop fiber is shown in Figure 6.9. The optimum grating again has 18% reflectivity; the transmitter output power is reduced to 4 dBm (vs. 4.5 dBm). The experiment is repeated for a 10 and 20 km feeder without dispersion compensation; a BR is used at the OLT. The BER performance is given in Figure 6.10 for each feeder length. Compared to the local self-seeding, we note a power penalty of 1 dB for the 10 km case, and a BER floor

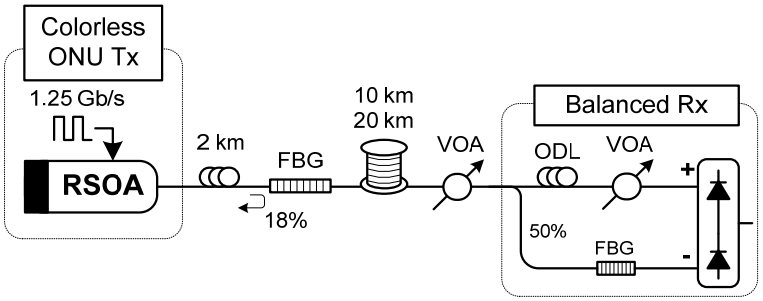

Figure 6.9. Experimental setup for remote self-seeding.

around 10^{-9} starts to appear for the 20 km feeder. The degradation in performance is attributed to the additional dispersion added by the DDF. Eye diagrams at -12 dBm are also provided. The BER simulation using FEC is also presented; a coding gain of 8.3 dB is achieved for the 10 km case and the BER floor is eliminated for the 20 km link.

Finally, these results are used to generate a power budget, presented in the final two rows of Table 6.1. For the transmitter output power of 4 dBm for remote self-seeding, we find the maximum PON capacity is unchanged when using FEC over a 10 km feeder; capacity is reduced from 128 to 64 for FEC over the 20 km link. Given the BER floor with remote self seeding, FEC is essential.

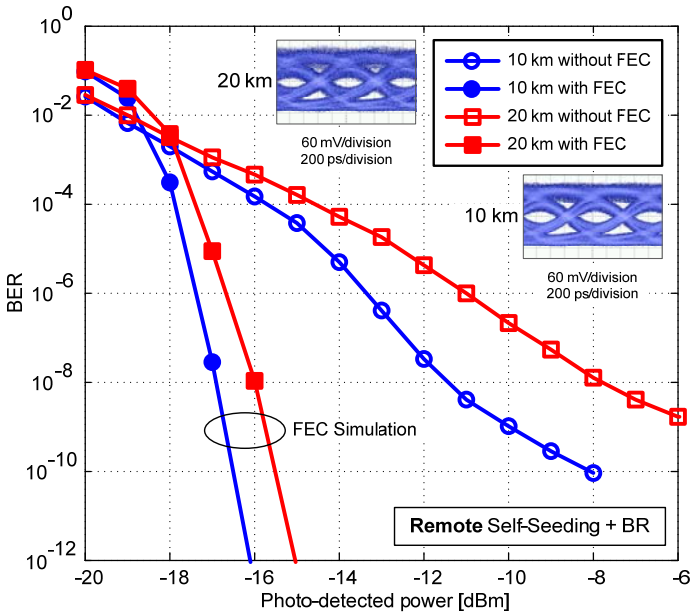

Figure 6.10. BER performance at 1.25 Gb/s with remote self-seeding and BR.

6.7. Summary and Conclusion

In this paper we proposed, for the first time to our knowledge, a self-seeded RSOA-based transmitter with a balanced receiver for dense spectrum-sliced WDM over the legacy TDM PON infrastructure. Our solution provides a gradual upgrade and supports hybrid TDM and SS-WDM operation over the same PON infrastructure. Both local and remote

self-seeding were demonstrated using a *p*% reflective FBG. The reflectivity was optimized to tradeoff self-seeding versus noise cleaning. The extinction ratio is also optimized to favor data erasure and reliable communication. For comparison we considered both a degenerate receiver with no filtering prior to photodetection and the conventional receiver with a CSF. We experimentally showed that despite a 3 dB penalty in implementing the BR, it outperforms the CR by preserving the noise cleaning without sacrificing spectral efficiency [19]. We measured BER better than 10^{-10} for local self-seeding over a 20 km feeder, whereas a BER floor around 10^{-9} appears for remote-self-seeding. For a 10 km feeder, error free is achieved for both cases.

Using our optimized transmitter with 4.5 dBm output power within a 25 GHz channel, and because of the use of the BR, even without FEC up to 32 users can be easily supported over the existing PON infrastructure; up to 64 users can be supported when using reasonable amplification at the OLT. We further simulated the coding gain when using a RS(255,239) FEC and showed that supporting 128 users is possible. Due to the flexibility in the design of FBGs compared to AWGs and due to the ability of the BR to maintain noise cleaning, our proposed PON achieves a higher spectral efficiency than that of traditional AWG-based SS-WDM PONs.

Acknowledgements

The authors would like to thank Serge Doucet for designing and fabricating the FBGs. The authors would like to thank also the anonymous reviewers whose careful reading resulted in clarification and increased quality of this paper.

Chapter 7

Conclusions and Future Work

7.1. Summary and Conclusions

In this thesis, we presented a general overview of the different PON standards focusing mainly on the design of the physical layer. We also reported the state of the art research in next generation gigabit capable PONs. Both OCDMA and WDM were considered in this literature review. The use of SOAs and RSOAs in PONs, their characteristics, their noise cleaning capabilities, and their advantages were also discussed. We introduced the self-seeded RSOA transmitters for SS-WDM systems. Such transmitters are powerful enough so that they eliminate the need for a centralized light source and they avoid the

use of remotely pumped EDFAs. We presented different methods that provide full duplex communication over single-feeder PON architectures. Remodulation techniques, sub-carrier multiplexing and the use of different modulation formats were discussed.

Concerning OCDMA for future PONs, we proposed and experimentally demonstrated the uplink of a 7×622 Mb/s SAC-OCDMA PON with burst-mode operation. Both LS and CLS architectures were considered, and examined over a 20 km link (with DCF). Extra splitting and propagation losses exist for CLS architectures as the uplink signal travels through the network back and forth. A power penalty of less than 2 dB was measured at a BER of 10^{-9} under certain assumptions on the relative power of the sources. We showed that the selection of the appropriate light sources plays an important role in the power budget, and can help increase the link margin. Using a Reed-Solomon RS(255,239) FEC, a coding gain of 2.5 dB was reported for a single-user system, and error free transmission (BER < 10^{-9}) was achieved for a fully loaded PON for the two architectures. Due to a CPA algorithm, even with zero preamble bits we report a zero PLR for up to four simultaneous users, and more than two orders of magnitude improvement in the PLR for a fully loaded PON.

Despite the good results we obtained for our SAC-OCDMA solution, the power budget was critical and therefore OLT amplification was required even for LS architectures. Putting aside the splitting losses at the RN, the use of an external modulator, together with the OCDMA encoding and decoding contributed to more than 20 dB of losses. SS-WDM (*i.e.*, incoherent WDM) can support the same number of users as SAC-OCDMA for the same number of frequency bins; therefore, there is no advantage for SAC-OCDMA over SS-WDM in terms of capacity. Moreover, writing FBGs for SS-WDM is simpler, and narrower slices can be obtained, which makes SS-WDM more attractive in terms of spectral efficiency and bandwidth usage.

In order to upgrade the legacy PONs from shared TDM to dedicated high speed SS-WDM over the existing infrastructure, we proposed using a powerful self-seeded RSOA transmitter together with a BR that avoids filtering and preserves the noise cleaning. The performance of a proof of concept self-seeded RSOA transmitter has been experimentally

studied in terms of BER for instance, with only a DR. The ER has been optimized to tradeoff data erasure versus reliable communication. At 1.25 Gb/s, we reported error free transmission (BER < 10^{-10}) over a 20 km link without dispersion compensation for a 55 GHz wide channel. We further studied the wavelength coverage of the transmitter over the C-band and its noise cleaning capability. We showed that despite a 1.5 dB power variation over a 40 nm band there is a 3 dB power penalty measured at 10^{-10} BER which was explained by the wavelength dependence of the noise cleaning, the gain squeezing and data erasure. We also demonstrated experimentally that the performance is degraded when using a conventional WDM receiver with a CSF prior to the detection.

Finally, we proposed a novel self-seeded RSOA transmitter using a *p*% reflective FBG. We have optimized the reflectivity to tradeoff the output power versus the noise cleaning. We measured the BER for the DR, the CR and the BR, and experimentally showed that the BR outperforms the CR without sacrificing the spectral efficiency, as expected. We found out that using the optimum FBG with $p = 18 \pm 2\%$, we can transmit up to 4.5 dBm of power within a 25 GHz channel.

The migration path from TDM to dense SS-WDM over the existing infrastructure and using our optimized transmitter and the BR has been investigated. We showed how our proposed solution can provide a gradual rollout for network operators, and how it can support hybrid TDM and SS-WDM operation over the same PON infrastructure. Furthermore, we addressed the possibility of colorless ONU operation by placing the FBG at the remote node. At 1.25 Gb/s error free transmission (BER < 10^{-10}) was achieved over a 20 km feeder with the BR for local self-seeding, whereas a BER floor around 10^{-9} was reported for the remote-self-seeding. For a 10 km feeder, error free was achieved for both cases. The power budget allowed up to 32 users to be supported over the existing PON infrastructure without OLT amplification. Through simulations we estimated that the capacity can be increased to 128 users when a FEC is used. We showed that despite the high splitting losses at the RN, our solution achieves a higher spectral efficiency than that of traditional AWG-based SS-WDM PONs.

7.2. Future Research Avenues

Although the objectives of this research have been achieved, probing deeper, there are still other research opportunities to be investigated. Below, we propose directions for future research that could be derived from the work we presented in this thesis:

- Concerning SAC-OCDMA for next generation PONs, the power budget was one of the major limitations even for a 1:8 splitting ratio. Replacing the external EAM at the ONUs with a directly modulated RSOA would release that constraint for both LS and CLS architectures. Moving the FBG encoders to the RN makes the ONU transmitters colorless and helps reduce the cost. These reflective ONUs can be seeded with a centralized source to get more output power. Adding a remotely pumped EDFA would also be an interesting solution.
- Another interesting point would be to find a new SAC-OCDMA family of codes, where the cardinality (number of codes) is larger than the code length. Also, writing FBGs with narrower frequency bins (comparable to WDM slices) would increase the spectral efficiency.
- Regarding self-seeded RSOA transmitters for SS-WDM systems, it would be interesting to design new FBGs more flat-topped and with faster rollover, to allow tightly spacing the channels. Also, optimizing the shape of the slicing/self-seeding FBG with that of a traditional CSF or with that of the notch filter of a BR.
- In this thesis, our self-seeded RSOA transmitter was operated in the continuous mode. The transient effects associated with self-seeded RSOA transmitters, create some challenges when the transmitter is operated in burst-mode. Understanding these transients and combining self-seeding with burst-mode operation is another research topic. We are currently working on that using an inexpensive TO-CAN packaged RSOA (RSOA-18-TO-C-FA) from Kamelian[1].
- Creating good simulation tools for the proposed SAC-OCDMA and SS-WDM systems could help to estimate the performance for larger systems under different conditions and network parameters.

[1] http://www.kamelian.com/data/rsoa_15_ds.pdf

- It is important not to forget that a good MAC layer can work in conjunction with the physical layer to improve the system performance by complementing the physical layer. For example simulating the throughput and the average packet delay using different protocols would be interesting. Implementing such protocols on FPGAs and doing joint experiments between the physical layer and MAC layer is also important.

The results we reported in this thesis provide a strong foundation for future work. In this section we just presented some suggestions and examples for future work.

Bibliography

[1] C. Lin, *Broadband optical access networks and fiber-to-the-home: Systems technologies and deployment strategies*, West Sussex, England: John Wiley & Sons Ltd., September 2006.

[2] A. Girard, *FTTx PON technology and testing*, Quebec City, Canada: Electro-Optical Engineering Inc., 2005.

[3] J. Prat, P. E. Balaguer, J. M. Gené, O. Díaz, and S. Figuerola, *Fiber-to-the-home technologies*, Boston, MA: Kluwer, 2002.

[4] P. W. Shumate, "Fiber-to-the-Home: 1977-2007," *IEEE J. Lightwave Technology*, vol. 26, no. 9, pp. 1093-1103, May 2008.

[5] C.-H. Lee, W. V. Sorin, and B. Y. Kim, "Fiber to the home using a PON infrastructure," *IEEE J. Lightwave Technology*, vol. 24, no. 12, pp. 4568-4583, December 2006.

[6] R. E. Wagner, J. R. Igel, R. Whitman, M. D. Vaughn, A. B. Ruffin, and S. Bickham, "Fiber-based broadband-access deployment in the United States," *IEEE J. Lightwave Technology*, vol. 24, no. 12, pp. 4526-4540, December 2006.

[7] "GPON FTTH market and technology overview," *Passave, Inc.,* September 2005.

[8] M. Abrams, P. C. Becker, Y. Fujimoto, V. O'Byrne, and D. Piehler, "FTTP deployments in the United States and Japan-equipment choices and service provider imperatives," *IEEE J. Lightwave Technology*, vol. 23, no. 1, pp. 236-246, January 2005.

[9] J. Moran, "Moving beyond the standard: Creating additional bandwidth through extending DOCSIS 2.0," *Motorola Broadband Communication Sector*, white paper, September 2003.

[10] Cable Television Laboratories, Inc., http://www.cablemodem.com, 2006.

[11] A. Leon-Garcia, and I. Widjaja, *Communication networks: Fundamental concepts and key architectures*, New York, NY: McGraw-Hill, 2nd Edition, May 2003.

[12] A. Banerjee, Y. Park, F. Clarke, H. Song, S. Yang, G. Kramer, K. Kim, and B. Mukherjee, "Wavelength-division-multiplexed passive optical network (WDM-PON) technologies for broadband access: A review," *OSA J. Optical Networking*, vol. 4, no. 11, pp. 737-758, November 2005.

[13] R. Feldman, E. Harstead, S. Jiang, T. Wood, and M. Zirngibl, "An evaluation of architectures incorporating wavelength division multiplexing for broad-band fiber access", *IEEE J. Lightwave Technology*, vol. 16, no. 9, pp. 1546-1559, September 1998.

[14] M. P. McGarry, M. Reisslein, and M. Maier, "WDM Ethernet passive optical networks," *IEEE Communication Magazine*, vol. 44, no. 2, pp. 15-22, February 2006.

[15] P. R. Prucnal, *Optical code division multiple access: Fundamentals and applications*, Boca Raton, FL: Taylor & Francis, December 2005.

[16] Z. A. El-Sahn, B. J. Shastri, M. Zeng, N. Kheder, D. V. Plant, and L. A. Rusch, "Experimental demonstration of a SAC-OCDMA PON with burst-mode reception: local versus centralized sources," *IEEE J. Lightwave Technology*, vol. 26, no. 10, pp. 1192-1203, June 2008.

[17] Z. A. El-Sahn, M. Zeng, B. J. Shastri, N. Kheder, D. V. Plant, and L. A. Rusch, "Dual architecture uplink demonstration of a 7×622 Mbps SAC-OCDMA PON using a burst-mode receiver," in *Proc. Optical Fiber Communication (OFC)*, San Diego, California, USA, Paper OMR3, February 2008.

[18] Z. A. El-Sahn, W. Mathlouthi, H. Fathallah, S. LaRochelle, and L. A. Rusch, "Dense SS-WDM over legacy PONs: Smooth upgrade of existing FTTH networks," accepted in *IEEE J. Lightwave Technology*, February 2010.

[19] W. Mathlouthi, F. Vacondio, and L. A. Rusch, "High-bit-rate dense SS-WDM PON using SOA-based noise reduction with a novel balanced detection," *IEEE J. Lightwave Technology*, vol. 27, no. 22, pp. 5045-5055, November 2009.

[20] P. Ossieur, X. Qiu, J. Bauwelinck, D. Verhulst, Y. Martens, J. Vandewege, and B. Stubbe, "An overview of passive optical networks," in *Proc. International Symposium on Signals, Circuits, and Systems*, vol. 1, pp. 113-116, July 2003.

[21] X. Qiu, P. Ossieur, J. Bauwelinck, Y. Yi, D. Verhulst, J. Vandewege, B. D. Vos, and P. Solina, "Development of GPON upstream physical-media-dependent prototypes," *IEEE J. Lightwave Technology*, vol. 22, no. 11, pp. 2498-2508, November 2004.

[22] S. Lallukka, and P. Raatikainen, "Link utilization and comparison of EPON and GPON access network cost," in *Proc. Global Telecommunication Conference (GLOBECOM),* St. Louis, MO, USA, pp. 301-305, December 2005.

[23] G. Kramer, G. Pesavento, "Ethernet passive optical network (EPON): Building a next-generation optical access network," *IEEE Communication Magazine*, vol. 40, no. 2, pp. 66-73, February 2002.

[24] ITU-T, "General characteristics of gigabit-capable passive optical networks (GPON)," *Recommendation G.984.1*, 2003.

[25] ITU-T, "Gigabit-capable passive optical networks (GPON): Physical media dependent (PMD) layer specification," *Recommendation G.984.2*, 2003.

[26] P. Ossieur, D. Verhulst, Y. Martens, Wei Chen, J. Bauwelinck, Xing-Zhi Qiu, J. Vandewege, "A 1.25-Gb/s burst-mode receiver for GPON applications," *IEEE, J. Solid-State Circuits*, vol. 40, no. 5, pp. 1180-1189, May 2005.

[27] J. S. Shaik, and N. R. Patil, "FTTH deployment options for telecom operators," *Sterlite Optical Technologies Ltd.*

[28] "PON & FTTx update," *Light Reading Inc.,* August 2005.

[29] R. Menendez, and D. Waring, "Technology options for optical access networks offering increased bandwidth," invited paper, *Bechtel Corporation*, vol. 4, no. 2, pp. 55-67, June 2006.

[30] S-J. Park, C-H. Lee, K-T. Jeong, H-J. Park, J-G. Ahn, and K-H. Song, "Fiber-to-the-home services based on wavelength-division-multiplexing passive optical

networks," *IEEE J. Lightwave Technology*, vol. 22, no. 11, pp. 2582-2591, November 2004.

[31] P. Garvey, "Economics of FTTx in municipality overbuilds," *OSP (Outside Plant) Expo Technical Presentation*, November 2005.

[32] W.-P. Huang, X. Li, C.-Q. Xu, X. Hong, C. Xu, and W. Liang, "Optical transceivers for fiber-to-the-premises applications: System requirements and enabling technologies," *IEEE J. Lightwave Technology*, vol. 25, no. 1, pp. 11-27, January 2007.

[33] W. J. Tomlinson, "Evolution of passive optical component technologies for fiber-optic communication systems," *IEEE J. Lightwave Technology*, vol. 26, no. 9, pp. 1046-1063, May 2008.

[34] R P. Davey, D. B. Grossman, M. Rasztovits-Wiech, D. B. Payne, D. Nesset, A. E. Kelly, A. Rafel, S. Appathurai, and S.-H. Yang, "Long-reach passive optical networks," *IEEE J. Lightwave Technology*, vol. 27, no. 3, pp. 273-291, January 2009.

[35] D. Nesset, S. Appathurai, R. Davey, and T. Kelly, "Extended reach GPON using high gain semiconductor optical amplifiers," in *Proc. Optical Fiber Communication (OFC)*, San Diego, California, USA, Paper JWA107, February 2008.

[36] J. Baliga, R. Ayre, W. V. Sorin, K. Hinton, and R. S. Tucker, "Energy consumption in access networks," in *Proc. Optical Fiber Communication (OFC)*, San Diego, California, USA, Paper OThT6, February 2008.

[37] C. Lange, M. Braune, and N. Gieschen, "On the energy consumption of FTTB and FTTH access networks," in *Proc. Optical Fiber Communication (OFC)*, San Diego, California, USA, Paper JWA105, February 2008.

[38] C. Lange, and A. Gladisch, "On the energy consumption of FTTH access networks," in *Proc. Optical Fiber Communication (OFC)*, San Diego, California, USA, Paper JThA79, March 2009.

[39] F. Payoux, P. Chanclou, and N. Genay, "WDM-PON with colorless ONUs," in *Proc. Optical Fiber Communication (OFC)*, Anaheim, California, USA, Paper OTuG5, March 2007.

[40] F. Payoux, P. Chanclou, T. Soret, and N. Genay, "Demonstration of a RSOA-based wavelength remodulation scheme in 1.25 Gbit/s bidirectional hybrid WDM-TDM PON," in *Proc. Optical Fiber Communications (OFC)*, Anaheim, California, USA, Paper OTuC4, March 2006.

[41] Z. Belfqih, P. Chanclou, and F. Saliou, "Hybrid WDM-TDM passive optical network in burst mode configuration with RSOA," in *Proc. Optical Fiber Communication (OFC)*, San Diego, California, USA, Paper JThA96, February 2008.

[42] N. Calabretta, M. Presi, R. Proietti, G. Contestabile, and E. Ciaramella, "A bidirectional WDM/TDM-PON using DQPSK downstream signals and a narrowband AWG," *IEEE Photonics Technology Letters*, vol. 19, no. 16, pp. 1227-1229, August 2007.

[43] J. Kang, and S.-K. Han, "A novel hybrid WDM/SCM-PON sharing wavelength for up- and down-link using reflective semiconductor optical amplifier," *IEEE Photonics Technology Letters*, vol. 18, no. 3, pp. 502-504, February 2006.

[44] J. Kang, Y.-Y. Won, S.-H. Lee, and S.-K. Han, "Modulation characteristics of RSOA in hybrid WDM/SCM-PON optical link," in *Proc. Optical Fiber Communications (OFC)*, Anaheim, California, USA, Paper JThB68, March 2006.

[45] K.-I. Kitayama, X. Wang, and N. Wada, "OCDMA over WDM PON-solution path to gigabit-symmetric FTTH," *IEEE J. Lightwave Technology*, vol. 24, no. 4, pp. 1654-1662, April 2006.

[46] C. Arellano, C. Bock, J. Prat, and K.-D. Langer, "RSOA-based optical network units for WDM-PON," in *Proc. Optical Fiber Communications (OFC)*, Anaheim, California, USA, March. 2006.

[47] J. Prat, C. Arellano, V. Polo, and C. Bock, "Optical network unit based on a bidirectional reflective semiconductor optical amplifier for Fiber-to-the-Home

networks," *IEEE Photonics Technology Letters*, vol. 18, no. 1, pp. 250-252, January 2005.

[48] S.-B. Park, D. K. Jung, D. J. Shin, H. S. Shin, I. K. Yun, J. S. Lee, Y. K. Oh, and Y. J. Oh, "Colorless operation of WDM-PON employing uncooled spectrum-sliced reflective semiconductor optical amplifiers," *IEEE Photonics Technology Letters*, vol. 19, no. 4, pp. 248-250, February 2007.

[49] M. J. Connelly, "Wideband semiconductor optical amplifier steady-state numerical model," *IEEE J. Lightwave Technology*, vol. 37, no. 3, pp. 439-447, March 2001.

[50] G. P. Agrawal, and N. A. Olson, "Self-phase modulation and spectral broadening of optical pulses in semiconductor laser amplifiers," *IEEE J. Selected Topics in Quantum Electronics*, vol. 25, no. 11, pp. 2297-2306, November 1989.

[51] Y. Katagiri, K. Suzuki, and K. Aida, "Intensity stabilisation of spectrum-sliced Gaussian radiation based on amplitude squeezing using semiconductor optical amplifiers with gain saturation," *IEEE Electronics Letters*, vol. 35, no. 16, pp. 1362-1364, August 1999.

[52] K. Sato, and H. Toba, "Reduction of mode partition noise by using semiconductor optical amplifiers," *IEEE J. Selected Topics in Quantum Electronics*, vol. 7, no. 2, pp. 328-333, March/April 2001.

[53] S. Kim, J. Han, J. Lee, and C. Park, "Intensity noise suppression in spectrum-sliced incoherent light communication systems using a gain-saturated semiconductor optical amplifier," *IEEE Photonics Technology Lett*ers, vol. 11, no. 8, pp. 1042-1044, August 1999.

[54] A. D. McCoy, P. Horak, B. C. Thomsen, M. Ibsen, and D. J. Richardson, "Noise suppression of incoherent light using a gain-saturated SOA: implications for spectrum-sliced WDM systems," *IEEE J. Lightwave Tech*nology, vol. 23, no. 8, pp. 2399-2409, August 2005.

[55] A. D. McCoy, P. Horak, M. Ibsen and D. J. Richardson, "Performance comparison of spectrum-slicing techniques employing SOA-based noise suppression at the

transmitter or receiver," *IEEE Photonics Technology Letters*, vol. 18, no. 14, pp. 1494-1496, July 2006.

[56] W. Mathlouthi, P. Lemieux, and L. A. Rusch, "Optimal SOA-based noise reduction schemes for incoherent spectrum-sliced PONs," in *Proc. European Conference on Optical Communication (ECOC)*, Cannes, France, Paper Tu3.5.4, September 2006.

[57] A. D. McCoy, M. Ibsen, P. Horak, B. C. Thomsen, and D. J. Richardson, "Feasibility study of SOA-based noise suppression for spectral amplitude coded OCDMA," *IEEE J. Lightwave Technology*, vol. 25, no. 1, pp. 394-401, January 2007.

[58] J. Penon, W. Mathlouthi, S. LaRochelle, and L. A. Rusch, "An innovative receiver for incoherent SAC-OCDMA enabling SOA-based noise cleaning: Experimental validation," *IEEE J. Lightwave Technology*, vol. 27, no. 2, pp. 108-116, January 2009.

[59] W. Mathlouthi, L. A. Rusch, P. Lemieux, Z. A. El-Sahn, and H. Fathallah, "Transmitter and receiver for optical communication systems," *International Patent Application (pending)*, Ref: 6013-225PCT, May 2008.

[60] K. Fouli, and M. Maier, "OCDMA and Optical Coding: Principles, Applications and Challenges," *IEEE Communication Magazine*, vol. 45, no. 8, pp. 27-34, August 2007.

[61] L. Nguyen, T. Dennis, B. Aazhang, and J. F. Young, "Experimental demonstration of bipolar codes for optical spectral amplitude CDMA communication," *IEEE J. Lightwave Technology,* vol. 15, no. 9, pp. 1647-1653, September 1997.

[62] Z.Wei, H. M. H. Shalaby, and H. G. Shiraz, "Modified quadratic congruence codes for fiber Bragg-grating-based spectral-amplitude-coding optical CDMA systems," *IEEE J. Lightwave Technology,* vol. 19, no. 9, pp. 1274-1281, September 2001.

[63] M. Rochette, S. Ayotte, and L. A. Rusch, "Analysis of the spectral efficiency of frequency-encoded OCDMA systems with incoherent sources," *IEEE J. Lightwave Technology*, vol. 23, no. 4, pp. 1610-1619, April 2005.

[64] K. Kitayama, X. Wang, and H. Sotobayashi, "Gigabit-symmetric FTTH-OCDMA over WDM PON," in *Proc. 9th Conference Optical Network Design & Modeling (ONDM)*, Milan, Italy, pp. 273-281, February 2005.

[65] H. Lundqvist, and G. Karlsson, "On error-correction coding for CDMA PON," *IEEE J. Lightwave Technology,* vol. 23, no. 8, pp. 2342-2351, August 2005.

[66] T. Hamanaka, X. Wang, N. Wada, A. Nishiki, and K.-I. Kitayama, "Ten-user truly asynchronous gigabit OCDMA transmission experiment with a 511-chip SSFBG en/decoder," *IEEE J. Lightwave Technology*, vol. 24, no. 1, pp. 95-102, January 2006.

[67] D. Zaccarin, and M. Kavehrad, "An optical CDMA system based on spectral encoding of LED," *IEEE Photonics Technology Letters*, vol. 5, no. 4, pp. 479-482, April 1993.

[68] M. Kavehrad, and D. Zaccarin, "Optical code-division-multiplexed systems based on spectral encoding of noncoherent sources," *IEEE J. Lightwave Technology*, vol. 13, no. 3, pp. 534-545, March 1995.

[69] J. Magne, D.-P. Wei, S. Ayotte, L. A. Rusch, and S. LaRochelle, "Experimental demonstration of frequency-encoded optical CDMA using superimposed fiber Bragg gratings," in *Proc. Conference Bragg Gratings, Poling & Photosensitivity in Glass Waveguides (BGPP)*, pp. 294-296, Monterey, California, USA, September 2003.

[70] J. Penon, Z. A. El-Sahn, L. A. Rusch, and S. LaRochelle, "Spectral-amplitude-coded OCDMA optimized for a realistic FBG frequency response," *IEEE J. Lightwave Technology*, vol. 25, no. 5, pp. 1256-1263, May 2007.

[71] S. Ayotte, and L. A. Rusch, "Increasing the capacity of SAC-OCDMA: Forward error correction or coherent sources?," *IEEE J. Selected Topics in Quantum Electronics*, vol. 13, no. 5, Part 2, pp. 1422-1428, September/October 2007.

[72] J. W. Goodman, *Statistical optics*, New York: Wiley, July 2000.

[73] T. Erdogan, "Fiber grating spectra," *IEEE J. Lightwave Technology,* vol. 15, no. 8, pp. 1277-1294, August 1997.

[74] S. Ayotte, M. Rochette, J. Magne, L. A. Rusch, and S. LaRochelle, " Experimental verification and capacity prediction of FE-OCDMA using superimposed FBG," *IEEE J. Lightwave Technology*, vol. 23, no. 2, pp. 724-731, February 2005.

[75] P. Kamath, J. Touch, and J. Bannister, "The need for media access control in optical CDMA networks," in *Proc. IEEE Infocom*, Hong Kong, March 2004.

[76] D. Raychaudhuri, "Performance analysis of random access packet switched code division multiple access systems," *IEEE Transactions on Communications*, vol. 29, no. 6, pp. 895-901, June 1981.

[77] H. M. H. Shalaby, "Optical CDMA random access protocols with and without pretransmission coordination," *IEEE J. Lightwave Technology*, vol. 21, no. 11, pp. 2455-2462, November 2003.

[78] H. M. H. Shalaby, "Performance analysis of an optical CDMA random access protocol," *IEEE J. Lightwave Technology*, vol. 22, no. 5, pp. 1233-1241, May 2004.

[79] Z. A. El-Sahn, J. Penon, and L. A. Rusch, "Simulation of real SAC-OCDMA under both S-ALOHA and R^3T random access protocols," in *Proc. IEEE LEOS Annual Meeting*, Montreal, Quebec, Canada, Paper ThW3, October 2006.

[80] D. Jung, S. Shin, C.-H. Lee, and Y. Chung, "Wavelength-division-multiplexed passive optical network based on spectrum slicing techniques," *IEEE Photonics Technology Letters*, vol. 10, no. 9, pp. 1334-1336, June 1998.

[81] M. Reeve, A. Hunwicks, S. Methley, L. Bickers, and S. Hornung, "LED spectral slicing for single-mode local loop application," *IEEE Electronics Letters*, vol. 24, no. 7, pp. 389-390, March 1988.

[82] G. Pendock, and D. Sampson, "Transmission performance of high bit rate spectrum-sliced WDM systems," *IEEE J. Lightwave Tech*nology, vol. 14, no. 10, pp. 2141-2148, October 1996.

[83] J. M. Oh, S. G. Koo, D. Lee, and S.-J. Park, "Enhancement of the performance of a reflective SOA-based hybrid WDM/TDM PON system with a remotely pumped erbium-doped fiber amplifier," *IEEE J. Lightwave Technology*, vol. 26, no. 1, pp. 144-149, January 2008.

[84] E. Wong, K. L. Lee, and T. B. Anderson, "Low-cost WDM passive optical network with directly-modulated self-seeding reflective SOA," *IEEE Electronics Letters*, vol. 42, no. 5, pp. 299-301, March 2006.

[85] E. Wong, K. L. Lee, and T. B. Anderson, "Directly modulated self-seeding reflective semiconductor optical amplifiers as colorless transmitters in wavelength division multiplexed passive optical networks," *IEEE J. Lightwave Technology*, vol. 25, no. 1, pp. 67-74, January 2007.

[86] H.-C. Kwon, Y.-Y. Won, and S.-K. Han, "A self-seeded reflective SOA-based optical network unit for optical beat interference robust WDM/SCM-PON link," *IEEE Photonics Technology Letters*, vol. 18, no. 17, pp. 1852-1854, September 2006.

[87] N. Nadarajah, K. L. Lee, and A. Nirmalathas, "Upstream access and local area networking in passive optical networks using self-seeded reflective semiconductor optical amplifier," *IEEE Photonics Technology Letters*, vol. 19, no. 19, pp. 1559-1561, October 2007.

[88] S.-M. Lee, K.-M. Choi, S.-G. Mun, J.-H. Moon, and C.-H. Lee, "Dense WDM-PON based on wavelength-locked Fabry-Perot laser diodes," *IEEE Photonics Technology Letters*, vol. 17, no. 7, pp. 1579-1581, July 2005.

[89] B. Zhang, C. Lin, L. Huo, Z. Wang, and C.-K. Chan, "A simple high-speed WDM PON utilizing a centralized supercontinuum broadband light source for colorless ONU," in *Proc. Optical Fiber Communications (OFC)*, Anaheim, California, USA, March 2006.

[90] H. Takesue, N. Yoshimoto, Y. Shibata, T. Ito, Y. Tohmori, and T. Sugie, "Wavelength channel data rewriter using semiconductor optical saturator/ modulator," *IEEE J. Lightwave Technology*, vol. 24, no. 6, pp. 2347-2354, June 2006.

[91] H. Takesue, and T. Sugie, "Wavelength channel data rewrite using saturated SOA modulator for WDM networks with centralized light sources," *IEEE J. Lightwave Technology*, vol. 21, no. 11, pp. 2546-2556, November 2003.

[92] J. -H. Yu, N. Kim, and B. W. Kim, "Remodulation schemes with reflective SOA for colorless DWDM PON," *OSA J. Optical Networking*, vol. 6, no. 8, pp. 1041-1054, August 2007.

[93] M. Fujiwara, H. Suzuki, and K. Iwatsuki, "Reducing the backreflection impact by using gain-saturated SOA in WDM single-fiber loopback access networks," in *Proc. Optical Fiber Communications (OFC)*, Anaheim, California, USA, Paper OTuC2, March 2006.

[94] K. Y. Cho, A. Murakami, Y. J. Lee, A. Agata, Y. Takushima, and Y. Chung, "Demonstration of RSOA-based WDM PON operating at symmetric rate of 1.25 Gb/s with high reflection tolerance," in *Proc. Optical Fiber Communication (OFC)*, San Diego, California, USA, Paper OTuH4, February 2008.

[95] K. Y. Cho, Y. J. Lee, H. Y. Choi, A. Murakami, A. Agata, Y. Takushima, and Y. C. Chung, "Effects of reflection in RSOA-based WDM PON utilizing remodulation technique," *IEEE J. Lightwave Tech*nology, vol. 27, no. 10, pp. 1286-1295, May 2009.

[96] M. McGarry, M. Maier, and M. Reisslein, "Ethernet PONs: A survey of dynamic bandwidth allocation (DBA) algorithms," *IEEE Communication Magazine*, vol. 42, no. 8, pp. 8-15, August 2004.

[97] Z. Wei, and H. Ghafouri-Shiraz "Codes for spectral-amplitude-coding optical CDMA systems," *IEEE J. Lightwave Technology,* vol. 20, no. 8, pp. 1284-1291, August 2002.

[98] D. Pastor, W. Amaya, and R. Garcia-Olcina, "Design of high reflectivity superstructured FBG for coherent OCDMA employing synthesis approach," *IEEE Electronics Letters*, vol. 43, no. 15, pp. 824-825, July 2007.

[99] A. Li, J. Faucher, and D. V. Plant, "Burst-mode clock and data recovery in optical multiaccess networks using broad-band PLLs," *IEEE Photonics Technology Letters*, vol. 18, no. 1, pp. 73-75, January 2006.

[100] J. Faucher, M. Y. Mukadam, A. Li, and D. V. Plant, "622/1244 Mb/s burst-mode CDR for GPONs," in *Proc. IEEE LEOS Annual Meeting*, Paper TuDD3, Montreal, Quebec, Canada, October 2006.

[101] J. Faucher, S. Ayotte, Z. A. El-Sahn, M. Mukadam, L. A. Rusch, and D.V. Plant, "A standalone receiver with multiple access interference rejection, clock and data recovery, and FEC for 2D λ-t OCDMA," *IEEE Photonics Technology Letters*, vol. 18, no. 20, pp. 2123-2125, October 2006.

[102] B. Sklar, *Digital communications: Fundamentals and applications*, Upper Saddle River, NJ: Prentice Hall, 2nd Edition, January 2001.

[103] A. Liu, R. Jones, L. Liao, D. Samara, D. Rubin, O. Cohen, R. Nicolaescu, and M. Paniccia, "A high-speed silicon optical modulator based on a metal-oxide-semiconductor capacitor," *Nature*, vol. 427, pp. 615-618, February 2004.

[104] S. Kaneko, J.-I. Kani, K. Iwatsuki, A. Ohki, M. Sugo, and S. Kamei, "Scalability of spectrum-sliced DWDM transmission and its expansion using forward error correction," *IEEE J. Lightwave Technology*, vol. 24, no. 3, pp. 1295-1301, March 2006.

[105] K. Cho, K. Fukuda, H. Esaki, and A. Kato, "The impact and implication of the growth in residential user-to-user traffic," in *Proc. ACM/SIGCOMM*, Pisa, Italy, pp. 207-218, September 2006.

[106] A. J. Keating, and D. D. Sampson, "Reduction of excess intensity noise in spectrum-sliced incoherent light for WDM applications," *IEEE J. Lightwave Technology*, vol. 15, no. 1, pp. 53-61, January 1999.

[107] A. Ghazisaeidi, F. Vacondio, A. Bononi, and L. A. Rusch, "SOA intensity noise suppression in spectrum sliced systems: A multicanonical Monte Carlo simulator of extremely low BER," *IEEE J. Lightwave Technology*, vol. 27, no. 14, pp. 2667-2677, July 2009.

[108] M. D. Vaughn, D. Kozischek, D. Meis, A. Bosckovic, and R. E. Wagner, "Value of reach-and-split ratio increase in FTTH access networks," *IEEE J. Lightwave Technology*, vol. 22, no. 11, pp. 2617-2622, November 2004.

[109] G. W. Yoffe, P. A. Krug, F. Ouellette, and D. A. Thorncraft, "Passive temperature-compensating package for optical fiber gratings," *OSA J. Applied Optics*, vol. 34, no. 30, pp. 6859-6861, October 1995.

[110] A. B. Carlson, P. B. Crilly, and J. C. Rutledge, *Communication Systems: An introduction to signals and noise in electrical communication*, New York, NY: McGraw Hill, 4th Ed., 2001.

[111] M. R. Mokhtar, C.S. Goh, S.A. Butler, S.Y. Set, K. Kikuchi, D.J. Richardson, and M. Ibsen, "Fibre Bragg grating compression-tuned over 110 nm," *IEEE Electronics Letters*, vol. 39, no. 6, pp. 509-510, March 2003.